Study, Design and Modeling of a PV-powered DC-Home with Optimized-Storage Appliance for Rural Electrification: The Case of Tullo Gudo Island, Ethiopia

Kebede Abebe Mamo

A Thesis Submitted to

The Department of Electrical Power and Control Engineering

School of Electrical Engineering and Computing

Presented in Partial Fulfillment of the Requirement for the Master of Science Degree in Electrical Power and Control Engineering (Power Engineering)

Office of Graduate Studies

Adama Science and Technology University

October 2020

Adama, Ethiopia

Study, Design and Modeling of a PV-powered DC-Home with Optimized-Storage Appliance for Rural Electrification: The Case of Tullo Gudo Island, Ethiopia

Kebede Abebe Mamo

Advisor: Dr.-Ing. Getachew Biru Worku

A Thesis Submitted to
The Department of Electrical Power and Control Engineering
School of Electrical Engineering and Computing

Presented in Partial Fulfillment of the Requirement for the Master of Science Degree in Electrical Power and Control Engineering (Power Engineering)

Office of Graduate Studies
Adama Science and Technology University

October 2020
Adama, Ethiopia

APPROVAL OF BOARD OF EXAMINERS

We, the undersigned, members of the Board of Examiners of the final open defense by Kebede Abebe have read and evaluated his thesis entitled “Study, Design and Modeling of PV Powered DC-Home with Optimized Storage Appliance for Rural Electrification” and examine the candidate. This is, therefore, to certify that the thesis has accepted in partial fulfillment of the requirement of the Degree of Masters of Science in Electrical Power and Control Engineering Program (Specialization in Electrical Power Engineering).

Name of Student	Signature	Date
Advisor/Supervisor	Signature	Date
External Examiner	Signature	Date
Internal Examiner	Signature	Date
Chairperson	Signature	Date
Head of Department	Signature	Date
School Dean	Signature	Date
Postgraduate Dean	Signature	Date

DECLARATION

I, the undersigned, declare that this thesis is my original work, has not been presented for a degree in this or other universities, all sources of materials used for this thesis work have been fully acknowledged.

Student's Name: ____________________

Signature: ______________

This thesis has submitted for examination with my approval as a university advisor.

Advisor's Name: ___________________________

Signature __________________

Date of Submission: _______________________________

ADVISOR APPROVAL SHEET

To: Department of Electrical Power and Control Engineering (EPCE)

Subject: Thesis Submission

This is to certify that the thesis entitled "Study, Design and Modeling of PV Powered DC-Home with Optimized Storage Appliance for Rural Electrification" submitted in partial fulfillment of the requirements of the Master of Science Degree in Electrical Power and Control Engineering, postgraduate in Electrical Power Engineering, and has been carried out by Kebede Abebe Mamo Id No. PGR/18409/11 under my supervision. Therefore, I recommend that the student has fulfilled the requirements and hereby he can submit the thesis to the department.

______________________	________________	______________
Name of advisor	Signature	Date

ACKNOWLEDGEMENT

First, I take this opportunity to give glory to the almighty God without him the completion of this work would have been impossible.

Next, I would like to express my sincere gratitude to my advisor Dr.-Ing. Getachew Biru for his skillful guidance, constructive comments, suggestions and encouragement without him this work could have not been complete. He has been a constant source of my motivation throughout lifespan of my study.

I owe my greatest gratitude to my family (my mother, my brothers and my sisters), who has been the inspirations of my life; your passion for education has contributed immensely to the completion of this study; this is for you.

I would moreover like to thank Mr. Sintayehu Alamnew for your contribution, your patience, helpful attitude, and for the completion of this study.

I am also very grateful to Mr. Minyamer Gelawe and Mr. Menlik Sahilu for lots of advice and helping in preparing the thesis documentation.

Finally, I would also like to thanks the EPCE department head Mr. Hinsermu Alemayehu and all staff members of EPCE and SOEEC dean Dr. Dereje Teklu.

TABLE OF CONTENTS

LIST OF FIGURES

LIST OF TABLES

LIST OF ABBREVIATIONS AND ACRONYMS

AC	Alternating Current
ALCC	Annual Life Cycle Cost
BES	Battery Energy Storage
BESS	Battery Energy Storage System
CCM	Continuous Conduction Mode
CdTe	Cadmium Selenide
CIGS	Cadmium Indium Gallium Selenide
CRF	Capacity Recovery Factor
DBS	Direct Current Bus Signaling
DC	Direct Current
DOD	Depth of Discharge
ESS	Energy Storage System
EU	European Union
EV	Electric Vehicle
FBES	Flow Battery Energy Storage
GW	Gigga Watt
HESS	Hybrid Energy Storage System
IEA	International Energy Agency
IGBT	Insulated Gate Bipolar Transistor
KCL	Kirchhoff's Current Law
LCC	Life Cycle Cost
LED	Light Emitting Diode
MATLAB	Matrix Laboratory
MPP	Maximum Power Point
MPPT	Maximum Power Point Tracking
NaS	Sodium Sulphide
NASA	National Aeronautics and Space Administration
NiCd	Nickel-Cadmium
NiCd	Nickel Cadmium
NiMH	Nickel-Metal Hydride
NPV	Net Present Value

O & M	Operation and Maintenance
P & O	Perturb and Observe
PID	Proportional Integrator Derivative
PSB	Poly Sulphide Bromide
PSCAD	Power System Computer Aided Design
PV	Photovoltaic
RES	Renewable Energy Storage
RMS	Root Mean Square
SC	Super-capacitor
SISO	Single Input Single Output
SMPS	Switch Mode Power Supply
SOC	State of Charge
TV	Television
UPS	Uninterrupted Power Supply
VRB	Vanadium Redox Battery
ZnBr	Zinc Bromine

ABSTRACT

Energy storage will be important to overcome the intermittency and changeability of renewable energy sources. Due to the rapidly changing nature of the weather, renewable energy harvesters – e.g. photovoltaic cells, energy storage systems (ESS) needed to balance energy demand from renewable energy supply. This research optimally sizes the energy storage systems based on days of autonomy. As the number of days of autonomy increases, the size of battery increases, and the battery should be large enough to store sufficient energy to operate the appliances at night and cloudy days, which is costly. This research focuses on the study, design, and modeling of storage optimization for solar-powered DC home appliances for rural electrification system. A hypothetical house assumed to have several household appliances is modeled in detail. Finally, the optimization of storage system is studied for PV-powered DC home with the aim of rural electrification application using HOMER pro software, the model of DC load is modeled, and the converter voltage controller is modeled and simulated by MATLAB/Simulink software. The DC bus system is 130V for 4.801kW household load sample. Constant load voltage is maintained using PID controller coupled with buck convertor irrespective of variation of load and irradiance. In order to determine the optimal days for battery autonomy (energy storage), five different conditions are discussed to determine the optimal day based on their cost of energy (COE) in $/kWh and net present cost (NPC) in $. The cost of energy for condition I (when days of autonomy's are two), condition II (when days of autonomy's are three), condition III (when days of autonomy's are four), condition IV (when days of autonomy's are five), and condition V (when days of autonomy's are six) are $0.689/kWh, $0.912/kWh, $1.16/kWh, $1.4/kWh, and $1.64/kWh; their net present costs are $46,290, $ 61,291, $77,861, $94,223, and $110,540 respectively. Two autonomy days is determined as the optimal time for the battery (energy storage) for the particular rural electrification site (Tullu Gudo Island) with minimum net present costs (NPC) of $46,291 and cost of energy (COE) of $0.689/kWh.

Key word: *Energy storage optimization, Household load modeling, PV Power, Standalone micro grid, Annual life cycle cost (ALCC), Life cycle cost (LCC), Net Present Cost (NPC), Cost of Energy (COE).*

CHAPTER 1

INTRODUCTION

1.1 Background

Population growth has brought an increase in energy demand and cost that has a meaningful effect on personal and governmental expenditures [1]. In 2018, about 55.02% of the populations in Ethiopia live without electricity according to the World Bank collection of development data. Due to insufficient power generation, insufficient and in efficient power transmission and distribution networks to rural areas, high poverty index and these unaffordability of available electrification options, very low household power demands tied with very low productive use of electricity in rural areas [2].

In rural areas of Ethiopia, renewable energies could be alternative sources. For the development of sustainable energy sources, wind and solar energy is very important for the reduction of fossil fuel. So, the stand-alone Photovoltaic systems where chosen in remote locations, due to the cost involved in extending the national grid. To make this renewable energy system more reliable and cost effective, energy storage devices are very important. This storage device in standalone solar PV systems guarantees energy supply during times when there is no sunlight or when it is available but not at the required intensity as on cloudy days. Battery and Super Capacitor (SC) where used for energy storage purposes [3] [4].

With the growing role of variable generation and changing demand profiles, grid operators have limited resources to maintain this dynamic balance. If energy storage has suitably installed, gives the grid operators a flexible and fast responding resource to effectively manage variability in generation and demand [5].

1.2 Statement of the Problem

The standalone DC micro grid project is a solution to challenges of rural electrification. It will provide for independences of DC power through various forms of renewable energy such as photovoltaic, wind, and hydropower. These renewable forms of standalone DC micro-grid energy will replace the currently used liquid fuel, gas, biomass or animal waste, to sustain the daily energy necessities of Ziway Lake Island (Tullu Gudo Island), Ethiopia. The DC micro-grid are used to provide the most basic living necessities such as room lighting, electric stove for cooking, TV, mobile charger, and refrigeration. These standalone PV systems have been attractive to supply electricity to rural areas with the required power quality, reliability, sustainability, and environment friendly characteristics, especially for communities living far in areas where grid extension is not appropriate.

Solar energy is not always reliable, because solar radiation varies from time to time and frequently changes, due to unpredictable nature and dependence on weather and climate changes. Hence, generated energy does not match with load demand all the time. Net metering is critical for PV systems because their generation does not align well with typical load profiles. Energy storage may soon provide a feasible alternative to net metering by shifting PV generation from mid-day to the evening.

The size and cost of energy storage systems depends on days of autonomy (duration for which the battery is capable of meeting the dispatch as a backup without charging). As the number of days of autonomy increases, the size of battery should also be increased. The battery should be large enough to store sufficient energy to operate the appliances at night and cloudy days, which is costly. In this research, PV-powered source is designed, modeled, and associated energy storage system is optimized to electrify a sample home at Ziway Lake Tullu Gudo highland (Tullu Gudo Island), which is found in Oromia regional state, Ethiopia.

1.3 Objectives of the Study

1.3.1 General Objective

The general objective of this research is to study, design, and model of PV-powered DC-home with optimized storage appliance for rural area (Case study: Lake Ziway Highland; Tullu Gudo Island; Ethiopia).

1.3.2 Specific Objectives

The following specific objectives are formulated to accomplish the general objective of the study:

- To assess the energy resource and power requirement of the sample home at the selected site.
- To design PV-powered DC home systems and optimization of the energy storage system (optimization in terms of solar insulation and cost).
- To simulate the system by using MATLAB/Simulink, HOMER Pro software and evaluate the performance of the system.

1.4 Scope and Limitations of the Study

The scope of this thesis mainly focused on modeling, designing, and optimization of energy storage system for PV-powered DC home appliance. In this research, the energy storage (ES) system is optimized based on days of autonomy by using HOMER Pro and variable DC loads are modeled by using MATLAB/Simulink. However, this thesis is limited to the simulation of the system using MATLAB/Simulink 2016a and Homer Pro software by showing how the different components of the system interact with each other. The reason behind this is the implementation of the real system, which is difficult to obtain the components. Along with it takes the additional time and cost incurred in making the real prototype implementation.

1.5 Significance of the Study

- The study has great significance for the people living without electrical power, to get reliable and clear energy for household needs like mobile charging, lighting, TV, refrigeration etc. for peoples living on Tullu Gudo Island.
- The study will benefit the governmental and non-governmental organizations working on rural development to electrify remote villages in affordable way. This study will be initiator to investors to invest in micro-grid market in remote areas like, Tullu Gudo Island in Ethiopia.
- Reduction of total investment costs of energy storage (battery) system.

1.6 Organization of the Thesis

The study, modeling and designing energy storage system of PV-powered DC home appliance for rural area is the focus of this thesis. The thesis organized into the following chapters. Chapter 2 describes the theoretical background of PV system (PV panel, charge controller, MPPT, storage devices, converter, etc.). Recent related papers are reviewed.

Chapter 3 describes the design and modeling of the PV system and optimization of energy storage devices are also discussed taking into consideration the solar inputs and load profiles.

Chapter 4 describes the whole system model is developed for the simulation on MATLAB/Simulink and optimization of energy storage system is developed on HOMER Pro software and the simulation results of designed system is discussed.

Finally, the conclusions, recommendations and future research works are discussed in chapter five. Results obtained from this thesis work are summarized and relevant conclusions were drawn. Further recommendations for future works in the area of energy storage system are then proposed.

CHAPTER 2

THEORETICAL BACKGROUND AND LITERATURE REVIEW

2.1 Theoretical Background

Early 20th century, wrangle begun between alternating (rotating) current (AC) and direct (coordinate) current (DC) frameworks by two scientists (Tesla and Michael Faraday). Tesla designed induction motor (induction machines) for the lion's share of industrial (mechanical) applications. In any case, Michael Faraday illustrated his dynamo electric generator. In spite of, DC displayed a major issue transmitting it over longer separations, the wires misplaced control had to be re-energized utilizing extra circuitry. Besides, stepping-up or stepping-down DC voltage too required complicated circuits. This advancement concreated the way for the AC foundation to construct over the past century. This driven to the dominance of substituting AC over DC for generation, transmission, and largely the utilization of power [6] [7].

2.1.1 Comparison of AC vs DC Distribution Systems

One of the many disadvantages of an AC transmission line is its limited capacity in transferring power. The root-mean square (RMS) voltage of a conductor in an AC system is limited to 70.7% of the peak value. Because the peak and RMS values in DC are same, a like conductor in DC transmission can transmit approximately 30% more power. In addition, the current density of alternating electric current is non-uniform and more current flows near the surface of the conductor than the core, known as the skin effect, free from inductance, dielectric losses, have very low corona losses and interference with communication system.

The absence of inductance in DC system makes voltage drop very low. While the absence of skin effect the small cross section conductor is required in DC system comparing with AC. This reduces the line conductor weight. This condition decreases the amount of power that transmitted through a conductor because the middle portion of the conductor is not used. As shown in Figure 2.1, the current density for a DC conductor is uniform throughout, which is not true in AC conductor. In an AC conductor, skin depth decreases as the frequency of current increases, the DC lines also have very low corona losses thus current only flows mainly near the surface of the conductor [7] [8].

As previously mentioned, the skin effect is where alternating current tends to avoid travel through the center of a solid conductor, limiting itself to conduction near the surface. This effectively limits the cross-sectional conductor area available to carry alternating electron flow, increasing the resistance of that conductor above what it would normally be for direct current:

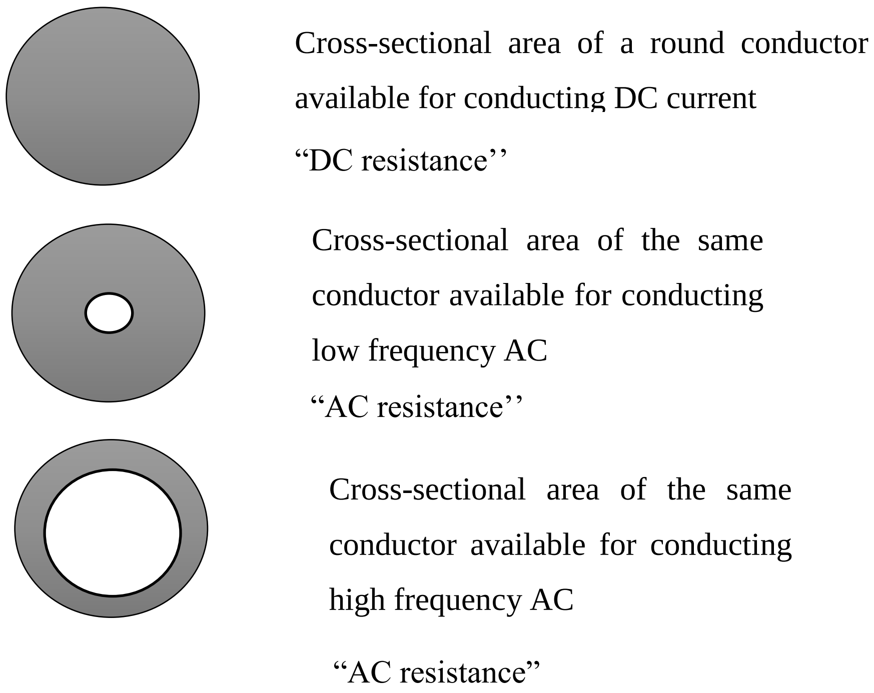

Figure 2. 1 Skin effect [7]

The “DC resistance” of electrical conductor is proportional with its cross-sectional area. The “AC resistance” of the same conductor refers to a higher Figure resulting from the skin effect. As you can see, at high frequencies the AC current avoids traveling through most of the conductor’s cross-sectional area. For conducting current, the wire might as well be hollow [7]. Additionally, DC is becoming more and more prevalent in homes, because; communication technologies and all consumer electronics, such as computers, telephones, televisions, compact fluorescent lighting with electronic ballast, light emitting diodes (LEDs), and efficient DC motors internally applied DC. A wide range of devices from lighting products to electronics fundamentally require DC power to drive semiconductors, charge batteries, and provide other useful services to end users. For this application, the renewable energy sources (RES) are an important because, it is inexhaustible, abundant, renewable, environmentally clean and friendly [8].

For stand-alone micro-grid, common DC transport is the favored choice due to different reasons. To begin with, most ESS components and renewable vitality generators work in DC voltage. Subsequently, keeping up a DC transport minimizes the requirements of control converter. Moment, DC transport does not require synchronization, which incredibly decreases the complexity of the generally framework. As result, DC coupling is more productive and lower taken a toll than comparable AC transport frameworks [9].

2.1.2 Renewable Energy

Grid expansion to such areas is practically impossible to satisfy the need of the society due to either financially high cost or practically not feasible, as these locations are geographically isolated, sparsely populated and have a very low power demand. Using diesel generators for electricity has also harmful effect on the environment in addition to their higher cost of fuel, maintenance and operation. Consequently, rural areas are dependent on local solutions for electricity to get its supply. These are as have been using sources of electricity with multi dimension high impact, such as Kerosene for lighting, diesel for milling and pumping, traditional biomass as source of energy for cooking and dry cells for radio and tape recorders. However, the current increase in oil price and the negative effects of fossil fuels on the environment motivates to search for other alternative (preferably renewable) sources of energy [8].

Due to increasing demand and environment concern, the integration of renewable energy source (RES) to power system is increasing day by day. The RES such as solar, wind turbine, fuel cells are intrinsically DC power sources [10]. Presently, sun powered energy is considered as the foremost promising sources with the highest potential to gain energy compared to other RESs. As the ratio of installed PV capacity to the system load increases, the required equipment needed to maintain a stable AC grid increases, forcing an optimum amount of PV power in a given system [11].

2.1.2.1 Overview of Photovoltaic (PV) System

Photovoltaic (PV) may be a strategy of producing electrical power by changing over sun powered radiation into the stream of electrons to get coordinate current power utilizing semiconductors that display photo-voltaic impact. To coordinate current (DC) power from sun oriented, certain sun powered boards comprising a number of cells containing a semiconducting fabric, which, utilizing to change over sun powered vitality into a usable frame of vitality, required. When the sunlight is sparkling on the sun-oriented cell, there is a stream of electrons and hence produces power. When there is no light sparkling to the board, no power created. The sun based cells that come to on the board (panel) and utilized on calculators and satellites are photovoltaic cells or modules. This PV module comprises of numerous PV cells wired in parallel arrange to extend current and in arrangement to deliver the next voltage [8].

In a PV cell, there are two doped semiconductor layers, P-type (hole) and N-type layer (electron) which, isolated to each other by a junction. A spontaneous electric field developed at the boundary, which characterizes the heading of the current stream over the junction. In arrange to urge power from a PV; the daylight ought to enter a glass cover and antireflection coating. The show created to tackle sun-powered vitality was from the western, planned building centralized power era and transmitting power by transmission wires to the buyers. Energy effectiveness of sun-powered photovoltaic calculated as the power yield from the PV isolated by the sun based radiation radiated to the sun based cluster region [12].

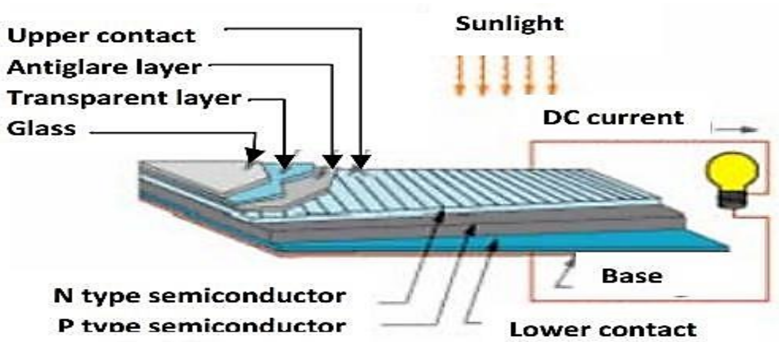

Figure 2. 2 Typical PV cells [12]

Worldwide growth of photovoltaic has been close to exponential between 1992 and 2018. During this period, photovoltaic (PV), also known as solar PV, evolved from a role market of small-scale applications to a mainstream electricity source. When solar PV systems were first recognized as a promising renewable energy technology, funding programs, such as; feed-in tariffs, were implement by a number of governments in order to provide economic incentives for investments. For several years, growth of photovoltaic has mainly driven by Japan and pioneering European countries. Therefore, cost of solar declined significantly due to experience curve effects like improvements in technology and economies of scale.

In the early 21st century a market for utility scale, plants emerged, to complement rooftop and other distributed applications. By 2015, some 30 countries had reached grid parity [13]. Projections for photovoltaic growth are difficult and burdened with many uncertainties. Official agencies, such as the International Energy Agency (IEA) have consistently increased their estimates for decades, while still falling far short of projecting actual deployment in every forecast. Bloomberg NEF projects global solar installations to grow in 2019, adding another 125–141 GW resulting in a total capacity of 637–653 GW by the end of the year. By 2020, the IEA forecasts solar PV to reach 770 GW in its high-renewable scenario, of which more than half will be deployed in China and India, making solar power the world's largest source of electricity.

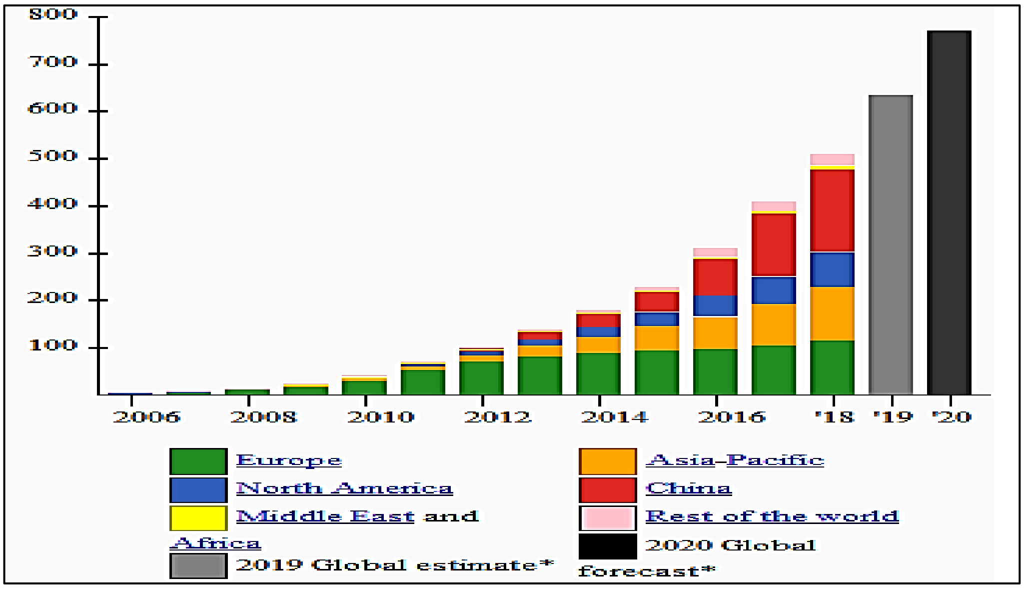

Figure 2. 3 Worldwide growth of photovoltaic [13]

Table 2. 1 Recent and estimated capacity of photovoltaic (GW) [13]

Year-end	2014	2015	2016	2017	2018	2019E	2020F
Growing	178.4	229.3	306.5	403.3	512	633	*~770*
Annual new	40.1	50.9	76.8	99	109	121	*121-154*
Total growth	28%	29%	32%	32%	27%	24%	

2.1.2.2 Classification of Solar Cells

Alexandre-Edmond Becquerel first observed the photovoltaic (PV) effect in 1839. Subsequently, in 1946 Russel Ohl invented the first modern solar cell made of silicon. Earlier photovoltaic solar cells are thin silicon wafers that transform sunlight energy into electrical power [14]. The modern photovoltaic technology based on the principle of electron hole creation in each cell composed of two different layers (p-type and n-type materials) of a semiconductor material, as shown in Figure 2.2. In this arrangement of the structure, when a photon of sufficient energy strike on the p-type and n-type junction, an electron is ejected by gaining energy from the striking photon and moves from one layer to another. This creates an electron and a hole in the process and this process generates electrical power. The various types of materials applied for photovoltaic solar cells includes mainly in the form of silicon (single crystal, multi-crystalline, amorphous silicon), cadmium-telluride, copper-indium-gallium-selenide, copper-indium-gallium-sulfide and third generation type of PV cells are discussed in the following Tables 2.2, 2.3, and 2.4.

Table 2. 2 Characteristics of crystalline PV cells with their performance [14]

Parameters	Crystalline cells (First generation)	
	Mono crystalline	Polly crystalline
Efficiency	14% - 17.5%	12% - 14%
High temperature Performance	Not good at high temperatures	Not good at high temperatures
Size	Significantly less volume to produce the same amount of power	Significantly less volume to produce the same amount of power
Cost	Two time more expensive compared to thin-film	Two time more expensive compared to thin-film.
Additional details	Oldest PV technology	Economical choice

Table 2. 3 Characteristics of thin film of PV cells with their performance [14]

Parameters	Thin Film (Second Generation)		
	CdTe	CIGS	Amorphous silicon
Efficiency	9% - 11%	10% - 12%	4% - 8%
High temperature performance	Good in cool as well as high temperature	Good in cool as well as high temperature	Good in cool as well as high temperature conditions
Size	Offering a wide range of product design form flexible, light, durable	Offering a wide range of product design form, flexible, light, durable	Offering a wide range of product design form, flexible, light, durable
Cost	50% less expensive than conventional silicon cells	50% less expensive than conventional silicon cells	50% less expensive than conventional silicon cells
Additional details	Toxic due to Cd	Some CIGS have impressive 20% efficiency	Needs long installation time and large space

Table 2. 4 Characteristics of third generation PV cell with their performance [14]

Parameters	Third Generation				
	Nano crystal	Dye Sensitized	Polymer	Concentrated	Perovskites
Efficiency	7% - 8%	10%	3% - 10%	40%	31%
High temperature performance	Excellent thermal stability	Not good in high temperature conditions	Not good in high temperature conditions	Excellent thermal stability	Excellent thermal Stability
Size	Offering a wide range of product design form, flexible, light, durable	Offering a wide range of product design form, flexible, light, durable	Offering a wide range of product design form, flexible, light, durable	Offering a Specialized range of product design	Offering a specialized range of product design
Cost	50% less expensive than conventional silicon cells	50% less expensive than conventional silicon cells	50% less expensive than conventional silicon cells	50% less expensive than conventional silicon cells	50% less expensive than conventional silicon cells
Additional details	Needs long installation time and large space	Needs long installation time and large space	Needs long installation time and large space	Needs long installation time and large space	Latest technology. Needs short installation time and min. space

2.1.3 Storage Devices

For any hybrid renewable energy systems, there is an extra and shortage of energy at any instant of time. If the renewable energy resources produces excess energy than the power demanded by the load, the additional energy should be stored. In addition, if the renewable resources system produces less energy than the power demanded by the load, then storage system should satisfy the load. Therefore, storage system is an essential for any renewable energy stand-alone systems [15].

2.1.3.1 Battery Energy Storage System (BESS)

A battery (energy storage) system is a storage unit that acts as a source in the power network by converting the stored energy into electrical energy for use in case of a need [16]. Batteries allow for the storage of solar photovoltaic energy; it is possible to use during nighttime; or when weather elements keep sunlight from reaching PV panels. Not only used in homes, but also batteries are playing an increasingly important role for utilities. As customers feed solar energy back into the grid, batteries can store it so it returned to customers later. The increased use of batteries will help modernize and stabilize our country's electric grid [17].

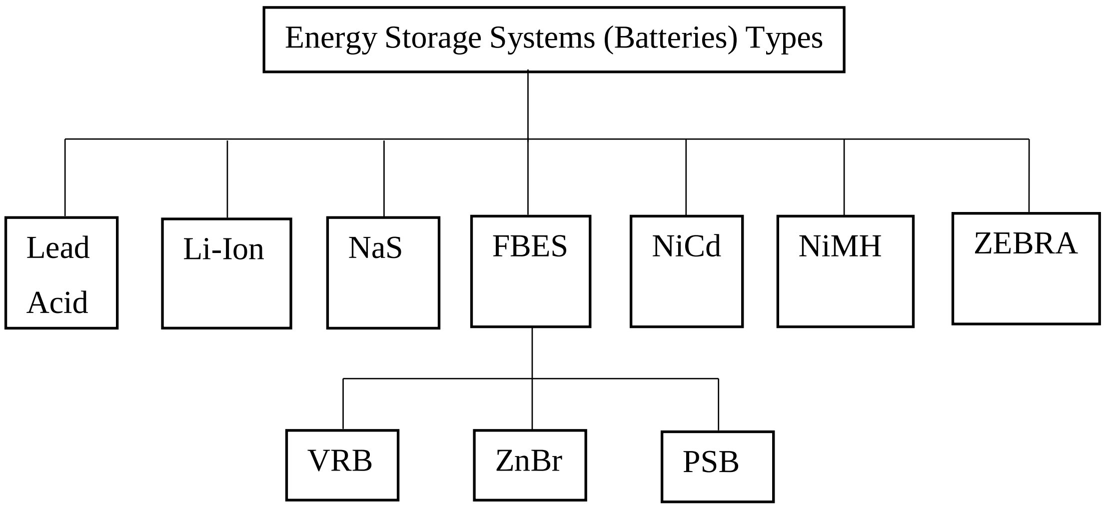

Figure 2. 4 Electro-chemical batteries classification

In a BESS system, electro-chemical cells connected in series or parallel to generate electricity for a desired voltage. Energy converted in bi-directional way i.e. between electrical and chemical energy with the help of the cells. Batteries can have a wider range of applications in energy management and transportation system [18]. Some important BES technologies represented below:

1. Lead-Acid Battery**:** These batteries are the oldest rechargeable battery [19] [18]. In the electrolyte is sulphuric acid, anode is made of Pb, and cathode is made of PbO2. Lead acid is rugged, forgiving if a bused and is economically priced, but it has a low specific energy and limited cycle count [19]. Lead acid used for wheelchairs, golf cars, personnel carriers, emergency lighting and uninterruptible power supply (UPS). These batteries act as backup power supplies for energy management application in stationary devices. Their performance at low temperature is poor which compensated by using thermal management system [18]. Lead is toxic and cannot be disposed in landfills [19].
2. Lithium-Ion Battery**:** In this type of battery, the electrolyte present is a non-aqueous organic liquid. Here anode made up of graphite carbon whereas cathode is made up of Lithium Metal Oxide (LiMO2) [18]. Li-ion is replacing many applications that previously served by lead and nickel-based batteries. Lithium-ion batteries have become the most common rechargeable batteries for consumer electronics, due to their high energy densities, relatively high cell voltages and low weight to volume ratios. They predicted to become commonplace for industrial, transportation and power storage applications, even if they tend to be more expensive than equivalent battery technologies with aqueous electrolytes. Due to safety concerns, Li-ion needs a protection circuit [20]. lifetime can be affected by cycle DOD but high cycle count and low maintenance, their cycle efficiency is up to 97%, reduce the cost per cycle over many other chemistries. It acts as a good candidate where small dimension and response time are important. Now a days these types of batteries are also used for electric vehicles [19] [18].
3. Sodium Sulphur battery (NaS): These batteries used beta alumina as solid electrolyte and molten form of sodium and Sulphur as the two electrodes. They have relatively high energy density and high rated capacity compared to other type of batteries. It has high-recycled ability up to 99%. They have high power electric energy storage applications.
4. Nickel-Cadmium battery (NiCd): These batteries have aqueous solution of alkali as an electrolyte. It uses nickel hydroxide (Knish) and cadmium in metallic form i.e.

(Cd) as the two electrodes respectively [18]. Mature and well understood; NiCd is used where long service life, high discharge current and extreme temperatures are required. NiCd is one of the most rugged and enduring batteries. This is the only chemistry that allows ultra-fast charging with minimal stress [19]. The main applications are; power tools, medical devices, aviation and UPS. Due to environmental concerns, NiCad replaced with other chemistries, but it retains its status in an aircraft due to good safety record. Its main drawbacks are arced and Ni are toxic heavy metals and it suffers from memory effect [18].

5. Nickel-Metal Hydride (NiMH): use hydrogen-absorbing alloy as an electrode. It has high energy density compare to NiCd batteries, which uses Cd as an electrode. In addition, these batteries are environment friendly and longer cycle life [19] [18]. NiMH used for medical instruments, hybrid cars and industrial applications [19].
6. Sodium Nickel Chloride (ZEBRA): are somewhat analogous to NaS batteries. They have free cell maintenance, low self-discharging and high life cycle relatively. The main shortcoming is that it takes 12-15 hours to heat up after its solidification.
7. Flow Battery Energy Storage system (FBES): This battery-stored energy in the two soluble redox couple switch is stored in exterior liquid electrolyte tank. The operation performed here includes reduction-oxidation reactions of electrolyte solution. They are cate go rise depending on dissolving properties of electro active components in the electrolyte, which are redox flow and hybrid flow batteries. Power of FBES system does not depend on its storage capacity. The main drawbacks are low performance, large maintenance cost and complex system compared to other types of batteries. Some type of flow battery technology is described below:

   A, Vanadium Redox Flow battery (VRB): It is the highly matured flow battery system, which stored energy using vanadium redox in two electrolyte tanks. The chemical reactions, which occur, are:

$$V^{4+} \rightarrow V^{5+} + e^{-} \text{ and } V^{3+} + e^{-} \rightarrow V^{2+}$$

   They have quick response and high efficiency relatively and provide continuous power. One drawback is its high operating cost. It has wide range of use in enhancing power qualities and UPS devices, power security and load leveling.

B, Zinc Bromine flow battery (ZnBr): It is a hybrid flow battery. In this, the reactive components kept in two aqueous electrolyte solution based upon zinc and bromine elements. The chemical reactions, which occurred, is as:

$$2Br^{-} \rightarrow Br_2 + 2e^{-} \text{ and } Zn^{2+} + 2e \rightarrow Zn$$

It has high energy density and good reversibility. It has some drawbacks as material corrosion, low cycle efficiency compared to other batteries. It has a narrow range of temperature.

C, Poly sulphide Bromide flow battery (PSB): It includes of sodium bromide (NaBr) and sodium polysulfide (NaPS) as electrolyte of salt solution. The chemical reaction that occurs is as:

$$3Br^{-} \rightarrow Br_3^{-} + 2e^{-} \text{ and } 2S_2^{-} \rightarrow S_4^{-} + 2e^{-}$$

Its main feature is cost effective abundant material of two electrolytes fast response time. This type of battery used for frequency and voltage control of power system.

In the aspect of technology, the rechargeable battery improved from lead acid battery to nickel-based battery and from nickel-based battery to lithium-ion (Li-ion) battery. Lithium-ion battery has higher terminal voltage, higher power density, higher energy density, higher efficiency, higher life cycle, higher lifetime and maintenance free compared to the other rechargeable batteries. Nowadays, Li-ion battery is widely adopted in portable electronic devices, such as laptop computers, smart phones, and digital cameras and in different storage devices. The most common form of lithium-ion batteries is comprised of positive electrode (cathode) of lithium oxides, negative electrode (anode) of graphite, electrolytes of lithium salt, and solvent molecule as shown in Figure 2.5.

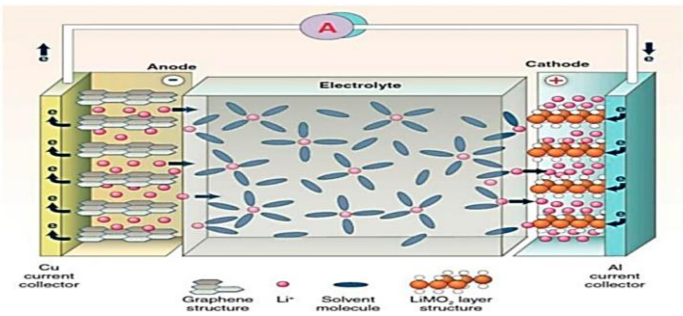

Figure 2. 5 The structure of a lithium-ion (Li-ion) battery [17]

Table 2. 5 Comparisons of the four commonly used rechargeable battery systems [21]

Specifications	Lead Acid	NiCd	NiMH	Li-ion		
				Cobalt	Manganese	Phosphate
Specific energy density (Wh/kg)	30-50	45-80	60-120	150-190	100-135	90-120
Internal resistance (mΩ)	<10 12Vpack	100-200 6V pack	200-300 6V pack	150-300 7.2V	25-75 Per cell	25-50 Per cell
Cycle life (80% discharge)	200-300	1000	300-500	500-1000	500-1000	1000-2000
Fast charge time	8-16h	1h typical	2-4h	2-4h	1h or less	1h or less
Overcharge Tolerance	High	Moderate	Low	Low. Cannot tolerate trickle charge		
Self-discharge/month (at room temp)	5%	20%	30%	< 10%		
Cell temperature (nominal)	2V	1.2V	1.2V	3.6V	3.8V	3.3V
Charge cutoff voltage (V/cell, 1C)	2.40 float 2.24	Full charge detection By voltage signature		4.2		3.6
Discharge cutoff voltage (V/cell, 1C)	1.75	1		2.5 - 3		2.8
Charge temperature	-20 - 50°	0 - 45°		0 - 45°		
Maintenance requirement	3-6 month	30-60 days	60-90 days	Not required		
Safety requirements	Thermally stable	Thermally stable, fuse protection common		Protection circuit mandatory		

Charge and discharge mechanisms of Li-ion battery: As with most batteries, they have an outer case made of metal. This metal case holds a long spiral comprising three thin sheets pressed together:

- A Positive electrode (cathode)
- A Negative electrode (anode)
- A separator

The separator is a very thin sheet of micro-perforated plastic, which separates the positive and negative electrodes while allowing ions to pass through. The positive electrode is made of Lithium Cobalt Oxide (LiCoO2). The negative electrode is made of Carbon as shown Figure 2.6, that during discharge, Lithium (Li+) ions carry the current from the negative to the positive electrode, through the electrolyte and separator diaphragm.

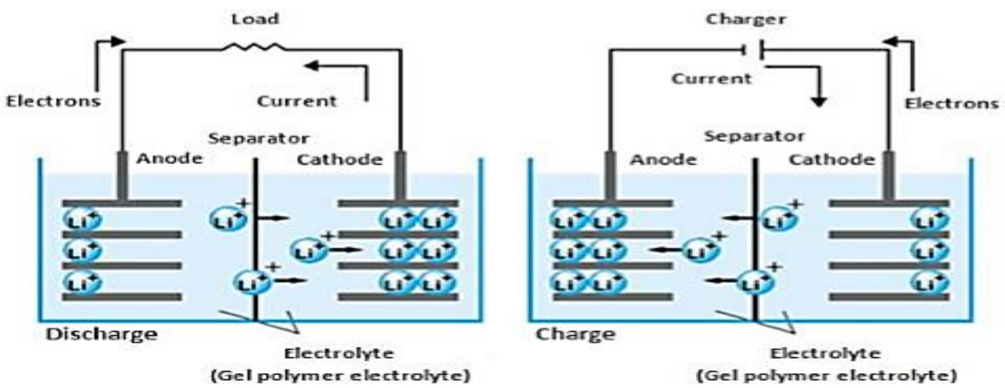

Figure 2. 6 Charge and discharge mechanism of Li-Ion rechargeable batteries

During charging, an external electrical power source applies an over-voltage than that produced by the battery, forcing the current to pass in the reverse direction. The lithium-ions then migrate from the positive to the negative electrode, where they embedded in the porous electrode material in a process known as intercalation.

2.1.4 Maximum Power Point Tracking (MPPT)

The photovoltaic system has a non-linear current-voltage and power-voltage characteristics that continuously varies with irradiation and temperature. In order to track the continuously varying maximum power point of the solar array the MPPT (maximum power point tracking) control technique plays an important role in the PV systems. The task of a maximum power point tracking (MPPT) network in a photovoltaic (PV) system is to continuously tune the system so that it draws maximum power from the solar array regardless of weather or load conditions [22].

Perturb and Observe (P & O): The P&O, algorithm also called “hill-climbing”, while both names refer to the same algorithm depending on how it implemented. Hill-climbing consist of a perturbation on the duty cycle of the power converter and P&O a perturbation in the operating voltage of the DC link between the PV array and the power converter. In the case of the Hill-climbing, perturb the duty cycle of the power converter implies modifying the voltage of the DC link between the PV array and the power converter, so both names refer to the same technique.

In this method, the sign of the last perturbation and the sign of the last increment in the power used to decide what the next perturbation should be on the left of the MPP incrementing the voltage increases the power whereas on the right decrementing the voltage increases the power. This algorithm is the most popular MPPT methods due to their ease of implementation and good performance when the irradiation is constant. The advantages of both methods are the simplicity and low computational power they need. The shortcomings are also well known: oscillations around the MPP and they can get lost and track the MPP in the wrong direction during rapidly changing atmospheric conditions.

2.1.5 Charge Controller

Charge controller is an essential component in PV systems where a storage system is required. In other words, the battery charge controller works as a voltage regulator. It protects the battery against both excessive overcharge by a generating unit system and deep discharge by a load. Charge controller shall disconnect the load when a certain state of discharge reached, also shall switch off the battery from the DC bus when it is fully charged. Charge controller adjusts to deal with different charging and discharging conditions. The controllers average efficiencies range from 95% to 98% [23].

2.1.6 DC Home Systems

The DC home system is a critical power to people who live off the electrical grid. It meant to supplement the living conditions of a family that does not have access to typical grid tied

AC power sources. The DC house will serve as a means for renewable energy sources uses for power an off-grid home as shown Figure 2.7 [24].

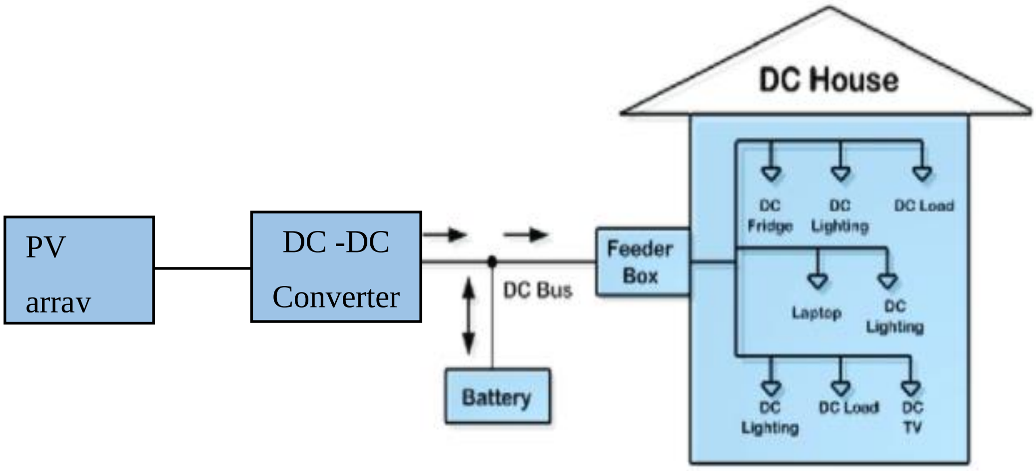

Figure 2. 7 Simple block diagram of stand-alone DC house

Figure 2.7 shows simple block diagram of the proposed design for standalone DC micro-grid distribution network.

This will bring power to those who do not have grid access, and increase the opportunity for the use of clean renewable energy sources. In remote areas, where it is difficult or costly to connect to the utility grid, stand-alone PV and wind power systems are gaining commercial attention, stand-alone photovoltaic systems are most common because it is visible in everywhere in Ethiopia. A typical stand-alone system incorporates a PV panel, regulator, energy storage system, DC–DC converter, bidirectional and load.

This type of configuration is suitable for remote villages with widely disperse population and it can have one or multiple renewable sources generating DC power. In addition, it allows the exchange of power in a small cluster of DC homes and suitable for remote villages.

2.1.6.1 Types of DC Home Appliances

Depending on the construction and operation, household appliances are classified in to three groups.

Resistive Loads**:** Current AC home appliances that are considered as resistive loads (heaters) include Stoves, Electric-Mitad, Ovens, dryers, toasters, kettle, coffee machine, LED lamps , DC fan, refrigerators, water purifier, Freezers or fridges, incandescent lamp and tungsten halogen lamp. Since these loads effectively modeled as a resistance, they directly supplied with DC distribution system without any modification [25].

Appliances equipped with motors (rotating machines): washing machines, mixers, vacuum cleaners, automatic gates, garage doors, dishwashers, ventilation fans, cloth washers and cloth dryers, are one of the most popular appliances that are available commercially with DC input power [25].

Electronic Loads**:** Laptop computer, TVs, satellite receivers, phone chargers and security cameras are the major electronic loads, which can be make efficient or even energy star just by replacing input ac/DC converter with the buck-boost converter [25]. Old electronic loads use a low-frequency transformer to step down the voltage, which is then rectified using a diode bridge. This type works only with a certain voltage amplitude and frequency. However, due to the introduction of switch mode power supply (SMPS), the load connected to a wide range of inputs. However, SMPS operated with DC without any design modifications as long as the DC voltage is in the same range as the appliance's voltage requirement.

2.1.6.2 DC Voltage Level Selection

Commercially, most appliances are readily available with an input voltage of 12 and 24V [26]. Some appliances are available with an input voltage of 48V [27]. Majority of DC appliances are available in 12V, 24V, and 48V DC voltage levels. Increasing nominal voltage level beyond 48V DC (i.e.120V, 240V, and 380V DC), the cable size requirement and rating of controller will decrease. This may result in saving in cost and improve safety. 120V is set as the optimal for Low voltage DC appliances because lower demand currents, making feeder less losses considerable, and the overall appliance efficiency is higher [28].

2.1.7 Optimal Sizing of Energy Storage (Battery) in Terms of Cost Based on Days of Autonomy's

Optimization is the method of achieving the best possible result of the defined optimization problem under given circumstances. The best possible, or optimal, system configuration is that satisfies the user specified constraints at the lowest total purchasing cost and unit energy cost. The goal of the optimization process is to determine the optimal value of autonomy days. Days of autonomy indicate the duration for which the battery is capable of meeting the dispatch as a backup without charging. As the number of days of autonomy increased, the size of battery is too increased and the battery should be large enough to store sufficient energy to operate the appliances at night and cloudy days, which is costive.

2.2 Literature Review

This portion discusses the more closely related works.

Over the past, few years several researchers carried out research on hybrid power systems. In [29] the author developed the HESS (Hybrid Energy Storage System) for renewable energy applications. A HESS characterized by a coupling of two or more energy storage technologies with supplementary operating characteristics (such as energy and power density, self-discharge rate, efficiency, lifetime, etc.). The paper discusses typical HESS applications, storage coupling architectures and basic energy management systems. However, the storage optimization of the HESS not discussed.

The author in [30] presented a DC Micro-grid platform for solar energy sources, and for practical applications such as lighting, cooking and computing. DC micro-grids can optimize the use of electronic devices, electrical storage, and distributed generation by using power server (DC-AC-DC). This power server accepts both AC and DC as power inputs and then produces only DC power output. According to the researcher, those two (DC-AC-DC) conversions yield an approximate 10-40% power loss and if the number of tests point is increased, a greater number of sections checked systematically.

Author [31] proposed AC-DC micro grid, DC and AC power sources supplying AC and DC loads. AC buses supply power full devices like air conditioner, washing machine, etc. and DC buses supply lighting system, consumer electronics and provide charging electro mobile.

In addition, advantages of DC micro grid discussed. However, some gaps need further investigation in the field of DC micro grid. Example, development of DC micro grid distribution of DC current, Installation of DC distribution box in every house, etc.

In [32], the author studied the optimization of both the placement and controller parameters for BESSs to improve power system oscillation damping by using particle-swarm optimization algorithm. The proposed optimization approach demonstrated on 39-bus system to improve applicability and efficiency of the proposed system based on seasonal load changes and the minimum number of BESS (i.e. minimum cost of BESS) units placed considered. The proposed controller model adopted to reduce the damping ratio of inter-area of 0.657Hz to 1.68% by using gains with automatic voltage regulators and governors of seven generators.

Several modeling studies on PV-wind turbine power system conducted. Among them, in [33] the researcher developed a grid-connected photovoltaic model using PSCAD for electromagnetic transient analysis where a simple circuit model of the solar array used to simulate its inherent characteristics with the basic specification data. Author in [34] implemented an insulation-oriented PV model using the MATLAB/Simulink software package. Taking the effect of sunlight irradiance on the cell temperature, the model took ambient temperature as reference input and used the solar insolation as a unique varying parameter. The output current and power characteristics simulated and analyzed using the proposed PV model. The model verification finally confirmed through an experimental measurement.

In [35] and [36], the authors presented a model for maximum power point tracking (MPPT) system based on perturbation and observation. To allow the PV system to produce the maximum possible power, significant number of maximum power point tracking (MPPT) techniques and algorithms developed. The MPPT tested under varying insolation and load conditions. This MPPT shown that with the Perturbation and Observation algorithm, the controller took a relatively moderate time to track the maximum power point.

In [37] the researcher studied the DC-DC power electronic interfaces of batteries used in micro-grid. The study conducted to investigate how the stability of the islanded micro-grid depends on its response speed to the transients. The paper focused on inner and power controllers of the DC-DC bidirectional converters for interfacing batteries in micro-grid. The inner control techniques discussed and a control strategy for the operation of batteries in different modes was proposed.

The researcher described the control approach applied to dual bidirectional Voltage source converter for composite wind-solar-hydro power systems in [38]. In order for these systems to operate in grid-connected and islanded modes, a control technique devised based on sum of-product of load and utility voltages. The effectiveness of the control technique demonstrated through simulation of the proposed scheme under constant as well as changing meteorological and load conditions.

In this thesis, a detailed design, model, storage optimization and simulation of a solar standalone PV power generation system for DC homes with battery storage presented. Modeling and simulation carried out using the MATLAB/Simulink software package, specifically SimPowerSystems, to verify the effectiveness of the proposed system. SimPowerSystems enables engineers to use model-based designs to model and simulate electrical circuits and power systems within Simulink, and includes a comprehensive applications library, which makes the interfacing of all the components of the solar-battery system a straightforward process for the user. Storage (battery) optimization based on days of autonomy's are carried out by using HOMER Pro software. HOMER stands for hybrid optimization model for renewable energy sources and it is a micro-power optimization model that simplifies the tasks of finding the best arrangement for both off-grid and grid-connected power systems. This software performing three tasks for a various applications: simulation, optimization, and sensitivity.

CHAPTER 3

DESIGN AND MODELING OF PV WITH ENERGY STORAGE SYSTEM

3.1 Site Description and Solar Energy Data of Study Area

3.1.1 Site Description

Tullo Gudo is an island located around Ziway town, in the state of Oromia, Ethiopia (Africa) with the region font code of Africa/Middle East. Ziway is located about 166.6 km from south Addis Ababa on the border between the regions of Oromia and of the southern nations, nationalities, and peoples; the Woreda holding the Lakes Shore Line is Adami Tullu and Jido Kombolcha, Dugda Bora, and Ziway Dugda. In Ziway Lake highland, Ethiopia, Tullu Gudo is approximately 18km off the South Eastern coast of south Ziway, Ethiopia in the state of Oromia. It is an island and it has more than 900 Zay peoples.

On this island, there is no installed energy system of that area. Geographically, Tullu Gudo Island is a hot and humid island. It is a sunny island the equatorial belt. Thus, a completely clear or cloudless sky is common on this rift valley island. Tullo Gudo is also as Debra Tseyon, Kulu, Gudo Deset, and Mount-Zion [39]. Its coordinate is 7°55'60" North and 38°51'0" East in DMS (Degrees, Minutes, Seconds) or 7.5° North and 38.5° East (in decimal degrees). It is located at an elevation of 1,636m above sea level [40].

Figure 3. 1 Tullu Gudo Island

3.1.2 Solar Energy and Surface Metrological Data of Tullu Gudo Island

Tullu Gudo Island averagely receives 5.84 solar hours, 0.58 clearness index, and 18.92°C temperatures, daily on average. The Solar data and average monthly Solar irradiation of this island for 30-year Meteorological and Solar Monthly & Annual Climatology's (January 1984 - December 2013) were collected from NASA as shown in Table 3.1.

Table 3. 1 Average monthly solar insulation, temperature and clearness index

Parameter	Jan	Feb	Mar	Apr	My	Jun	Jul	Aug	Sep	Oct	Nov	Dc
Insulation (kWh/m^2)	6.02	6.41	6.35	6.04	5.95	5.42	4.83	5.02	5.64	6.04	6.25	6.1
Clearness index	0.65	0.64	0.61	0.57	0.57	0.53	0.47	0.48	0.53	0.6	0.66	0.7
Temp. (°C)	19	20.4	21.3	20.9	20.5	19	17.5	17.4	18	17.7	17.8	18

3.2 Load and Energy Demand Estimation for Tullu Gudo Island

PV systems convert solar energy into electricity. In rural areas without electricity grid access, standalone PV systems are an alternative energy generation option. The generated electricity can be instantaneously consumed or stored (e.g. in batteries) to be consumed at night. When planning a stand-alone system, the most important task is to match energy supply and demand. This can be a challenging task, mainly when considering the fluctuation of solar insolation in the winter rain season. Furthermore, the daily demand of such a facility is not always constant throughout the year. A crucial task in solar stand-alone systems planning is to analyses the energy demand [41].

3.2.1 Load Forecasting for Tullu Gudo Island

The DC load consumption is relatively low in islanding areas. For load flow calculations, the household appliances modeled as loads, which draw direct current from the DC distribution network [42].

In order to forecast the loads for the DC house, it is important to consider the demand of the people living in Tullu Gudo Island. Due to covid_19, I did not want to the area in order to collect the data. Therefore, I forecast the load by estimation. The selection strategy is shown in Table 3.2 below.

Table 3. 2 Load selection strategies with their required ratings [10]

Location and types of loads	Quantity (#)	Rating (W)	P (W) Total	Hrs/day	Hrs/d	Voltage (V)
Living + Dining Room						
Lighting (LED)	3	9	27	18:00 -22:00	4	24
Socket (TV)	1	56	56	11:00 – 14:00 19:00 – 22:00	6	24
DC fan	1	24	24	12:00 – 14:00	2	120
Laptop charger	2	50	100	11:00 – 14:00 19:00 – 22:00	6	19.5
Mobile charger	2	5	10	12:00 – 13:00 19:00 – 21:00	3	5
Refrigerator	1	72	72	Full day	24	120
Water Purifier	1	11	11	0:00 – 4:00	4	120
Coffee maker	1	150	150	12:00 –13:00	1	120
Bed Room x3						
Lighting (LED)	2	7	42	20:00 –22:00	2	24
Mobile charger	1	5	15	20:00 –22:00	2	5
Kitchen						
E-mitad (25A)	1	3000	3000	9:00 – 11:00	1	120
Stove(16A)	1	1000	1000	6:00 – 7:00 11:00 –13:00	4	120

				18:00 – 19:00		
Lighting (LED)	2	9	18	5:00 – 7:00 18:00 –20:00	4	24
Wash/Restroom						
Lighting (LED)	2	7	14	5:00 – 6:00 19:00 –20:00	2	24
Laptop charger	1	50	50	12:00 –13:00	1	19.5
Mobile charger	1	5	5	12:00 -13:00	1	5
Corridors/Verandah						
Lighting (LED)	2	7	14	18:00 -22:00	4	24
Washing machine	1	180	180	14:00 –16:00		120
Total Power (W)			4,800			

From Table 3.2 for installation and design purpose, all resistive and rotating machine loads are considered as 120V appliance and all electronic loads except mobile charger and laptop charger are considered as 24V appliance. Since the devices have their own voltage and DC –DC converters can be match the voltage, we can consider all loads as 120V appliances. Based on their construction and operation we can classify these loads:

Resistive loads: Stoves, E-mitad, DC Fan, Refrigerator, Water purifier, Coffee machine and LEDs.

Rotating machine: Washing machine.

Electronics loads: Laptop charger, TV, and Phone charger.

Table 3. 3 Required energy with their power rating

Hours per day	Load demands	Energy in *Wh*
0:00 – 1:00	Refrigerator, Water purifier	83
1:00 – 2:00	Refrigerator, Water purifier	83
2:00 – 3:00	Refrigerator, Water purifier	83
3:00 – 4:00	Refrigerator, Water purifier	83
4:00 – 5:00	Refrigerator	72
5:00 – 6:00	Refrigerator, LED (9Wx2), LED (7Wx2)	104
6:00 – 7:00	Refrigerator, Stove, LED (9Wx2)	1,090
7:00 – 8:00	Refrigerator	72
8:00 – 9:00	Refrigerator	72
9:00 – 10:00	Refrigerator, E-mitad	3,072
10:00 – 11:00	Refrigerator, E-mitad	3,072
11:00- 12:00	Refrigerator, Stove, TV	1,128
12:00 – 13:00	Refrigerator, Coffee maker, TV, Stove, DC fan, (Mobile and laptop) charger (x3)	1,467
13:00 – 14:00	Refrigerator, TV, DC fan, (Mobile and laptop) charger (x2)	262
14:00 – 15:00	Refrigerator, (mobile and laptop) charger (x2), Washing machine	362
15:00 – 16:00	Refrigerator, Washing machine	252
16:00 – 17:00	Refrigerator	72
17:00 – 18:00	Refrigerator	72
18:00 – 19:00	Refrigerator, Stove, LED (9Wx5), LED (7Wx2)	1131
19:00 – 20:00	Refrigerator, TV, LED (9Wx5), mobile and laptop charger (x3), LED (7Wx4)	366
20:00 – 21:00	Refrigerator, TV, LED (9Wx3), LED (7Wx3), Mobile and laptop charger(x5)	451
21:00 – 22:00	Refrigerator, TV, LED (9Wx3), LED (7Wx3)	176
22:00 – 23:00	Refrigerator	72

23:00 – 0:00	Refrigerator	72
	Total energy	14,242

In general, Tullu Gudo Island has more than 900 Zay peoples and the houses are widely dispersed. However, on some areas around five to ten houses are located near to each other. Each DC house in the village needs 4,800W peak power as discussed in Table 3.2 and one (1) for sample DC house considered for this thesis. The minimum DC voltage supplied to the DC bus is 130 Vdc.

3.2.1.1 Load Modeling for DC Home Appliance

A load model in this thesis is a mathematical representation of the relationship between voltage and current or power and voltage. The detailed power consumption of the home appliances is analyzed and the load profiles generated by taking different utilization modes of the devices in to account. In general, load model for the above-classified appliances are summarized as shown in Table 3.4.

Table 3. 4 Load modeling for DC home system [25]

Types of Loads		Model	Parameter
Resistive Loads	Heating Lighting	$R = R_o$ $R = R_1 + R_o$	R_o – from measurement R_1 – from measurement R_o – from rated power
Rotating Loads	Induction machine Universal machine	$R = R_o$ – for VSD $R = \frac{U^2}{P_o}$ for SMPS $I = Y_o U + I_o$	P_o – from measurement Y_o & I_o –from measurement
Electronic Loads	SMPS Lighting	$R = \frac{U^2}{P_o}$ $R = \frac{U}{I_o}$	P_o – from measurement I_o – from measurement

Since the household loads varies continuously throughout the day, the loads can't be represented directly in MATLAB/Simulink software as a Simscape power system lacks a formal block for a varying resistive load for evaluating the loads profiles. These variable load blocks designed as controlled current source and these model blocks accept Ro for heating loads, Po for SMPS and Io for electronic lighting loads from the load profile generator.

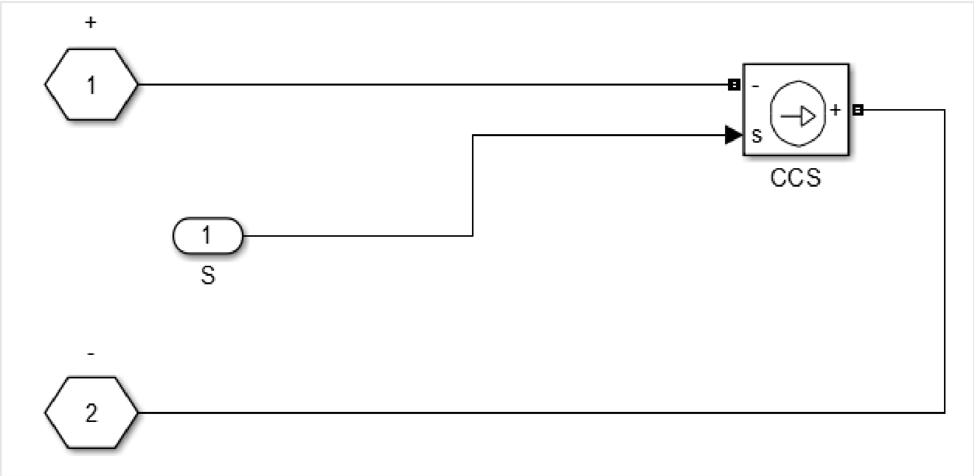

Figure 3. 2 Electronic lighting load models

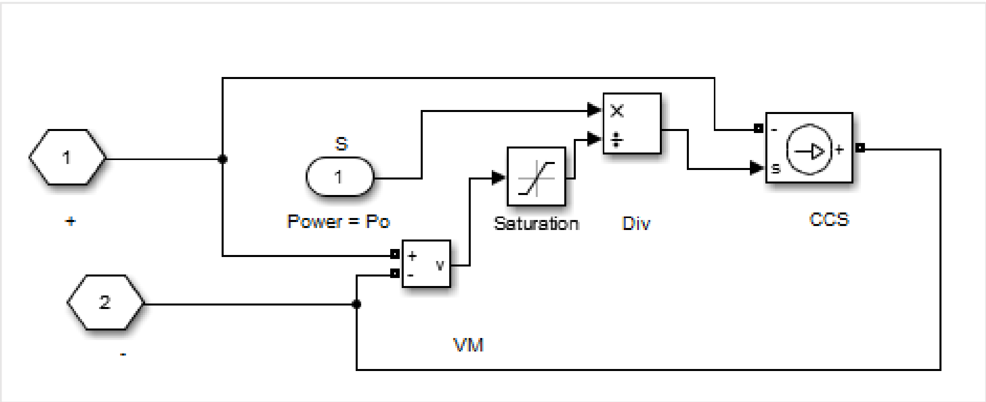

Figure 3. 3 SMPS load model

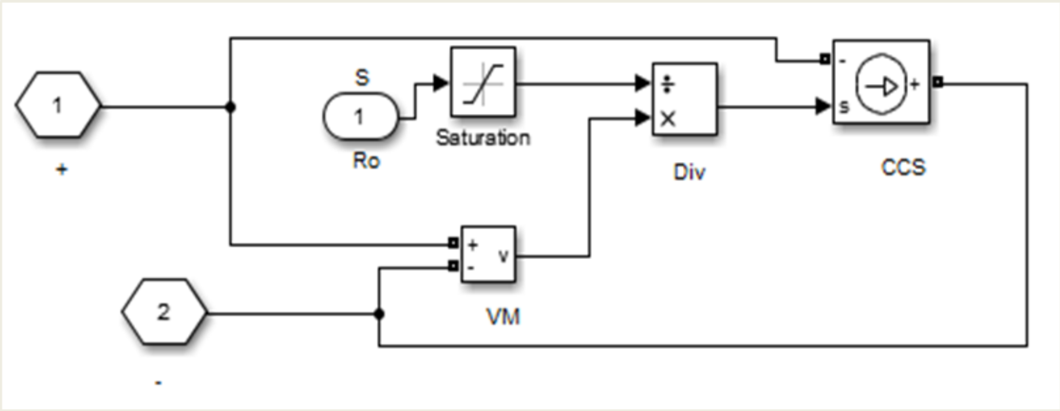

Figure 3. 4 Resistive load models

These load profiles are generated for the total loads using MATLAB software command program in Appendix (A) selected loads (resistive, rotating, and electronic loads). The software command accepts power consumption of appliances and their daily switching times and this program displays a graph of the variation of electrical load in watt versus time in hour.

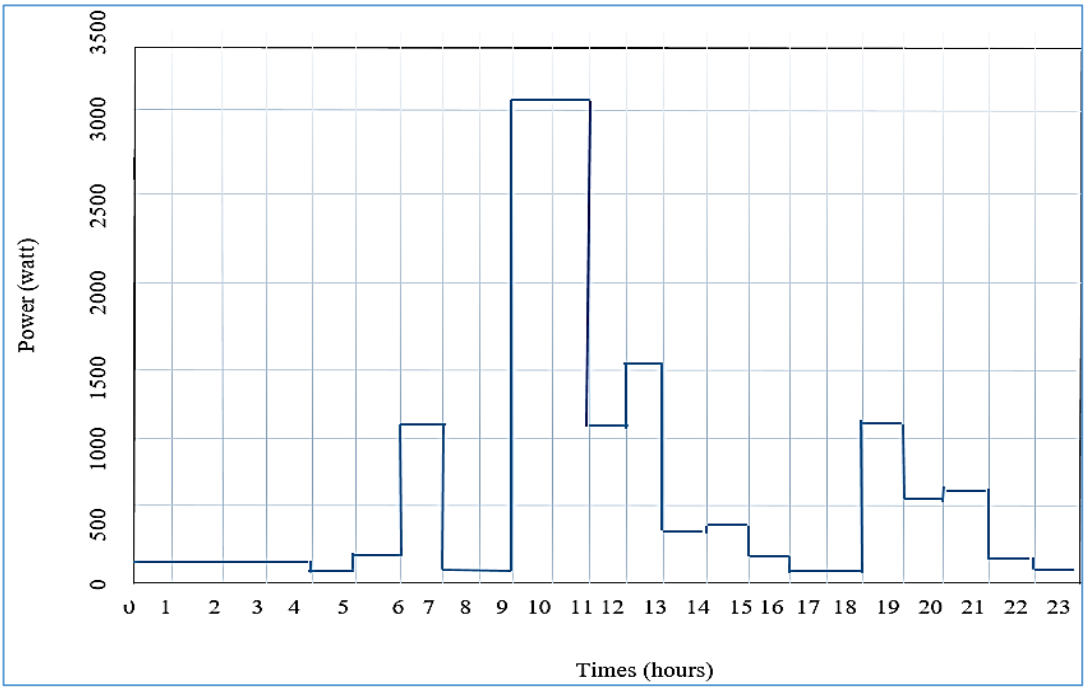

Figure 3. 5 Total loads characteristics of sampled household profile

The total household profile shows a maximum peak load of 3072W during times between 9:00 – 11:00hrs.

From total loads characteristics, it is also possible to determine some important parameters like maximum demand, daily average load and load factor.

$$\text{Maximum Demand} = \text{Daily Peak Load} = 3072\text{W}$$

$$\text{Average Load} = \frac{\text{Daily Energy in Wh}}{24\text{ hours}} = \frac{14,242\text{Wh}}{24\text{hrs}} = 593.42\text{W}$$

$$\text{Load Factor} = \frac{\text{Average Load}}{\text{Maximum Demand}} = \frac{593.42}{3072} = 0.1932$$

3.3 Design and Modeling of DC Home System

The daily peak power demand as discussed in Table 3.1 for this thesis 4.788kW stand-alone DC micro-grid system for DC home is required. This DC home system consists of a DC power supply, energy storage, DC loads and a power electronic interface to stand-alone DC micro-grid energy system. The proposed stand-alone DC micro-grid system supplies power lighting, some means of cooking, food storage, laptop charging, TV and the like for the sampled house. The distribution system is DC supplying DC loads.

The main renewable energy is PV and ES that controlled through DC-DC converters. Particularly, the photovoltaic arrays by a boost converter, the energy storages by a bidirectional converter. As stipulated in the introduction, multiple renewable sources used to generate power for the DC house as well as the system intended to power rural households must be cost effective; therefore, only solar energy system retained. Therefore, this thesis only focuses on solar power generation as the source of power for the stand-alone DC for DC homes as shown in Figure 2.7.

3.3.1 Photovoltaic Design and Modeling

3.3.1.1 Mathematical Modeling of Photovoltaic Cells

Photovoltaic cell are devices that transform the sun irradiance into DC current, as discussed in Table 2.2. In Figure 3.6, a simplified equivalent circuit model of the PV presented. The output current of a PV module obtained from the Equation (3.1).

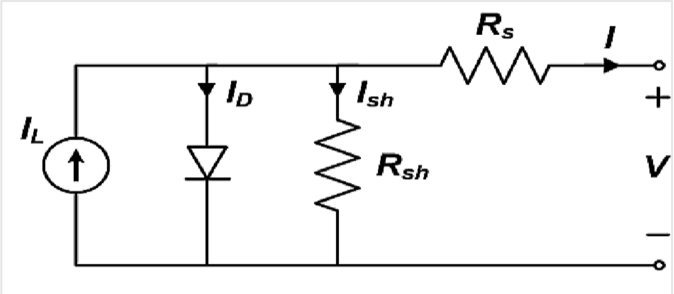

Figure 3. 6 Equivalent circuit models for a PV [43]

In practical model of single solar cell as shown in Figure 3.6, R_s represents series resistance of PN junction cell and R_{sh} represents shunt resistance, which is inversely in relation with leakage current to the ground. Series resistor has great impact on the I-V characteristic of solar cell. I_D and I_{sh} are diode current and shunt leakage current where output terminal current I is evaluated by applying KCL in equivalent circuit of solar cell [43].

$$I = I_{ph} - I_D - I_{sh} \tag{3.1}$$

Photon current is generating on absorption of solar radiation by solar cell hence photocurrent value directly related to variation in solar irradiance and temperature and that is:

$$I_{ph} = \left(I_{sc} + K_i \Delta T\right)\frac{G}{G_r} \tag{3.2}$$

$$I_D = I_O\left[\exp\left(\frac{q\left(V + IRs\right)}{AKT}\right) - 1\right] \tag{3.3}$$

$$I_O = I_{rs}\left(\frac{T}{T_{ref}}\right)^3 \exp\left[\left(\frac{qE_{go}}{AK}\right)\left(\frac{\Delta T}{T_{ref}T}\right)\right] \tag{3.4}$$

$$\text{But, } \frac{\Delta T}{Tref} = \frac{1}{Tref} - \frac{1}{T}$$

From Equation (3.3) & (3.4) $I_D = I_{rs}\left(\frac{T}{T_{ref}}\right)^3 \exp\left[\left(\frac{qEg_o}{AK}\right)\left(\frac{\Delta T}{T_{ref}T}\right)\right]\left[\exp\left(\frac{q\left(V + IR_s\right)}{AKT}\right) - 1\right]$

$$\text{But, } I_{rs} = \frac{I_{sc}}{\exp\left[\left(\frac{qV_{oc}}{AKN_sT}\right) - 1\right]}$$

$$I_{sh} = \frac{V + IR_s}{R_{sh}} \tag{3.5}$$

$$I = I_{ph} - I_o \left[\exp\left(\frac{q\left(V + IR_s\right)}{AKN_s T} \right) - 1 \right] - I_{sh} \tag{3.6}$$

Where:

I_o – Saturation current (A)

I – photovoltaic current (A)

I_{rs} – Reverse saturation current (A)

T – operating temperature (K)

T_{ref} – Nominal temperature (K) = 298

V – terminal voltage of diode (V)

G – Solar irradiation (w/m^2)

K – Boltzmann's constant (J/K) = 1.38*10 $^{-23}$

q – Electron charge (C) = 1.6 *10 $^{-19}$

V_{oc} – open circuit voltage (V)

A – Ideality factor of the diode = 1.3

I_{ph} – photon current (A)

I_{sc} – Short circuit current (A)

N_s – total series number of cells

E_{go} – Band gap energy of the semiconductor (eV) = 1.1

ΔT – The difference of operating temperature and nominal temperature (T $-T_{ref}$) in (K)

3.3.1.2 Photovoltaic Specification of the Selected Modules

For the PV array, the Kyocera solar KC200GT's model from BP solar manufacturer has been chosen. The parameters of the PV array are shown in Table 3.5.

Table 3. 5 Manufacturer data sheet of PV module (KC200GT) at STC [41]

Parameters	Values
Maximum Power ($P_{\max}$)	200.143W
Voltage at $P_{\max}$ ($V_{\max}$)	26.3V
Current at $P_{\max}$ (I_{mp})	7.61A
Short-circuit current (I_{sc})	8.21A
Open-circuit voltage (V_{oc})	32.9V
Number of cells in series	54
Temperature coefficient of I_{sc} (K_I)	0.0032A/K
Temperature coefficient of V_{oc} (K_V)	-0.123V/K

3.3.1.3 Modeling of Solar Module and Solar Array

Since a typical PV cell produces less than 3.5 W at 0.6V approximately, then high power can achieve by connecting many solar cells in series-parallel configuration [43]. This configuration can be setup by connecting PV module in series and parallel connections and this group of several PV modules assembled in a PV tray is called as solar array. Configuration of PV arrays depends on required rated voltage and current of a power plant.

$$I = N_p\left(I_{sc} + K_i \Delta T\right)\frac{G}{G_r} - N_p I_{rs}\left(\frac{T}{T_{ref}}\right)^3 \exp\left[\left(\frac{qEg_o}{AK}\right)\left(\frac{\Delta T}{T_{ref}T}\right)\right]\left[\exp\left(\frac{q\left(V + IR_s\right)}{AKN_sT}\right) - 1\right] - \frac{N_pV + N_sIR_s}{N_pR_{sh}} \tag{3.7}$$

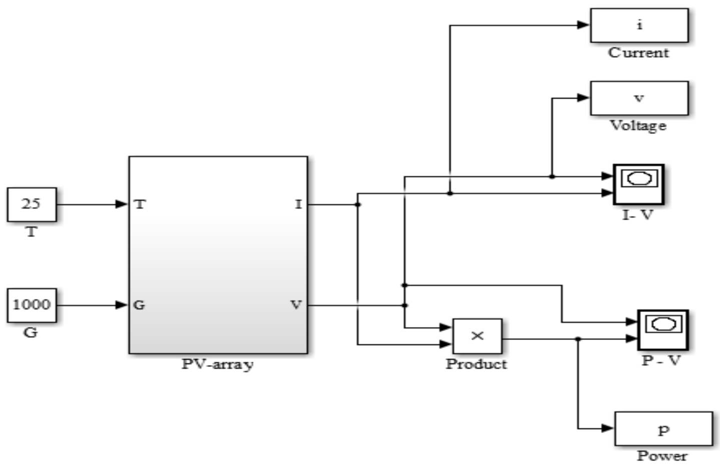

Figure 3. 7 Simulink model of selected PV array

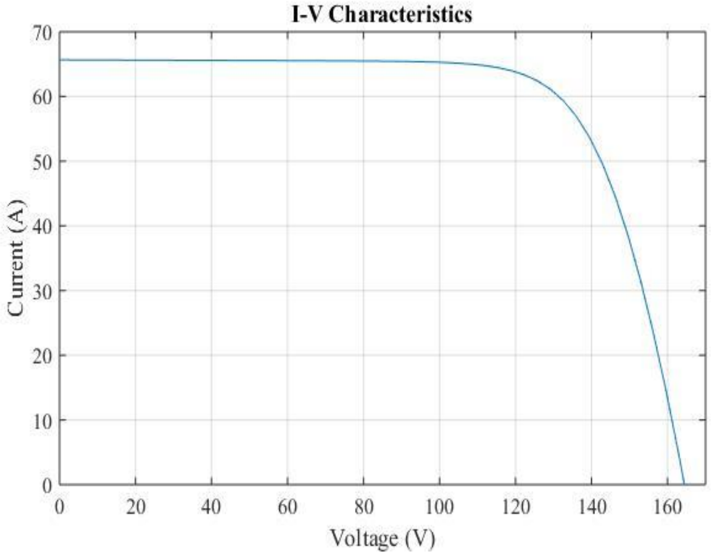

Figure 3. 8 I - V characteristics of selected PV array

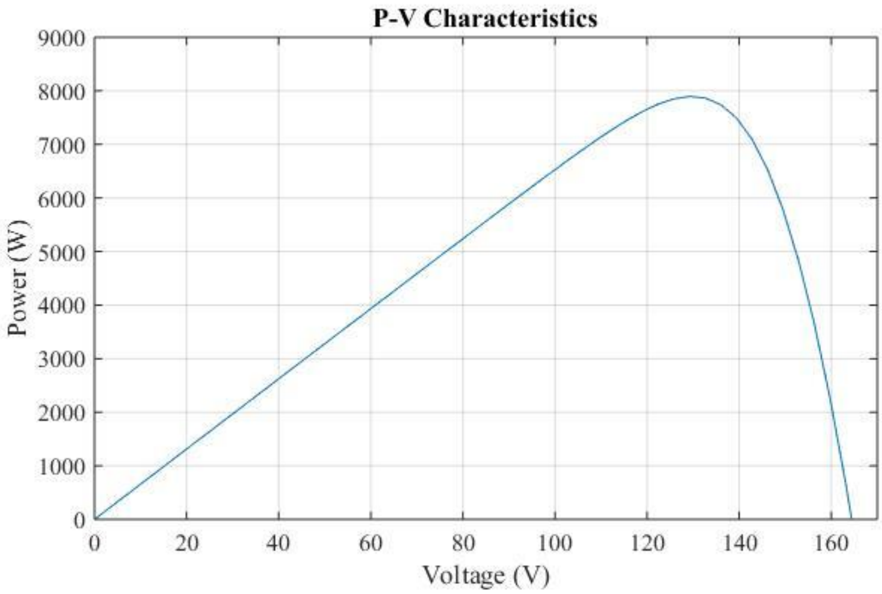

Figure 3. 9 P-V characteristics of selected PV array

Where:

N_p – Number of module connected in parallel =8

N_s – Number of string connected in series = 5

3.3.1.4 PV Modules/Array Calculation for Study Area

At this stage, the number of modules that needed to supply a load demand of 4.8kW for the sample of DC – Home system in the Island of Tullu Gudo, Ethiopia determined. To meet the load demand defined in Table 3.2, the renewable energy source (PV-arrays) with the storage devices must size properly so that efficient power utilization achieved. Additionally, the adequate sizing of PV array is also important to prolong the life of the system components, house appliances, and battery bank. PV array sizing based on the lowest solar insolation month (critical month) of the study area. From the data in Table 3.1, it is clear that the lowest insolation month in Tullu Gudo Island is July when the average insolation is 4.83kWh/m^2.

Kyocera solar KC200GT solar module is selected which produces 200W at 1kW/m^2 and 25ºC at STC (Table 3.5). Using the formulas in Equation (3.7), the power generated by the photovoltaic module is computed. These energy demand calculations take into consideration the energy required to charge the battery bank.

PV Modules and array sizing:

The total system efficiency (η_t) = 0.60

Selected PV module max power voltage (V_m) = 26.3V

Selected PV module guaranteed power output at STC = 200W

$$\text{Peak Sun Hours}\left(\text{PSH}\right)\text{ at design tilt for design month} = \frac{\text{Minimum Monthly Solar Insulation}\left(G_{min}\right)}{\text{Maximum Daily Solar Insulation}\left(G_{max}\right)}$$

$$= \frac{4.83(\frac{kWh}{m^2 / day})}{1(\frac{kW}{m^2})} = 4.83hr / day$$

G_{max} : - the average maximum solar radiation of the site for one day (kW/m^2)

Total number of modules

$$N_{R\text{-}M} = \frac{P_{pv}}{P_m} \tag{3.8}$$

$$P_{pv} = \frac{P_d}{\eta_t} = \frac{4.801kW}{0.6} = 8.001kW$$

Since there is a loss in all components of PV system, efficiency should be considered to get the desired power.

Therefore, the total number of PV required modules ($N_{R\text{-}M}$) are:

$$N_{R\text{-}M} = \frac{8001W}{200.143W} = 39.977 \approx 40 \text{ Where,}$$

Number of PV modules connected in series

$$N_{M\text{-}S} = \frac{V_{dc}}{V_m} \tag{3.9}$$

$$N_{M\text{-}S} = \frac{120V}{26V} = 4.615 \approx 5\text{, but } 5 \times 26 = 130V$$

So, since the total numbers of required modules are 40 and number of modules connected in series are 5, the total number of strings connected in parallel will be 8. The connection diagram is shown in Figure 3.10.

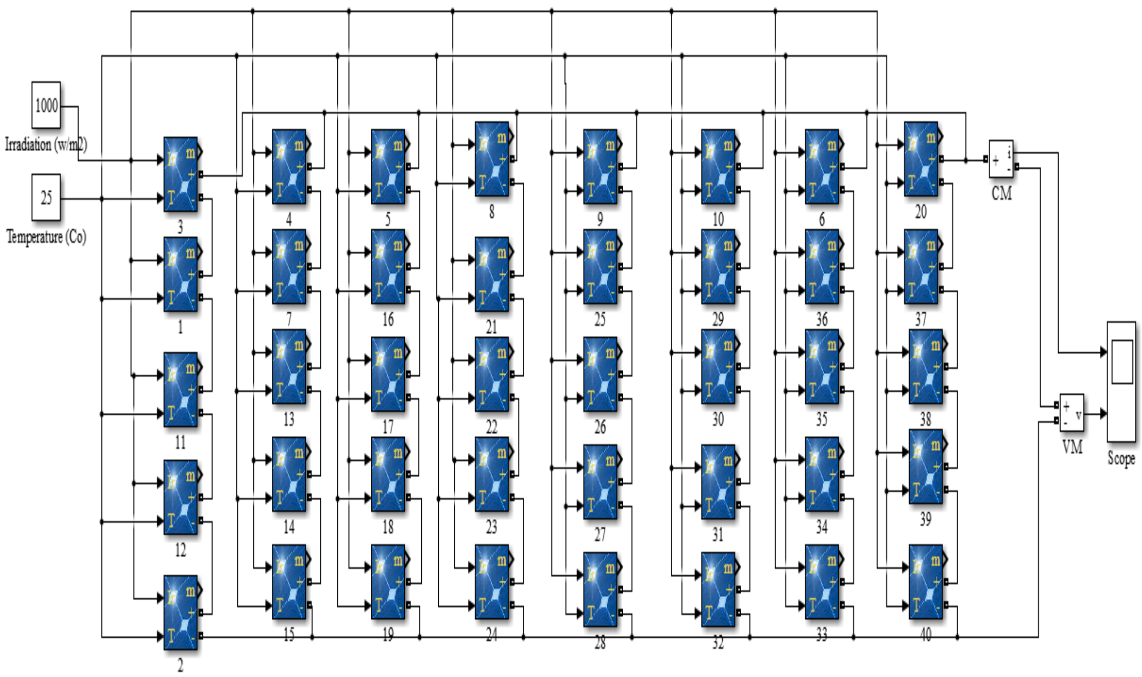

Figure 3. 10 Connection diagram of series parallel of required PV modules

Where: N_{M-S} number of modules/arrays connected in series

P_{pv} : - output power of required PV modules

P_m : - output power of individual module

η_t : - total system efficiency

P_d : - demand power

Series modules/array

V_{dc} : - DC bus Voltage (V)

V_m : - Module voltage (V)

3.3.1.5 Charge Control Sizing

The battery charge controller must comply with the systems voltage (V). The PV input should refer to the PV modules short-circuit current. According to standard practice, the sizing of solar charge controller is to take the short-circuit current (I_{sc}) of the PV array and multiply it by safety factors (C_F) due to losses, accumulation of dust on the module, to increase the system efficiency is around 1.3. The rated load output of the charge controller needs to comply with the sum of loads connected to the charge controller. Therefore, the maximum array to controller current estimated as:

$$I_{Controller} = N_{M\text{-}S} \times I_{sc} \times C_F \tag{3.10}$$

$I_{controller} = 8 \times 8.21 \times 1.3 = 85.384A$. The standard value of charge controller ratings are 80A, which is less than the desired value, and 100A, which is greater than the desired value. When we compared these charge controllers, the former has less safe and less cost and the later has safer and costive. However, the generated current from PV array is 66.7A, which is less than 80A. Therefore, it is possible to choose 80A charge controller that is cost effective.

3.3.1.6 Design and Modeling of DC – DC Converter

The advantage of using DC-DC converter is two folds: First is the efficiency. In ideal condition, not all the elements in the circuit, such as inductor, capacitor, switch and diode, consume any energy. In practice, the efficiency of DC-DC converter can exceed 90%, which is very high for power transformation [44]. The other advantage is the ease to control and integrate. The voltage transformation in DC/DC converter has achieved by changing the duty cycle of the pulse train, which called PWM (pulse width modulation). The power needed for pulse train is very small and neglected. Moreover, the pulse train can be easily constructed [44].

DC - DC Buck boost convertor design: Buck boost convertor coupled with maximum power point tracking implemented to make constant output voltage from the PV panel. The buck–boost converter is a type of DC-DC converter that has an output voltage magnitude that is either greater than or less than the input voltage magnitude. The equivalent circuit of buck boosts convertor as shown in Figure 3.11.

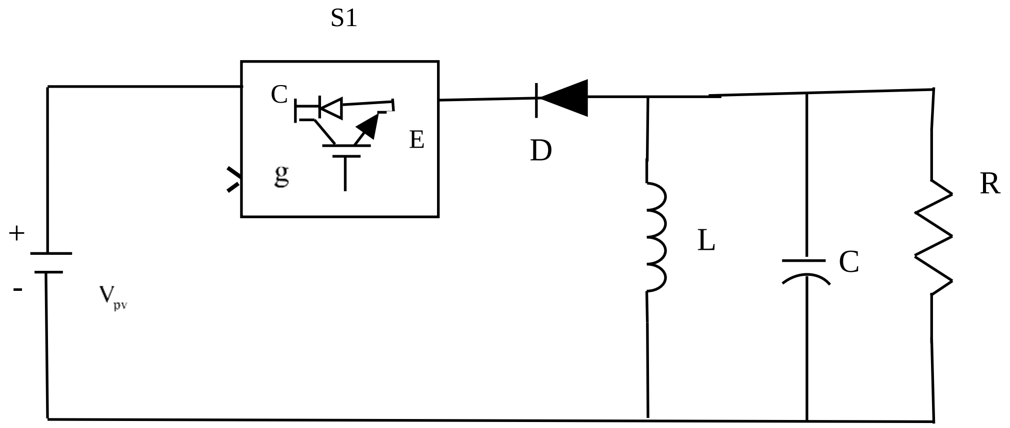

Figure 3. 11 DC – DC buck-boost converter circuit diagram

$$V_{bus} = \frac{D}{1-D} V_{pv} \tag{3.11}$$

$$V_{bus} = 130V, \; V_{pv} = 120V$$

Where V_{bus} : - is output value of convertor voltage

V_{pv} : - is output value of PV system

D: - is the duty cycle. From Equation (3.11)

$$\frac{D}{1-D} = \frac{V_{bus}}{V_{pv}} = \frac{130V}{120V} \text{ From this D = 0.52.}$$

Therefore, the duty ratio (D) of the converter is varies between 0.48 and 0.52.

Resistor (R) design:

$$R = \frac{V_{bus}{}^2}{P_{Load}} \tag{3.12}$$

As seen from total loads characteristics of household profile, the peak and the minimum, load is 3.072kW and 72W respectively and the corresponding load resistances for the buck boost convertor becomes:

$$R_{min} = \frac{V_{bus}{}^2}{P_{max}} = \frac{130^2}{3072} = 5.5\Omega$$

$$R_{max} = \frac{V_{bus}{}^2}{P_{min}} = \frac{130^2}{72} = 234.7\Omega$$

Inductor (L) designing:

$$L = \frac{R_{max}(1-D)}{2f_s} \tag{3.13}$$

$$L = \frac{234.7 \times (1-0.48)}{2 \times 20000} = 3.05mH$$

Capacitor (C) designing:

$$C = \frac{D}{2f_s R_{min}} \tag{3.14}$$

$$C = \frac{0.52}{2 \times 20000 \times 5.5} = 2.4\mu F$$

From the datasheet, a capacitor having magnitude of 300V, $150\mu F$ and an inductor with magnitude of 35mH, 70A that can resist the maximum rated current selected for the buck boost convertor [25].

MPPT Algorithm for Controlling Buck boost Convertor: An MPPT algorithm identifies the maximum power point and forces the solar panel to the MPP by providing suitable duty signal to the converter [45]. According to the theory of maximum power transfer, the power delivered to the load is maximal when the source internal impedance matches the load impedances [22].

Thus, the impedance seen from the converter side needs to match the internal impedance of the solar array. If there is an increment in the power, the perturbation should keep in the same direction and if- the power decreases, then the next perturbation should be in the opposite direction. Therefore, the Flow chart of Perturb and Observe of MPPT as shown in Figure 3.13 used to drive the boost converter interfacing the PV system to the DC micro-grid.

DC – DC Buck Converter Designing and Modeling: A buck converter is a step-down DC-DC converter consisting primarily of inductor and two switches (generally a transistor switch and diode) for controlling inductor. It fluctuates between connection of induction to source voltage to mount up energy in inductor and then discharging the inductor's energy to the load [46] as shown in Figure 3.12.

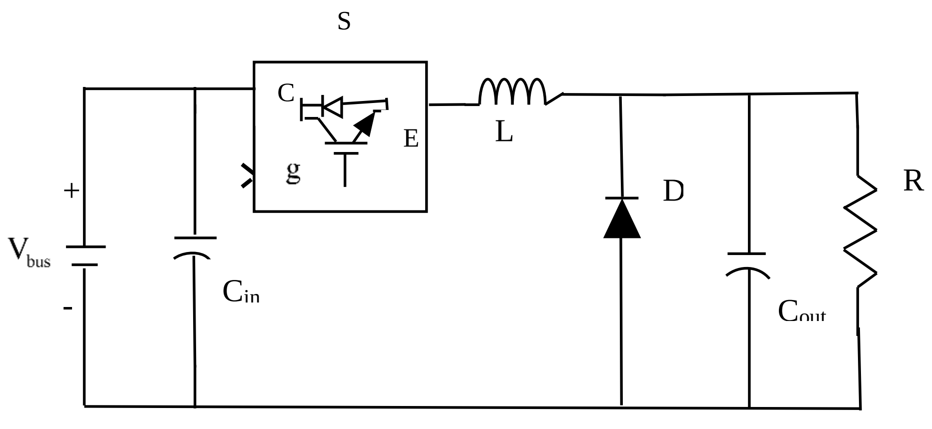

Figure 3. 12 DC – DC buck converter circuit diagram

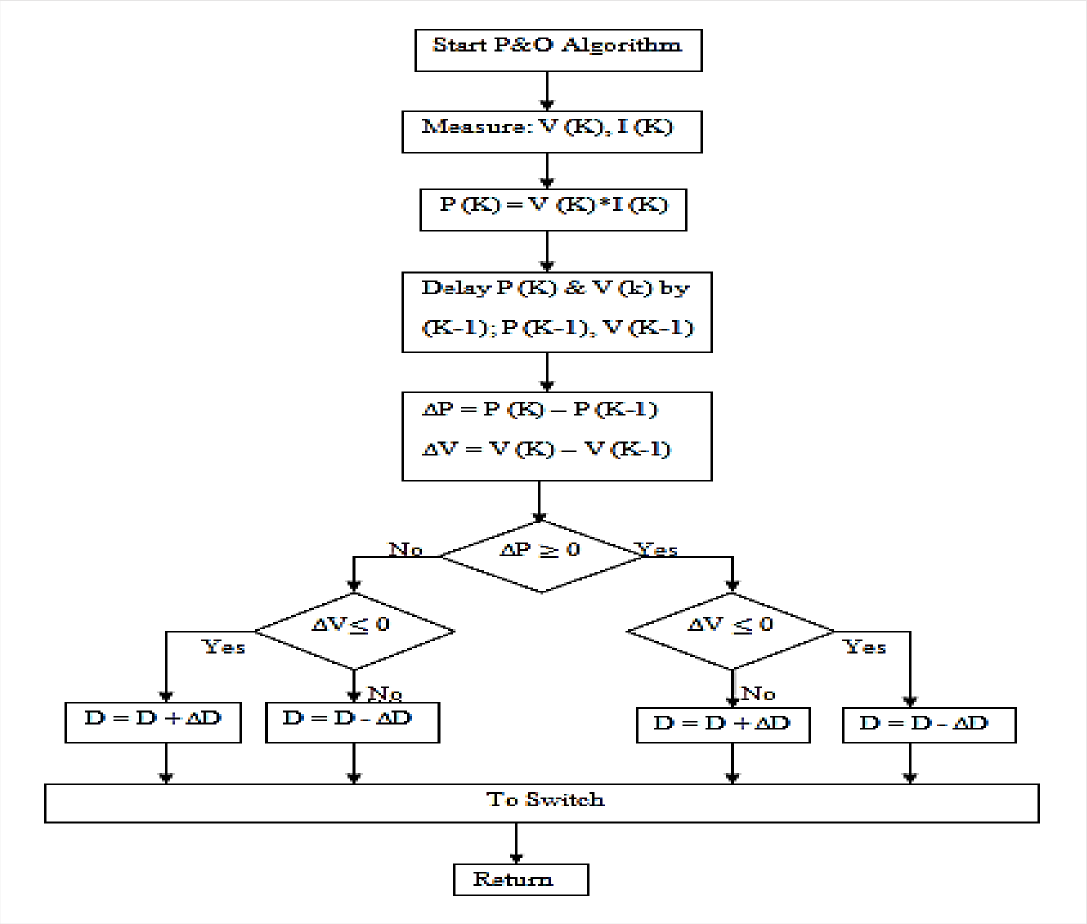

Figure 3. 13 Flow chart of P&O algorithm for buck boost converter

DC – DC Buck Converter Designing:

- When the switch pictured above is closed (i.e., on state), the voltage across the inductor is $V_L = V_{in} - V_o$. The current flowing through inductor linearly rises. The diode does not allow current to flow through it, since it is reverse-biased by voltage.
- When the switch is opened (i.e., off state), diode is forward biased and voltage is $V_L = -V_o$ (neglecting drop across diode) across inductor. The inductor current, which was rising in ON case, now decreases.

Case I DC – DC buck Converter design for 120V (Resistive and Rotating) (4294W)

Inductor Designing: The filter inductor value and its peak current are determined based on the specified maximum inductor current ripple [47].

$$L = \frac{R\left(1-D\right)}{2fs} \tag{3.15}$$

From Table 3.3; P = 4294W, V_o = 130V, V_{in} = 120V

$$R = \frac{V^2}{P} = \frac{130^2}{4294} = 3.94\Omega$$

$$V_o = 120V,\ V_{in} = 130V$$

$$D = \frac{V_o}{V_{in}} = \frac{120}{130} = 0.923$$

$$L = \frac{3.94\left(1-0.923\right)}{2\times 20000} = 7.6\mu F$$

Where, D = duty cycle (%), f_s = switching frequency (Hz), L = inductance (H) R = load resistance (Ω).

Capacitor designing: The function of the capacitor is to filter the inductor current ripple and passing a stable output voltage [47]. It also has to ensure that load steps at the output supported before the regulator is able to react.

$$C = \frac{1-D}{16L\times f_s} \tag{3.16}$$

$$C = \frac{1-0.923}{16\times 7.6\times 10^{-6}\times 20000^2} = 1.583\mu F$$

Case II DC – DC buck Converter design for 24V (Electronic) (207W)

Inductor designing:

$$V_{in} = 130V,\ V_o = 24V$$

$$R = \frac{V^2}{P} = \frac{130^2}{207} = 81.64\Omega$$

$$L = \frac{81.64\times(1-0.185)}{2\times 20000} = 1.664mH$$

Capacitor designing:

$$C = \frac{1-D}{16Lf_s} = \frac{1-0.185}{16\times 1.664\times 10^{-3}\times 20000^2} = 0.0765\mu F$$

Case III DC – DC buck converter design for 19.5V (Laptop charger) (270W)

Inductor designing:

$$V_{in} = 130V\,,\ V_o = 19.5V$$

$$D = \frac{V_o}{V_{in}} = \frac{19.5}{130} = 0.15$$

$$R = \frac{V^2}{P} = \frac{130^2}{270} = 62.6\Omega$$

$$L = \frac{R(1-D)}{2f_s} = \frac{62.6\times(1-0.15)}{2\times 20000} = 1.33mH$$

Capacitor designing:

$$C = \frac{1-D}{16L\times fs} = \frac{1-0.15}{16\times 1.33\times 10^{-3}\times 20000^2} = 0.01\mu F$$

Case IV DC – DC buck converter design for 5V (Mobile charger) (30W)

$$V_{in} = 130V \quad V_o = 5V \quad P = 30W$$

$$D = \frac{Vo}{Vin} = \frac{5}{130} = 0.0385$$

$$R = \frac{V^2}{P} = \frac{130^2}{30} = 563.3\Omega$$

Inductor designing:

$$L = \frac{R(1-D)}{2f_s} = \frac{563.3\times(1-0.0385)}{2\times 20000} = 13.54mH$$

Capacitor designing:

$$C = \frac{1-D}{16L\times f_s} = \frac{1-0.0385}{16\times 13.54\times 10^{-3}\times 20000^2} = 0.0111\mu F$$

Table 3. 6 Summary of parameters for different operating voltage

Parameter	For 120V	For 24V	For 19.5V	For 5V
Duty cycle	0.923	0.185	0.15	0.0385
Inductor	7.6mH	1.664mH	1.33mH	13.54mH
Capacitor	1.583µF	0.0765µF	0.01µF	0.0111µF
Resistance	3.94Ω	81.64Ω	62.6Ω	563.3Ω

From the datasheet, a capacitor having magnitude of 300V, 5µF and an inductor with magnitude of 25mH, 70A selected for the buck DC-DC convertor [48].

Buck Convertor Voltage Control: Buck convertor is connected to the load is used to provide constant output voltage of 5V, 19.5V, 24V and 120V DC. However, since there is a continuous variation of load throughout the day, the load voltage may not be constant. This is the case especially when high power consuming appliances like stoves and E-mitad are connected and disconnected from the system. To maintain constant voltage, buck convertor coupled with PID controller is used. Most commercial controllers provide full PID (also called three-term) control action. Including a term that is a function of the derivative of the error with high-order plants, provide a stable control solution [49].

Proportional plus Integral plus Derivative (PID) control action is expressed as:

$$PID(t) = K_p e(t) + K_i \int e(t)dt + K_d \frac{de(t)}{dt} \quad (3.17)$$

$$PID(s) = e(s) * G_p(s) = e(s)\left[K_p(s) + \frac{K_i(s)}{s} + sK_d(s) \right] \quad (3.18)$$

Equation (3.17) written in time domain and Equation (3.18) written in Laplace's transform. The advantages of the PID controller are controlling the object, which is highly nonlinear and uncertain [25].

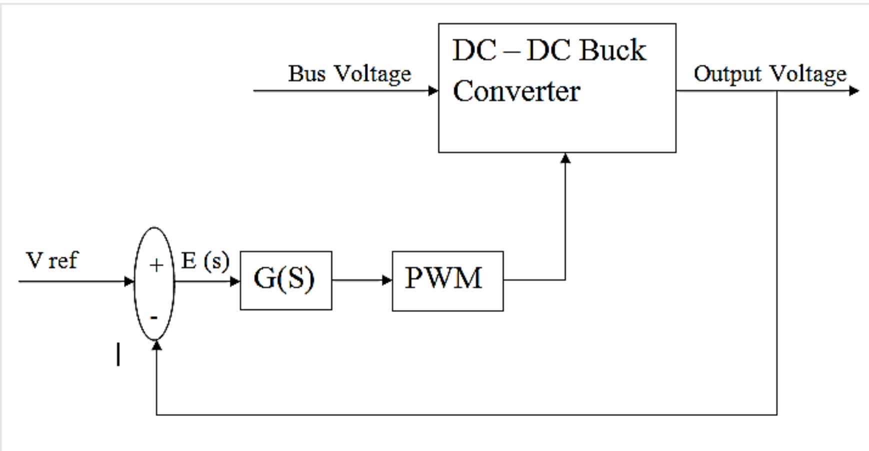

Figure 3. 14 Load voltage (buck convertor) control by using PID controller

The above control uses the output voltage of the convertor as a feedback and compares this output with the fixed reference value. Then, the error has given to the PID controller, which will then produce the corrected modulated voltage signal so that the buck convertor will produce a constant output voltage. The small signal SISO transfer function used to control buck convertor ($G_c(s)$) given by:

$$G_c(s) = \frac{\frac{V_{in}}{LC}}{S^2 + \frac{S}{RC} + \frac{1}{LC}} \quad (3.19)$$

Where V_{in} is the input voltage for the buck convertor and R, L, and C are the resistance, inductance and capacitance for the buck convertor respectively. Therefore, the system transfers functions G(s) is: -

$$G(s) = \frac{\frac{V_{in}}{LC} G_p(s)}{S^2 + \frac{1}{RC} S + \frac{1}{LC} + \frac{V_{in}}{LC} G_p(s)} \quad (3.20)$$

$$G(s) = \frac{\frac{V_{in}}{LC}\left(K_d S^2 + K_p S + K_i\right)}{S^3 + \left(\frac{1}{RC} + \frac{V_{in}}{LC} K_d\right) S^2 + \left(\frac{1}{LC} + \frac{V_{in}}{LC} K_p\right) S + K_i} \quad (3.21)$$

Using MATLAB program, the PID controller parameters are determined and given in table

Table 3. 7 PID control parameters for buck convertor

Controller parameters	Tuned (120V)	Tuned (24V)	Tuned (19.5V)	Tuned (5V)
K_p	0.1333	0.20024	1.7737	0.28924
K_i	10,659.7825	9662.3547	843,925.4818	16,007.3365
K_d	4.1672×10^{-7}	1.0375×10^{-6}	9.32×10^{-7}	1.3066×10^{-6}
Performance and Robustness	Tuned	Tuned	Tuned	Tuned
Rise time (second)	4.48×10^{-7}	1.94×10^{-6}	2.19×10^{-7}	1.6×10^{-6}
Settling time (second)	1.6×10^{-5}	3.02×10^{-6}	2.45×10^{-6}	6.81×10^{-6}
Overshoot (%)	1.4	1.72	3.96	2.25

By using these controller parameters, it is also possible to determine the system transfer function of buck converter.

G(s) = transfer function of plant * transfer function of PID controller

$$G(s) = \frac{433.4S^2 + 1.3863\times10^8 S + 1.11\times10^{13}}{S^3 + 107365.5S^2 + 1.466\times10^8 S + 1.11\times10^{13}} \quad (3.22)$$

Where G(s):- represents system transfer function.

3.3.2 Design, Modeling and Control of Energy Storage System

3.3.2.1 Energy Storage System

PV power generation varies with the amount of sunlight shining on the panels at an instance, which results in lack of power generation during nighttime and cloudy weather. At such times, energy storage used to control the voltage level and the power flow through a bidirectional converter, in order to provide smooth power to the DC loads continuously.

Some characteristic parameters of the battery, which apply to the DC micro grid, are the following:

- Power Capacity: - is the maximum instantaneous output power that an ES device can provide, usually measured in kilowatts (kW) or megawatts (MW).
- Energy Capacity: - the amount of electrical energy the device can store usually measured in kilowatt-hours (kWh) or megawatt-hours (MWh).
- Response Time: - is the length of time it takes the storage device to start releasing power from the moment it activated.
- Efficiency: - indicates the quantity of electricity, which recovered as a percentage of the electricity used to charge the device.
- Round-Trip Efficiency: - indicates the quantity of electricity, which recovered as a percentage of the electricity used to charge and discharge the device.
- Depth of Discharge (DOD): - is the fraction or percentage of the capacity that has been removed from the fully charged battery.
- State of Charge (SOC): - is the level of charge of an electric battery relative to its capacity.
- Day of Autonomy: - the number of consecutive days a stand-alone system battery bank will meet a defined load without solar energy input. The latitude location of the system is important to determine days of autonomy.

3.3.2.2 Modeling of Energy Storage (Battery) System

Lithium-ion Model: Rechargeable battery is an electro-chemical device that converts electrical energy to chemical energy during charging and converts chemical energy to electrical energy during discharging.

In the aspect of technology, the rechargeable battery improved from lead acid battery to nickel-based battery and from nickel-based battery to lithium-ion (Li-ion) battery. Lithium-ion battery has higher terminal voltage, higher power density and higher energy density compared to the other rechargeable batteries [50]. Nowadays, Li-ion battery is widely adopted in portable electronic devices, such as laptop computers, smart phones and digital cameras.

The storage capacity required for the battery bank depends on the number of days batteries can provide power to the load without recharging. Depth of Discharge (DOD) is the amount of energy drawn from a battery compared to its total storage capacity. For a PV system, two common terms related to DOD are maximum DOD and average daily DOD. Maximum DOD is the maximum amount of charge that drawn out of the battery. It also related to the autonomy capacity required to operate the system loads or given number of days with no generation from PV.

A system designed with very low DOD will have most of the battery energy available to the load but with a tradeoff for longer battery life. The average daily DOD is the amount of energy drawn from battery’s full capacity with the average daily load profile. A system designed for longer autonomy periods (more capacity) will have lower average daily DOD. For this system, DOD of 80% selected, which is typical for isolated PV storage systems.

Accurate battery information such as state-of-charge (SOC), current and voltage are vital for circuit designer to manage the energy consumption of battery-powered system [50]. Moreover, supervision on battery is necessary to avoid battery from overcharged or over-discharged. Therefore, an accurate battery model is vital as a guide in circuit design process to estimate the characteristics of battery.

Table 3. 8 Typical parameters of Lithium-ion battery *[20]*

Characteristics	Lithium-ion
Specific energy (Wh/kg)	150 – 200
Energy density (Wh/L)	200 – 500
Specific power (W/kg)	150 – 315
Nominal cell voltage (V)	3.2 – 3.7
Electrical efficiency (%)	0.99
Self-discharge (%)	0.1 – 0.3
Life time (years)	5 – 15
Life cycle	1000 – 10000 cycles
Range of operating temperature (℃)	-30 - +60

Advantages of Lithium-ion Battery:

- High energy density**:** This is one of the highlighted advantages of lithium-ion battery technology. With the increased density of energy, this battery technology used from smartphones to the high-end electric vehicles.
- Self-discharge**:** Other rechargeable batteries are not good with the rate of self-discharge. Due to the existence of Lithium-ion cells in the battery, the self-discharge rate is quite lower than others battery types. It is around 5% for the first four hours and drops to around 1-2% per month.
- Low maintenance**:** It does not require constant maintenance to continue its flawless performance.
- No requirement for priming**:** Some of the rechargeable cells need to get primed whenever they charged for the very first time but there is apparently no requirement in lithium ion cells and lithium ion battery.
- Availability of variety**:** There are several types of lithium-ion cells, which used accordingly as per the requirement for a particular application.
- Cell voltage**:** The voltage produced by each lithium ion cell is about 3.6 volts. This has many advantages. Being higher than that of the standard nickel cadmium, nickel metal hydride and even standard alkaline cells at around 1.5 volts and lead acid at around 2 volts per cell, the voltage of each lithium-ion cell is higher, requiring less

cells in many battery applications. For smartphones, a single cell is all that needed and this simplifies the power management [51].

Disadvantages of Lithium-ion Battery:

- Protection requirement**:** They are not as rough and tough as some other rechargeable technologies are and one should avoid its overcharging in order to keep protected. They also require a protection circuitry incorporated to ensure the safe operating limits.
- Ageing: One of the major disadvantages of this technology us that it may hurt the life drowning process battery ageing. The ageing of battery solely depends upon the numerous discharge cycles that are completed of this battery before the capacity falls. This can be an issue if they embedded alone in any of the equipment whereas the detachable one can be replaced easily [51].
- Cost: Again, one of the major disadvantages of this technology is the cost. The lithium ion batteries are typically 40% more expensive than nickel cadmium cells.
- Immature technology: Although it used by many but still, it is an undeveloped technology because, it resides in the developing area and a room of improvement still exists.

Applications: Rechargeable battery plays important role in future technology since it is potentially to be applied as energy storage element in green technology applications, such as electric vehicle (EV), portable electronics, but recently they have gained popularity in larger scale applications such as grid tied systems and electric vehicles and photo-voltaic (PV) system. The renewable energy source can be stored in battery packs and thus help to reduce the dependency on fossil fuels [50] [52]. When selecting a battery for residential applications, lifetime, and maintenance should considered. Lithium-ion battery packs have a higher round-trip efficiency than many other alternatives, which can lead to a longer lifetime compared to other battery types such as lead acid.

Battery Circuit Model:

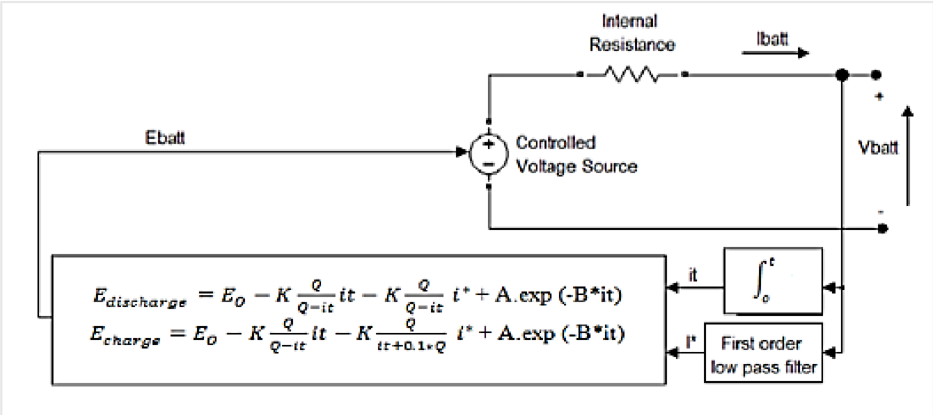

Figure 3. 15 Battery model equivalent circuits

This basic equivalent battery circuit represented by shepherd's equation as [52]:

Charging equation:

$$V_{batt}(t) = E_o - K\frac{Q}{Q-it}it - K\frac{Q}{it+0.1Q}i^* + Ae^{-B\times it} \tag{3.23}$$

Discharging equation:

$$V_{batt}(t) = E_o - K\frac{Q}{Q-it}it - K\frac{Q}{Q-it}i^* + Ae^{-B\times it} \tag{3.24}$$

The voltage at the battery terminal calculated as:

$$V_{batt} = E_{batt} - I_{batt} \times R_{batt} \tag{3.25}$$

But,

$$A = V_{full} - V_{exp}$$

$$B = \frac{2.3}{Q_{exp}}$$

$$K = 0.065*\left[V_{full} - V_{nom} + A\left(e^{-B\times Qnom} - 1\right)\right]*\frac{Q_{full} - Q_{nom}}{Q_{nom}}$$

Where:

E_o – Battery voltage constant (V)

E_{batt} – Internal battery voltage (V)

A – Exponential voltage amplitude constant (V)

Q – battery capacity (Ah)

R – internal resistance (Ω)

it – battery discharge capacity (Ah)

B – Exponential zonetime constant inverse (1/Ah)

i^* - Filtered current through polarization resistance

Battery state of charge

$$SOC(t) = SOC(t-1) + \frac{i(t)\times \Delta t}{Q} \text{ (If Q is in Ah)} \quad (3.26)$$

Or

$$SOC(t) = SOC(t-1) + \frac{P(t)\times \Delta t}{Q} \text{ (If Q is in } Wh\text{)} \quad (3.27).$$

The Simulink battery model available in MATLAB depicted in Figure 3.16:

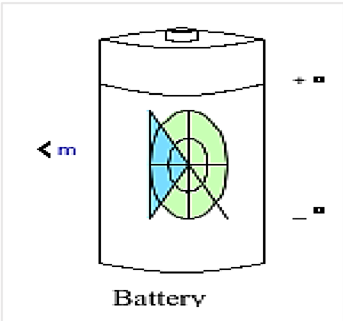

Figure 3. 16 Simulink battery model

The Simulink battery block implements a generic dynamic model parameterized to represent most popular types of rechargeable batteries.

Where m: the current of the battery, input signal and SOC, output signal.

As discussed in the previous section, Lithium-ion battery type is more efficient choice for the standalone PV backup than system.

Battery sizing: Batteries used to store the excess of energy generated by the PV array during sunny and high insolation of periods, and they provide power to the system during nighttime and low insolation of periods.

The battery type recommended for using in solar PV system is deep cycle battery. Deep cycle battery specifically designed for to discharge to low energy level and rapid recharged or cycle charged and discharged day after day for years. The battery should be large enough to store sufficient energy to operate the appliances at night and cloudy days. The required battery capacity for stand-alone PV system depends on load demands and desired autonomy. The autonomy day is the time during which a lonely battery provides power for load requirements, without any solar energy, beginning from a full state of charge [53]. Battery capacity (in Ah) is determined by using the total load (in Ah) required per day and the number of days the system is required to operate without energy generation (days of autonomy or days when there is no sunlight). Days of autonomy are the number of days a battery bank will supply a given load without recharged by a PV array or another source.

Normally, the days of autonomy are determined with experience in the field. Generally recommended values are:

Table 3. 9 Latitudes with associate days of autonomies

Latitude	Days of autonomy (D_A)
0^0 - 30^0	5 – 6
30^0 - 50^0	10 – 12
50^0 - 60^0	15

Since Ethiopia is in the range of 0° to 30°, the recommended days of autonomy are 5 – 6. Another important factor is the maximum depth of discharge of the battery. The depth of discharge refers to how much capacity used from the battery. Most systems designed for regular discharge values between 60 to 80 percent. When the battery is sizing, the following factors taken into consideration:

- Battery Efficiency: - Most batteries have an efficiency of about 85%, Li-ion= 99%+.
- Allowable Depth of Discharge: - The maximum percentage of full rated capacity that can withdraw from a battery known as its Allowable Depth of Discharge. The allowable depth of discharge for Lithium-ion Batteries (Li-ion Batteries) is 80%.
- Days with no sunshine/number of days of autonomy generally expressed as the days of storage in a PV system, autonomy refers to the time a fully charged battery can supply energy to the systems loads when there is no energy supplied by the PV modules. Number of days of autonomy typically ranges from 2 to 6. If the load supplied is not critical, then one autonomy day is commonly used.

Now let us size a battery bank needed to supply 14,242Wh per day to a DC electric load of Tullu Gudo Island. Assume that:

- The DC voltage of the battery bank is 120V.
- The number of autonomy days is 1 - 6 days in Ethiopia.
- The maximum depth of discharge is 65%.
- The selected rechargeable battery is (12V-100Ah) Li-ion.

In order to size the minimum capacity of battery bank, the estimated energy storage is first determined. The obtained energy value divided by the allowable depth of discharge of the battery to give a safe energy storage value of the required battery bank. At this point, the particular battery used was select and using its specifications, the capacity of the entire battery bank in Ampere-hours computed, and subsequently the total number of batteries in the bank computed.

Total energy demand per day (E_D) = 14,242Wh

$$I_c = \frac{E_D}{\eta_{batt} \times DOD \times V_{S\text{-}DC}} \tag{3.28}$$

$$I_c = \frac{14,242\text{Wh}}{0.96 \times 0.65 \times 120\text{V}} = 190\text{Ah}$$

$$B_{B\text{-}C} = I_c \times N_D \tag{3.29}$$

Where: E_D - is energy demand (Wh)

I_c : - is the ampere-hours consumed by the load (Ah)

$V_{S\text{-}DC}$: - is the nominal DC system voltage (V)

$B_{B\text{-}C}$: - is the required battery bank capacity (Ah)

N_D : - are days of autonomy

η_{batt} : - battery efficiency

Finally, the number of batteries in series and parallel branches of the bank are determined and an estimate of the cost of the battery bank (B_{bcost}) is made from the knowledge of the cost of the selected single battery (B_{cost}) for each cases. The number of batteries connected in parallel ($N_{B\text{-}P}$) to reach the Amp hours required by the system calculated as follow [54]:

$$N_{B\text{-}P} = \frac{B_{B\text{-}C}}{B_C} \tag{3.30}$$

Where B_C : - is the capacity of the selected battery (Ah).

While, the number of batteries connected in series ($N_{B\text{-}S}$) to reach the voltage required by the system calculated as follow:

$$N_{B\text{-}S} = \frac{V_{S\text{-}DC}}{V_B} \tag{3.31}$$

$$N_{B\text{-}S} = \frac{130V}{12V} = 10.833 \approx 11$$

Where V_{SDC} is the DC system voltage (V) and V_B is the battery voltage (V).

$$N_{B\text{-}R} = N_{B\text{-}P} \times N_{B\text{-}S} \tag{3.32}$$

Where: - $N_{B\text{-}R}$ is total number of batteries required

Table 3. 10 Summary of the required parameters for battery sizing

N_D	$B_{B\text{-}C}$ (Ah)	$N_{B\text{-}P}$	$N_{B\text{-}R}$	Total Ah required
2	380	3.8 ≈ 4	4x11 = 44	4,400
3	570	5.7 ≈ 6	6x11 = 66	6,600
4	760	7.6 ≈ 8	8x11 = 88	8,800
5	950	9.5 ≈ 10	10x11 = 110	11,000
6	1,140	11.4 ≈ 12	12x11 = 132	13,200

Greater autonomy days are associated with larger and higher cost of the battery banks. However, it drops the average daily depth of charge (DOD), and it provides longer lifetime for battery in this manner.

Bidirectional DC – DC Converter Modeling: A conventional buck-boost converter can manage the power flow in one direction only but power can flow in both the direction in bidirectional converter. Bidirectional DC-DC converters are the device for the purpose of step-up or step-down the voltage level with the capability of flow power either in forward directions or in backward direction. The bidirectional DC-DC converters work as regulator of power flow of the DC bus voltage in both the direction [55]. In the power generation by windmills and solar power systems, output fluctuates because of the changing environment condition. Bidirectional DC-DC converters are useful for switching between energy storage. When the power demand is lower than that provided, the excessive energy will be stored in the batteries, which is called charging mode. Conversely, when the power demand is higher than that provided by the PV system, the energy flows from batteries to the load, which is called discharging mode. This study proposes a bidirectional buck-boost converter to manage the storage and supply of power between photovoltaic power generation systems and batteries. Due to the circuit, structure of a bidirectional converter allows bidirectional power flows, two operation modes can be set for this converter depending on the direction of the power flow: boost and buck modes [56].

The charging/discharging mode defined as that the energy transferred from the DC bus to battery or from battery to DC-bus, since the battery voltage may be higher or lower than the DC-bus voltage during the entire operation as shown in Figure 3.17.

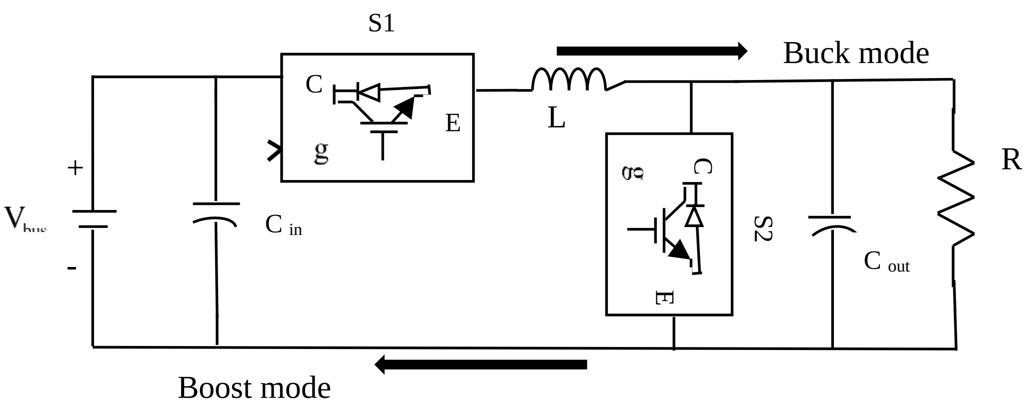

Figure 3. 17 Circuit diagram of universal bi-directional buck-boost convertor

For buck converter:

$$L = \frac{V_{bus} \times (V_{bus} - V_{batt})}{\Delta I_L \times f_s \times V_{batt}} \tag{3.33}$$

$$L = \frac{130 \times (130 - 120)}{11.1 \times 20000 \times 120} = 0.0488\text{mH}$$

$V_{bus} = 130\text{V}$, $V_{batt} = 120\text{V}$, $f_s = 20{,}000\text{Hz}$

$$I_o(\max) = \frac{P_{Load}}{V_{bus}} = \frac{4801\text{W}}{130\text{V}} = 37\text{A}$$

$$\Delta I_L = (0.2 \text{ to } 0.4) \times I_o(\max) = 0.3 * 37\text{A} = 11.1\text{A}$$

$$C_{batt}(\max) = \frac{\Delta I_L}{8 \times f_s \times V_{bus}(ESR)} \tag{3.34}$$

$$V_{bus}(ESR) = ESR \times \Delta I_L = 0.155\Omega \times 11.1\text{A} = 1.72\text{V}$$

$$C_{batt}(\max) = \frac{11.1}{8 \times 20000 \times 1.72} = 40.33\mu\text{F}$$

For boost converter:

$$L = \frac{V_{batt} \times (V_{bus} - V_{batt})}{\Delta I_L \times f_s \times V_{bus}} \tag{3.35}$$

$$L = \frac{120 \times (130 - 120)}{11.2 \times 20000 \times 130} = 0.0416\text{mH}$$

$$\Delta I_L = (0.2 \text{ to } 0.4) \times I_o(\max)$$

$$C_{bus}(\min) = \frac{I_o(\max) \times D}{f_s \times \Delta V_{bus}} \tag{3.36}$$

$$\Delta V_{bus} = 3\% \text{ of bus voltage} = 3.9\text{V}$$

$$D = 1 - \frac{V_{batt}}{V_{bus}}$$

$$D = 1 - \frac{120}{130} = 0.077$$

$$C_{bus}(\min) = \frac{37*0.077}{20000*3.9} = 36.5\mu F$$

From the datasheet C_{batt} = 250μF, 300V, C_{bus} = 50μF, and L = 80mH, 100A is selected for the bidirectional buck boost convertor [57].

Where V_{bus} : - is the desired bus voltage

V_{batt} : - typical battery voltage

ΔI_L : - estimated inductor ripple current

f_s : - minimum switching frequency

A good estimation for inductor ripple is 20% to 40% of output current.

$I_o(\max)$: - maximum output current

Table 3. 11 General working condition of PV and Battery system [58]

Condition	Action
PV Power = Load Battery SOC high	PV Supplies Load No Charging Battery
PV Power = Load Battery SOC low	PV Supplies Load No Charging Battery
PV Power > Load Battery SOC high	PV Supplies Load No Charging Battery
PV Power > Load Battery SOC low	PV Supplies Load PV Charge Battery
PV Power < Load Battery SOC high	PV Supplies Load Battery Supplies Load
PV Power < Load Battery SOC low	PV Supplies Load Batteries Supplies Load until minimum SOC reached the shutdown Load
No PV Power Battery SOC high	Batteries Supplies Load
No PV Power Battery SOC low	Shutdown Load

When Table 3.11 is generalized, battery (energy storage) system operated by comparing the load power consumption with the output power of the PV panel and the current state of charge of the battery. If the state of charge is greater than minimum (0.4), the load will be supplied by the battery and the battery becomes in discharging mode. When there is enough supply of solar radiation (when the power produced by PV modules is greater than the load), and the state of charge of the battery falls below maximum (0.8), the PV panel will supply power to the load and battery, otherwise the loads will be disconnected from the system. The relationship between maximum and minimum state of charge (SOC) related as shown in Equation (3.37):

$$SOC_{min} = SOC_{max}(1 - DOD_{max}) \tag{3.37}$$

Bi-directional Buck-Boost Controller: The main objective of the bidirectional converter controller is to control the ES, to maintain a constant DC-bus voltage, i.e. on the DC micro-grid.

3.3.3 Load Side Distribution Network Modeling

Feeder Box Panel: The feeder box is a panel located on the outside of the DC house and contains the 120V DC distribution panel and circuit breaker since the devices have their own voltage, DC – DC converter much the voltage.

Circuit breaker (CB): The circuit breakers protect the system from inrush (surge) current caused by the loads inside the DC House. These circuit breakers are very important for protection of the system. Therefore, since current add up when loads placed in parallel, the DC circuit breakers chosen based on the maximum current required to power the appliances on a certain branch. The goal here is to choose a circuit breaker size just above this maximum current rating so that it trips and open-circuits that particular branch if a short circuit occurs.

Figure 3.18 shows the power flow in a basic DC circuit. The power loss in a DC circuit is directly proportional to the conductor resistance and the amount of current flowing through the conductor as shown by following equation:

$$P_{Loss} = P_{Source} - P_L = V_{DC}I - V_2I = I^2R = V_{drop}I \tag{3.38}$$

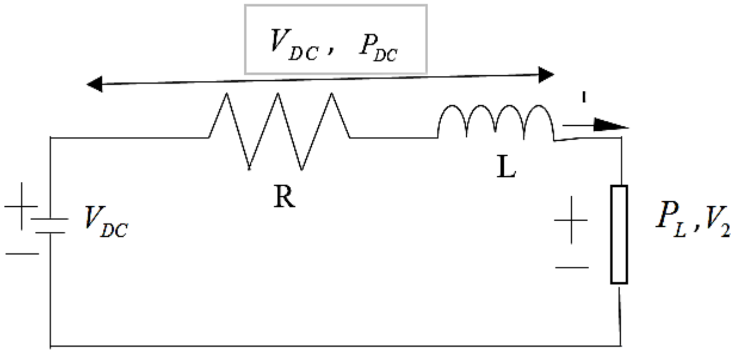

Figure 3. 18 DC equivalent circuit diagram

R: conductor resistance

L: conductor inductance

V_2 : Voltage at the load terminals

P_{Source} : Power source of DC circuit

P_L : active load power

V_{DC} : DC source voltage

P_{Loss} : power losses in DC circuit

At full load, the minimum current for one DC home is

$$I_{full\text{-}load} = \frac{P_{Load}}{V_2} \tag{3.39}$$

$$I_{full\text{-}load} = \frac{4294W}{120V} = 35.8A \text{ For } 120V$$

$$I_{full\text{-}load} = \frac{207W}{24V} = 8.625A \text{ For } 24V$$

$$I_{full\text{-}load} = \frac{270W}{19.5V} = 14A \text{ For } 19.5V$$

$$I_{full\text{-}load} = \frac{30W}{5V} = 6A \text{ For } 5V$$

Equation (3.39) shows distribution network will have different current ratings due to different distribution load voltages (for 5V, 19.5V, 24V and 120V).

Table 3. 12 Circuit breaker rating and cross-sectional area

Circuit	Description	Typical Current Rating (A)	Circuit Breaker Rating (A)	Cross-sectional Area (mm2)
1	Main Circuit Breaker	71 – 93	80	25
2	Sub-circuit Breaker1	30 – 39	32	6
3	Sub-circuit Breaker2	15.9 – 22	16	4
4	Sub-circuit Breaker3	< 15.9	10	2.5

3.4 System Cost Estimation

3.4.1 Photovoltaic Array Cost

Solar KC200GT solar module selected for the system due to its availability.

Table 3. 13 Technical parameters and cost assumptions for PV source *[59]*

Parameter	Unit	Value
Tilt angle	Degree	0
Azimuth angle	Degree	0 (West to South)
Ground reflectance	Percent (%)	20
DE rating factors	Percent (%)	95
Capital cost	USD/kW	1500
Replacement cost	USD/kW	1000
Operation and Maintenance (O&M) cost	USD/kW	50
Tracking system	-	No tracking
Life time	year	20

3.4.2 MPPT Charge Controller Cost

Table 3. 14 The costs of MPPT charge controllers required

PV system used for	MPPT controllers required	Total cost
2kW	1	$458.33
3kW	1	$458.33
4kW	1	$458.33
5kW	2	$916.66
6kW	2	$916.66
7kW	2	$916.66
8kW	2	$916.66
10kW	3	$1,374.99
12kW	4	$1,833.32
15kW	5	$2,291.65
20kW	6	$2,749.98
25kW	6	$2,749.98

The MPPT charge controller selected for the system is Outback FM-80 Flexmax. This charge controller takes the varying voltage from the PV array and produces a stable 120V voltage for the DC bus. Outback power FLEXmax 80 (FM80-150VDC) MPPT solar charge controller. A single controller has rating FM80-150VDC costs is $458.33 from Appendix C. Since the designed system is 8kW, the required charge controller is two (2) and the cost is $916.66.

3.4.3 Cost of Energy Storage System (ESS)

The purpose of the proposed standalone DC micro-grid system for our study area is to supply uninterruptible and maximum power quality to the DC loads in islanded mode. So, to achieve our purpose the cost of every kWh supplied by the ESS needed. The most important factors to calculate the costs and benefits ESS are the capital cost of the equipment, the cost for recharging energy and the replacements costs if they are needed [60]. The frequency of operation (charge and discharge cycles) is one of the most important parameters to calculate the life cycle.

Table 3. 15 The frequency of operation (charge and discharge cycles) of ESS *[61]*

Category/definition	Hours of storage	Use/Duty cycle	Representative application
Long-duration storage, frequent discharge	4 – 8	1cycle/day x 250 days/year	Load-leveling, Source following, arbitrage
Long-duration storage, infrequent discharge	4 – 8	20 times/year	Capacity credit
Short-duration storage, frequent discharge	0.25 – 1	4x15 min cycling x 250 days/year = 1000 cycles/year	Frequency or area regulation
Short-duration storage, infrequent discharge	0.25 – 1	20 times/year	Power quality, momentary carry-over

The applications for ESS can categorized by whether frequent cycling expected. This is important because depending on the application, the number of cycles by year will change. For an arbitrage application, the ESS will work more than 200 cycles by year. In the other hand, if the ESS used only for power quality the ESS will work only 20 times by year [61].

From Table 3.16 the energy storage subsystem (pack) cost of lithium-ion battery is 600$/kWh. However, today, the cost of energy storage subsystem (pack) is estimated about $200 per kWh by 2020 and to about $160 per kWh by 2025. Cost calculated by adding the cost of the storage unit with the cost of the full equipment systems; these are treated separately because they depend on ratings, power and energy. The cost of the power and energy storage is shown in Table 3.16 are used for comparative purpose, because the actual cost of storage systems depends on many factors and hypothesis, therefore the values shown are subjective and continue to be debated even among experts in the field.

Table 3. 16 The cost of ESS with their performance assumptions *[61]*

Technology	Power subsystem cost $/Kw	Energy storage subsystem cost $/kWh	Round-trip efficiency (%)	Cycles
Advanced Lead-acid Battery	400	330	80	2,000
Sodium/Sulfur Batteries	350	350	75	3,000
Lead-acid with carbon enhanced electrodes	400	330	75	20,000
Zink/Bromine Batteries	400	400	70	3,000
Vanadium Redox Batteries	400	600	65	5,000
Lithium-ion Batteries	400	600	85	4,000
Pumped hydro	1,200	75	85	25,000
Flywheels	600	1,600	95	25,000
Super-capacitor	500	10,000	95	25,000
Compressed air energy storage (CAES)	700	5	70	25,000

Table 3. 17 Assumptions for Life-cycle Benefit and Cost Analysis *[61]*

Parameter	Value
General inflation rate	2%
Discount rate	10%
Service life	10 years
Fuel cost, natural gas (surface CEAS only)	$5/MBTU
Electricity cost, charging	10¢/kWh

Capital Cost Calculation:

The capital cost calculation, in its simplest form is:

$$\text{Cost}(\$) = \text{Cost}_{pcs}(\$) + \text{Cost}_{storage}(\$) \qquad (3.40)$$

The cost of the power conversion equipment is proportional to the power rating of the system:

$$\text{Cost}_{pcs}(\$) = \text{Unit Cost}(\$/\text{kW})\text{P} \times (\text{kW}) \qquad (3.41)$$

For most systems, the cost of the storage unit is proportional to the amount of energy stored:

$$\text{Cost}_{storage}(\$) = \text{Unit Cost}_{storage}(\$/\text{kWh}) \times \text{E}(\text{kWh}) \qquad (3.42)$$

Where E: - is the stored energy capacity.

In the simplest case, E is equal to P × t, where P is Power and t is the discharge or storage time. All systems have some inefficiency. To account for this, Equation 3.42 modified as follows:

$$\text{Cost}_{storage}(\$) = \text{Unit Cost}_{storage}(\$/\text{kWh}) \times \text{E}(\text{kWh}/\eta) \qquad (3.43)$$

Where: - η is the efficiency of the battery.

Only when, the unit costs of the subsystems known, and the storage capacity in kWh known, it is possible to rewrite the capital cost in terms of the power rating:

$$\text{Cost}_{system}(\$/\text{kW}) = \text{Cost}_{total}(\$)/\text{P}(\text{kW}) \qquad (3.44)$$

The cost evaluation determines the most cost beneficial BESS. The unit energy cost (C_E) calculated by dividing the annual life cycle cost (ALCC) by annual energy consumption of load [62].

$$C_E = \frac{ALCC}{E_{yr}}(\$/\text{kWh}) \qquad (3.45)$$

Where: - E_{yr} is the yearly energy consumption of the household (in kWh).

The ALCC calculated by using Equation (3.46)

$$ALCC = LCC\left[\frac{(1+n)^t \times n}{(1+n)^t - 1}\right] \qquad (3.46)$$

$$CRF = \left[\frac{(1+n)^t \times n}{(1+n)^t - 1} \right]$$

Where t : is number of years

n : - is interest (discount) rate

CRF : - called capacity recovery factor.

$ALCC$: - is life cycle cost, which defined as the sum of present value of a system

$$LCC = C_p + C_{O\&M} + P_v \quad (3.47)$$

Where: - C_p is the purchasing cost.

$C_{O\&M}$: - is the present value of operation and maintenance cost, by understanding from the Homer Pro the operation and maintenance cost of lithium-ion battery is around 2% of the battery cost.

P_v : - is the present value (replacement) cost.

The battery (energy storage) system assumed replaced every ten years. Interest and inflation rate has taken as 10% and 2% respectively. The present value (replacement cost) of the item (P_v) calculated by:

$$P_v = C_p \left(\frac{1+i}{1+n} \right)^t \quad (3.48)$$

From the datasheet, the battery (energy storage) system assumed to replace in every ten (10) years. The operation and maintenance cost are about 2% of the battery cost.

Where i : - is inflation rate.

$\left(\frac{1+i}{1+n} \right)^t = \left(\frac{1+0.02}{1+0.1} \right)^{10} = 0.4699$: - is price reduction coefficient.

The cost of energy storage calculated by using Equation (3.50) and energy storage subsystem cost calculation Table 3.16 above.

Table 3. 18 Summary of the cost of the selected battery with days of autonomy

Number of days autonomy (N_D)	Total Ah required	Total energy generated in kWh	Yearly battery energy consumption of house hold in kWh	Total Cost in dollar ($)	Battery replacement cost ($)	O & M Cost ($)
2	4,400	48	17,520	9,600	4,512	192
3	6,600	72	26,280	14,400	6,768	288
4	8,800	96	35,040	19,200	9,024	384
5	11,000	120	43,800	24,000	11,280	480
6	13,200	144	52,560	28,800	13,536	576

By using Table 3.18, it is possible to determine the optimal autonomy days of the selected area by using optimal energy cost (HOMER Pro) based on days of autonomy.

CHAPTER 4

RESULTS AND DISCUSSIONS

4.1 Simulation Results from Homer Pro Software

The selection and sizing of components of the standalone (PV with Battery) energy system have been done, using HOMER-Pro software. Input information is provided to HOMER like daily load demand shown in Table 3.3, average solar insulation, clearness index, temperature as shown in Figure 4.2, 4.3, from NASA by using the latitude and longitude of the area and detailed costs. HOMER Pro is an optimization model, which does thousands of simulations and gives best possible design for the system. HOMER software show bargains with sun oriented PV cluster in terms of evaluated kW, not in m^2. The show considers that the yield of the PV cluster is directly proportional to the occurrence sun oriented radiation. If the sun-based radiation is 0.80kW/m2, the cluster will deliver 80% appraised yield [63].

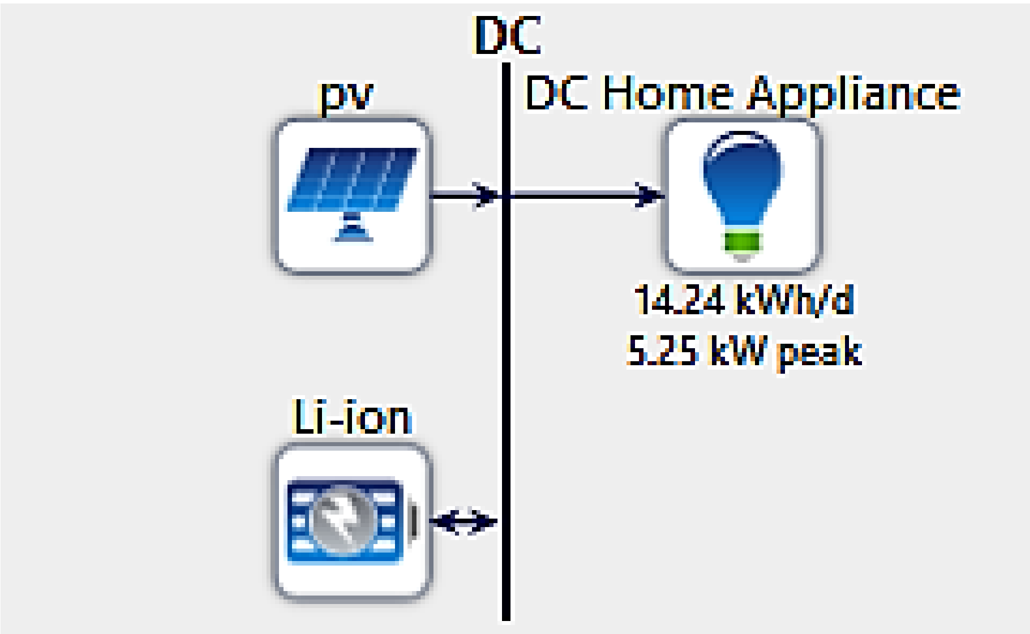

Figure 4. 1 Simple block diagram of PV with battery hybrid system

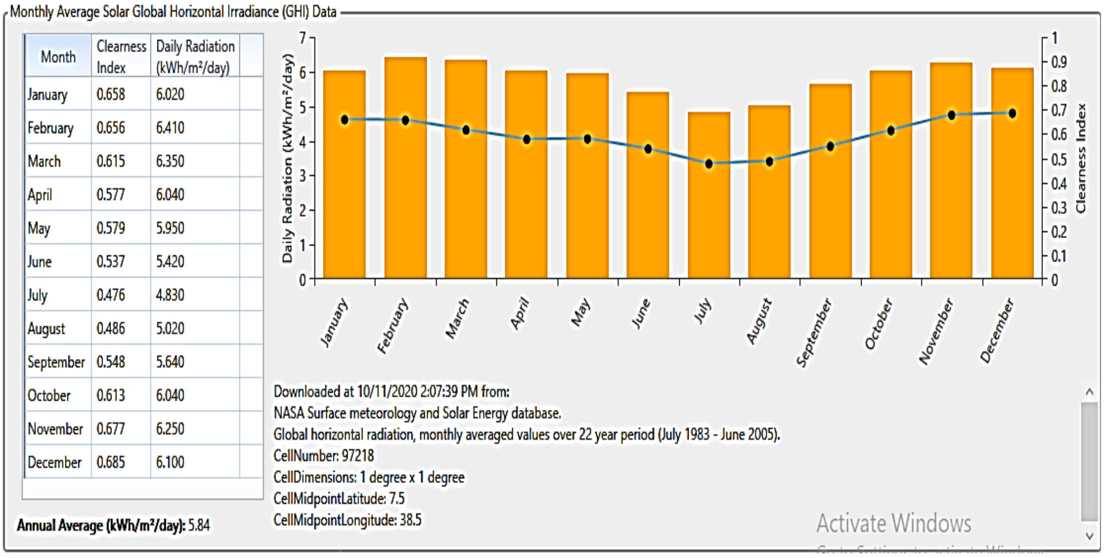

Figure 4. 2 Average monthly solar insulation and clearness index of the study area

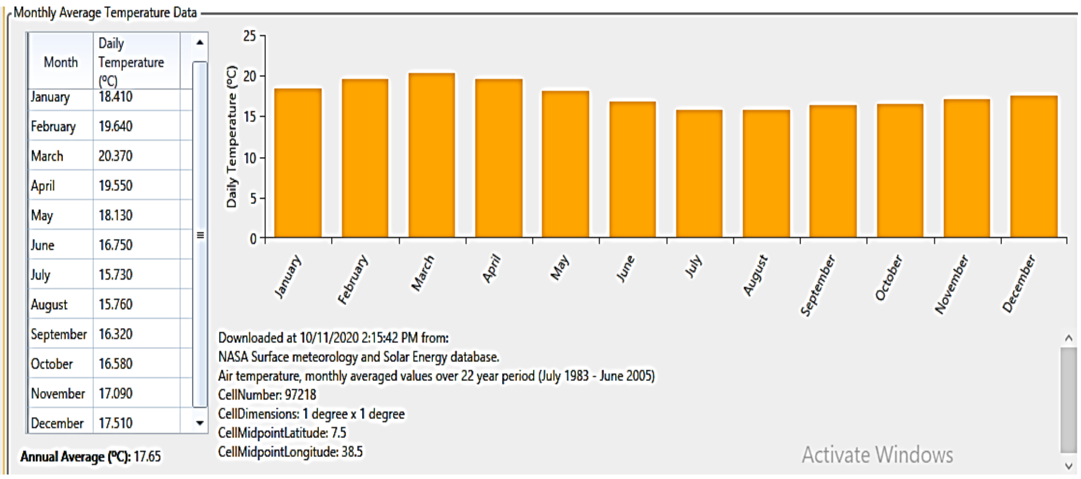

Figure 4. 3 Average monthly temperatures of study area

4.1.1 Sensitivity Results

The sensitivity factors such as solar insolation, temperature, clearness index, and cost are selected for this study. The search space may be extended by putting a range of options to select best possible arrangement. HOMER-Pro simulates each planes of their individual look space for every sensitivity values. An hourly time series simulation for every possible system type and arrangement is done for one-year. A feasible arrangement is defined as a solution for PV with battery hybrid system configuration that satisfy the demand. HOMER-Pro rejects all infeasible arrangements and positions the possible designs in accordance with ever-increasing net present cost (NPC). It more over permits so many parameters to be displayed against the sensitivity variables intended for selecting the best possible structure.

Case I when days of autonomy is two:

Export... | Export All... | **Sensitivity Cases** — Left Click on a sensitivity case to see its Optimization Results. | Compare Economics | Column Choices...

Architecture					Cost				System		PV Panel		Li-Ion	
PV Panel (kW)	PV Panel-MPPT (kW)	Li-Ion	Efficiency1	Dispatch	COE ($)	NPC ($)	Operating cost ($/yr)	Initial capital ($)	Ren Frac (%)	Total Fuel (L/yr)	Capital Cost ($)	Production (kWh/yr)	Autonomy (hr)	Annual Throughput (kWh/yr)
3.18	8.00	3	0	CC	$0.689	$46,290	$912.67	$34,492	100	0	5,692	6,095	238	2,627
3.24	8.00	3	0	CC	$0.689	$46,333	$909.29	$34,578	100	0	5,778	6,205	204	2,602
3.18	8.00	3	0	CC	$0.689	$46,290	$912.67	$34,492	100	0	5,692	6,095	238	2,627
3.24	8.00	3	0	CC	$0.689	$46,333	$909.29	$34,578	100	0	5,778	6,205	204	2,602
3.18	8.00	3	0	CC	$0.689	$46,290	$912.67	$34,492	100	0	5,692	6,095	238	2,627

Figure 4. 4 Sensitivity results when days of autonomy's are two

Case II when days of autonomy is three:

Export... | Export All... | **Sensitivity Cases** — Left Click on a sensitivity case to see its Optimization Results. | Compare Economics | Column Choices...

Architecture				Cost				System		PV Panel		Li-Ion		
PV Panel (kW)	PV Panel-MPPT (kW)	Li-Ion	Dispatch	COE ($)	NPC ($)	Operating cost ($/yr)	Initial capital ($)	Ren Frac (%)	Total Fuel (L/yr)	Capital Cost ($)	Production (kWh/yr)	Autonomy (hr)	Annual Throughput (kWh/yr)	Nomina (k
2.95	8.00	3	CC	$0.912	$61,291	$986.01	$48,545	100	0	5,345	5,653	357	2,727	302
3.05	8.00	3	CC	$0.914	$61,431	$985.85	$48,687	100	0	5,487	5,834	306	2,684	302
2.95	8.00	3	CC	$0.912	$61,291	$986.01	$48,545	100	0	5,345	5,653	357	2,727	302
3.05	8.00	3	CC	$0.914	$61,431	$985.85	$48,687	100	0	5,487	5,834	306	2,684	302
2.95	8.00	3	CC	$0.912	$61,291	$986.01	$48,545	100	0	5,345	5,653	357	2,727	302

Figure 4. 5 Sensitivity results when days of autonomy's are three

Case III when days of autonomy is four:

PV Panel (kW)	PV Panel-MPPT (kW)	Li-Ion	Dispatch	COE ($)	NPC ($)	Operating cost ($/yr)	Initial capital ($)	Ren Frac (%)	Total Fuel (L/yr)	Capital Cost ($)	Production (kWh/yr)	Autonomy (hr)	Annual Throughput (kWh/yr)	Nominal
3.00	8.00	3	CC	$1.16	$77,861	$1,149	$63,013	100	0	5,413	5,739	331	2,707	302
3.05	8.00	3	CC	$1.16	$77,934	$1,149	$63,087	100	0	5,487	5,834	306	2,685	302
3.00	8.00	3	CC	$1.16	$77,861	$1,149	$63,013	100	0	5,413	5,739	331	2,707	302
3.05	8.00	3	CC	$1.16	$77,934	$1,149	$63,087	100	0	5,487	5,834	306	2,685	302
3.00	8.00	3	CC	$1.16	$77,861	$1,149	$63,013	100	0	5,413	5,739	331	2,707	302
3.05	8.00	3	CC	$1.16	$77,934	$1,149	$63,087	100	0	5,487	5,834	306	2,685	302

Figure 4. 6 Sensitivity results when days of autonomy's are four

Case IV when days of autonomy is five:

PV Panel (kW)	PV Panel-MPPT (kW)	Li-Ion	Dispatch	COE ($)	NPC ($)	Operating cost ($/yr)	Initial capital ($)	Ren Frac (%)	Total Fuel (L/yr)	Capital Cost ($)	Production (kWh/yr)	Autonomy (hr)	Annual Throughput (kWh/yr)	Nominal
2.84	8.00	3	CC	$1.40	$94,223	$1,319	$77,170	100	0	5,170	5,429	442	2,781	403
2.86	8.00	3	CC	$1.40	$94,266	$1,319	$77,213	100	0	5,213	5,485	408	2,767	403
2.84	8.00	3	CC	$1.40	$94,223	$1,319	$77,170	100	0	5,170	5,429	442	2,781	403
2.86	8.00	3	CC	$1.40	$94,266	$1,319	$77,213	100	0	5,213	5,485	408	2,767	403
2.84	8.00	3	CC	$1.40	$94,223	$1,319	$77,170	100	0	5,170	5,429	442	2,781	403
2.86	8.00	3	CC	$1.40	$94,266	$1,319	$77,213	100	0	5,213	5,485	408	2,767	403

Figure 4. 7 Sensitivity results when days of autonomy's are five

Case V when days of autonomy is six:

PV Panel (kW)	PV Panel-MPPT (kW)	Li-Ion	Dispatch	COE ($)	NPC ($)	Operating cost ($/yr)	Initial capital ($)	Ren Frac (%)	Total Fuel (L/yr)	Capital Cost ($)	Production (kWh/yr)	Autonomy (hr)	Annual Throughput (kWh/yr)	Nominal
2.72	8.00	3	CC	$1.64	$110,540	$1,480	$91,404	100	0	5,004	5,217	595	2,835	504
2.81	8.00	3	CC	$1.65	$110,668	$1,480	$91,535	100	0	5,135	5,385	510	2,793	504
2.72	8.00	3	CC	$1.64	$110,540	$1,480	$91,404	100	0	5,004	5,217	595	2,835	504
2.81	8.00	3	CC	$1.65	$110,668	$1,480	$91,535	100	0	5,135	5,385	510	2,793	504
2.72	8.00	3	CC	$1.64	$110,540	$1,480	$91,404	100	0	5,004	5,217	595	2,835	504
2.81	8.00	3	CC	$1.65	$110,668	$1,480	$91,535	100	0	5,135	5,385	510	2,793	504

Figure 4. 8 Sensitivity results when days of autonomy's are six

4.1.2 Optimization Results

The HOMER model demonstrate simulations, optimization and sensitivity analysis in order to identify the most feasible hybrid system combination in terms of cost and technical aspects, based on the given constraints and inputs. The model presents optimum results under two categories: overall optimization and categorized optimization result tables according to their initial capital, NPC, COE, dispatch type, renewable energy penetration or fraction, and capacity shortage.

Case I when days of autonomy is two:

Export... | Optimization Results | Left Double Click on a particular system to see its detailed Simulation Results. | Categorized | Overall

Architecture					Cost				System		PV Panel		Li-Ion	
PV Panel (kW)	PV Panel-MPPT (kW)	Li-Ion	Efficiency1	Dispatch	COE ($)	NPC ($)	Operating cost ($/yr)	Initial capital ($)	Ren Frac (%)	Total Fuel (L/yr)	Capital Cost ($)	Production (kWh/yr)	Autonomy (hr)	Annual Throughput (kWh/yr)
3.18	8.00	3	0	CC	$0.689	$46,290	$912.67	$34,492	100	0	5,692	6,095	238	2,627
		114	0	CC	$18.79	$1.26M	$12,995	$1.09M	100	0			9,037	5,333

Figure 4. 9 Optimization result when days of autonomy's are two

Case II when days of autonomy is three:

Export... | Optimization Results | Left Double Click on a particular system to see its detailed Simulation Results. | Categorized | Overall

Architecture				Cost				System		PV Panel		Li-Ion		
PV Panel (kW)	PV Panel-MPPT (kW)	Li-Ion	Dispatch	COE ($)	NPC ($)	Operating cost ($/yr)	Initial capital ($)	Ren Frac (%)	Total Fuel (L/yr)	Capital Cost ($)	Production (kWh/yr)	Autonomy (hr)	Annual Throughput (kWh/yr)	Nominal Ca (kWh
2.95	8.00	3	CC	$0.912	$61,291	$986.01	$48,545	100	0	5,345	5,653	357	2,727	302
		78	CC	$19.28	$1.30M	$13,320	$1.12M	100	0			9,275	5,333	7,862

Figure 4. 10 Optimization results when days of autonomy's are three

Case III when days of autonomy is four:

Export... | Optimization Results | Left Double Click on a particular system to see its detailed Simulation Results. | Categorized | Overall

Architecture				Cost				System		PV Panel		Li-Ion		
PV Panel (kW)	PV Panel-MPPT (kW)	Li-Ion	Dispatch	COE ($)	NPC ($)	Operating cost ($/yr)	Initial capital ($)	Ren Frac (%)	Total Fuel (L/yr)	Capital Cost ($)	Production (kWh/yr)	Autonomy (hr)	Annual Throughput (kWh/yr)	Nominal Ca (kWh
3.00	8.00	3	CC	$1.16	$77,861	$1,149	$63,013	100	0	5,413	5,739	331	2,707	302
		84	CC	$27.63	$1.86M	$18,848	$1.61M	100	0			9,275	5,333	8,467

Figure 4. 11 Optimization results when days of autonomy's are four

Case IV when days of autonomy is five:

Export... **Optimization Results** Left Double Click on a particular system to see its detailed Simulation Results. ◉ Categorized ○ Overall

Architecture				Cost				System		PV Panel		Li-ion		
PV Panel (kW)	PV Panel-MPPT (kW)	Li-ion	Dispatch	COE ($)	NPC ($)	Operating cost ($/yr)	Initial capital ($)	Ren Frac (%)	Total Fuel (L/yr)	Capital Cost ($)	Production (kWh/yr)	Autonomy (hr)	Annual Throughput (kWh/yr)	Nominal Ca (kWh
2.84	8.00	3	CC	$1.40	$94,223	$1,319	$77,170	100	0	5,170	5,429	442	2,781	403
		63	CC	$25.91	$1.74M	$17,710	$1.51M	100	0			9,275	5,333	8,467

Figure 4. 12 Optimization results when days of autonomy's are five

Case V when days of autonomy is six:

Export... **Optimization Results** Left Double Click on a particular system to see its detailed Simulation Results. ◉ Categorized ○ Overall

Architecture				Cost				System		PV Panel		Li-Ion		
PV Panel (kW)	PV Panel-MPPT (kW)	Li-Ion	Dispatch	COE ($)	NPC ($)	Operating cost ($/yr)	Initial capital ($)	Ren Frac (%)	Total Fuel (L/yr)	Capital Cost ($)	Production (kWh/yr)	Autonomy (hr)	Annual Throughput (kWh/yr)	Nominal Ca (kWh
2.81	8.00	3	CC	$1.65	$110,668	$1,480	$91,535	100	0	5,135	5,385	510	2,793	504
		57	CC	$28.12	$1.89M	$19,173	$1.64M	100	0			9,682	5,333	9,576

Figure 4. 13 Optimization results when days of autonomy's are six

From the optimization result obtained from HOMER Pro software, the net present cost (NPC) and cost of energy (COE) is minimum (optimum), when days of autonomy's are two.

4.2 Simulation Results from MATLAB/Simulink software

In this research, modeling storage optimization for PV-powered DC home distribution system is analyzed. Almost all of home appliances get their source from ac system (although internally operate with direct current) and change this ac to dc using power electronic convertors. This conversion causes some power loss during normal and operating conditions. Injera Mitad and stoves (High power consuming devices) can operate directly with direct current without any modification. Similarly, with some modification made in the internal circuitry of rotating appliances, can be supplied directly with 120V dc and all electronic appliances, can be supplied directly with 24V, 19.5V and 5V dc system because all appliances have their own voltages.

Since the household loads varies continuously throughout the day, the loads can't be represented directly in MATLAB Simulink software as a Simscape power system lacks a formal block for a varying resistive load for evaluating the loads profiles. These variable load block can be designed as controlled current source, with the output current being determined by varying resistance value and voltage measurements.

The overall implementation of the energy storage system and PV-powered DC-home appliance is implemented using MATLAB/Simulink software for 24:00 hours. The simulation interprets that the proposed system will deliver constant voltage regardless of the load and power supply variations between solar PV and battery (energy storage) system for variation of irradiance and temperature. The input variables from source sides are solar insulation and cell temperature, and the output variables are PV voltage, PV current and PV power. From load side, the input variables are variable loads (forecasted power) with controlled voltage from DC bus and the output variables are load currents as shown in figure 4.14 below.

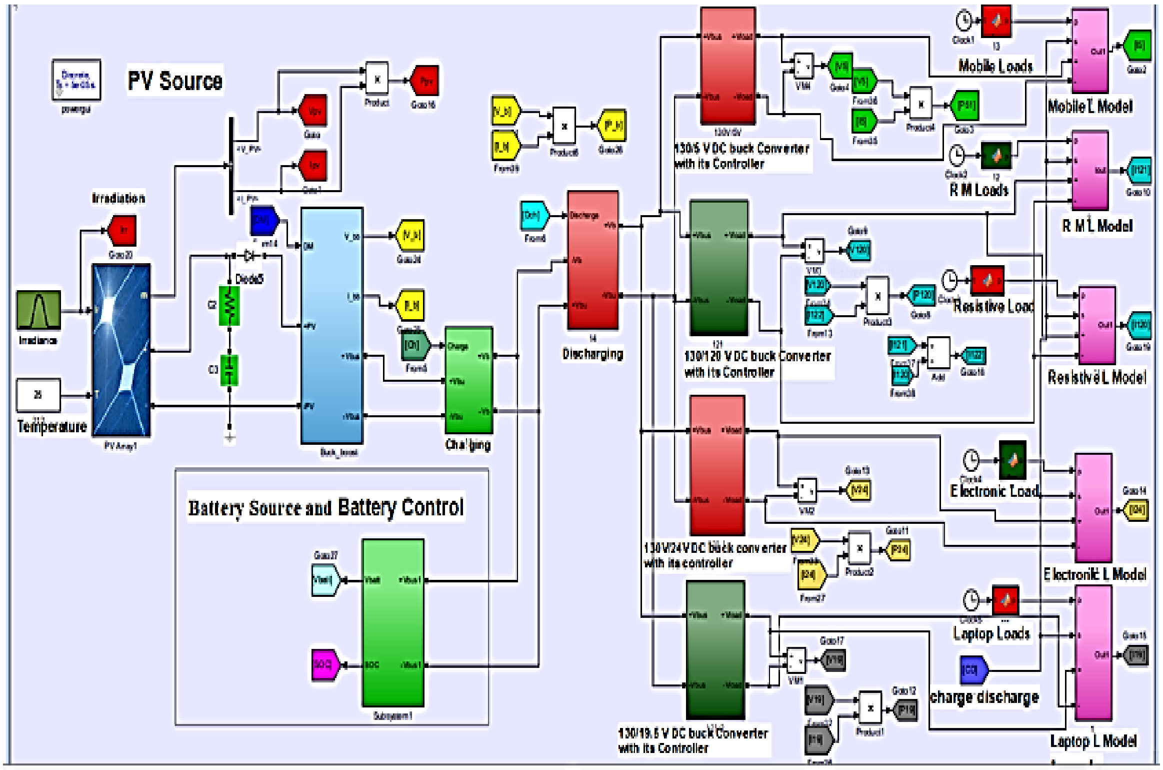

Figure 4. 14 Proposed system model for one sampled DC-home appliance

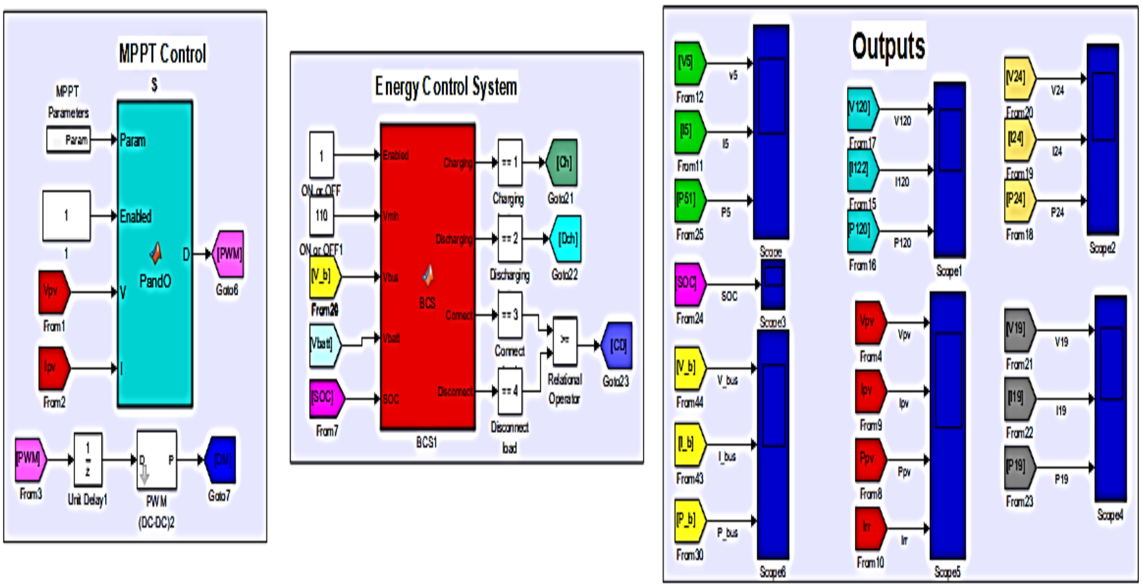

Figure 4. 15 Control system and outputs for proposed one sampled DC-home appliance

Figure 4.14 shows the proposed system for the overall implementation of the energy storage system and PV-powered DC-home appliance, which is implemented on MATLAB/Simulink software for 24:00 (24 hours) and Figure 4.15 shows the MPPT for buck-boost converter controller, battery control system, and the outputs for proposed system.

Figure 4.16 below shows the output of solar PV modules with maximum power point tracking. There is no voltage, current and power output from the panel before 06:00 and after 18:00 hours because there is no solar irradiation (insulation). Between 06:00 and 18:00, constant voltage of magnitude of 140V DC produced from the system. The irradiance curve in the fourth picture of Figure 4.16 shows that solar irradiation reaches its peak value of 1000 W/m^2 between 12:00 and 13:00.

4.2.1 Simulation Result with interpretation (MATLAB)

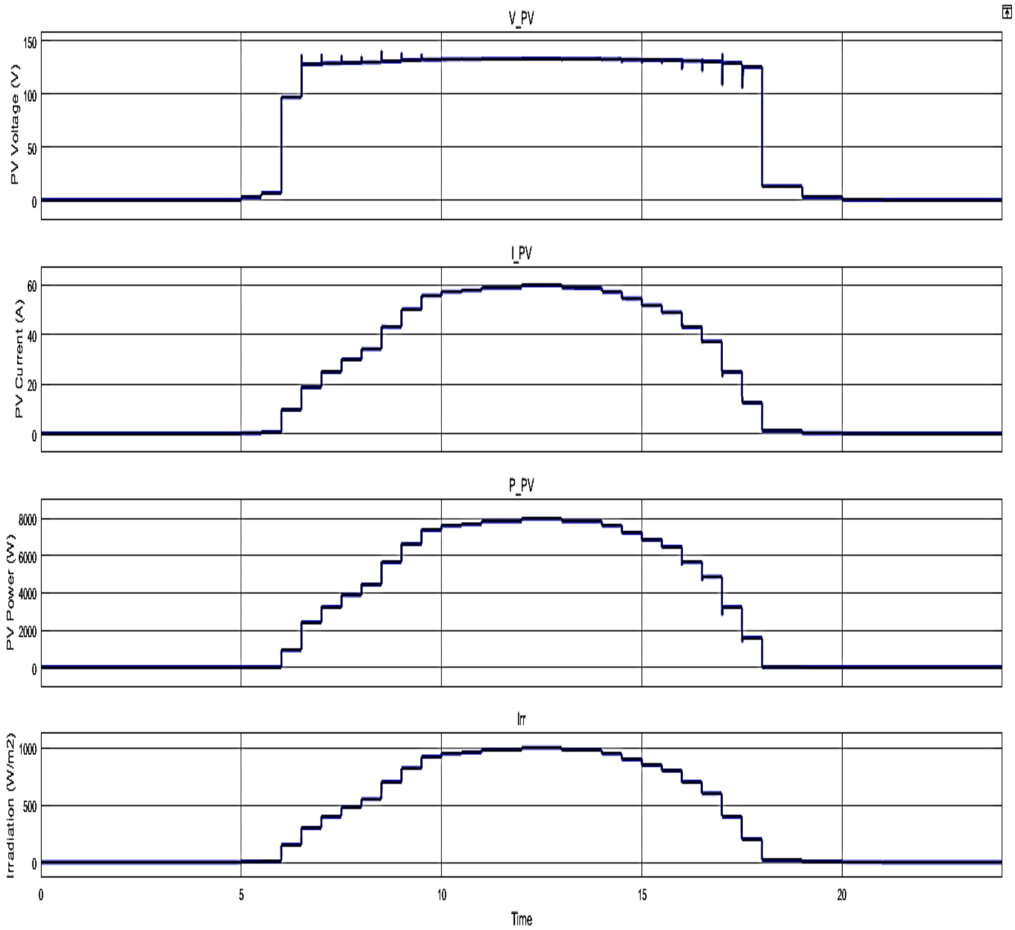

Figure 4. 16 The voltage, current, power and solar irradiation of the PV system

Buck-boost convertor is predictable to produce constant voltage with variation of irradiance throughout the day. Figure 4.17 below shows the output of the source buck-boost convertor. The convertor produces constant voltage of 130V DC when there is sunlight irradiation (insulation) between 06:00 and 18:00. As it seen from Figure 4.17 although the current designed to operate in continuous conduction mode, the buck boost convertor current enters in discontinuous conduction modes. Due to this effect, the output power of the buck boost convertor undergoes discontinuous conduction mode. The power output of the convertor becomes zero before 6:00 and after 18:00, as there is no solar radiation during these times.

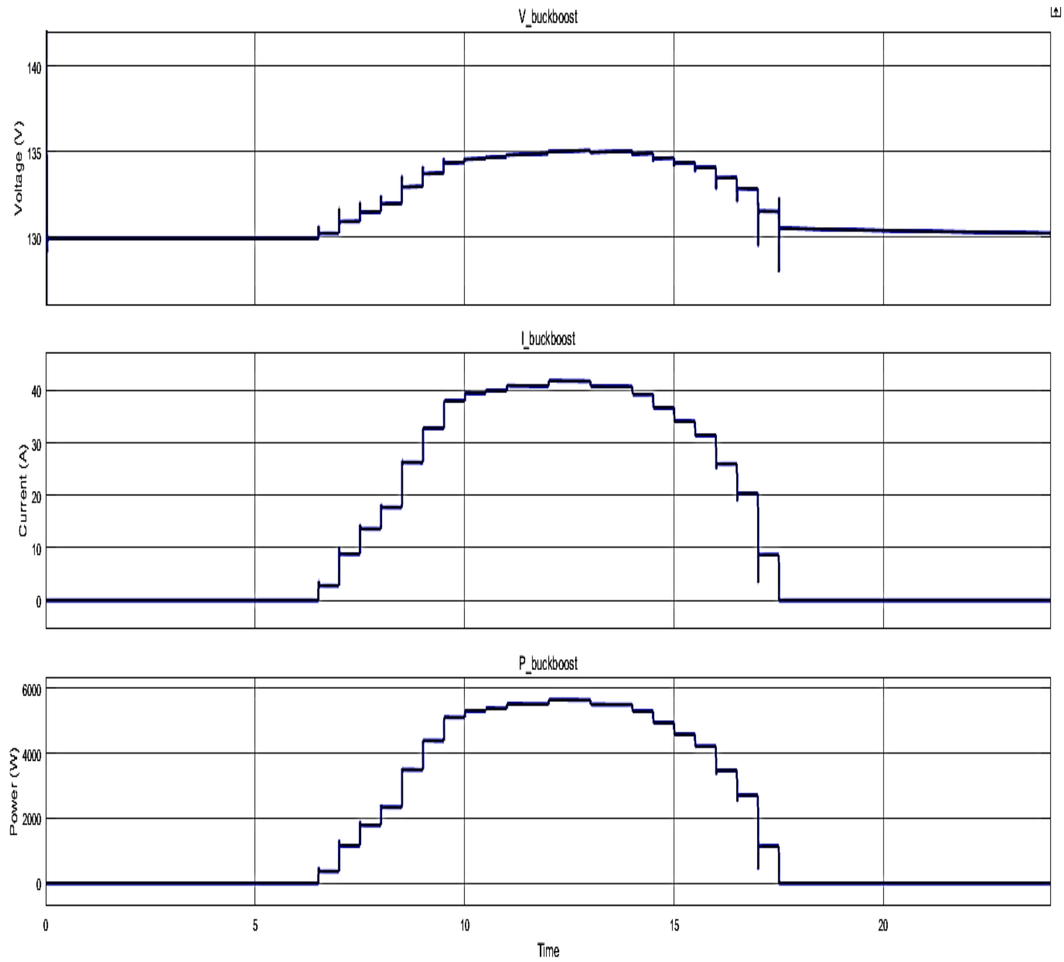

Figure 4. 17 The voltage, current and power output of the buck boost convertor for dc bus

The following Figure 4.18 shows, during nighttime's after dusk until early morning, there is no solar irradiation (insulation). Therefore, the loads not supplied by the PV power system. During this time, battery (energy storage) system supplies the power when the power output of the solar panels is less than the load demand requirement. In between 18:00 and 06:00 hours, the loads get their supply from the battery since there is no solar insulation during this time, which means the battery is in discharging mode. Between 06:00 and 18:00 hours, the PV panels produce sufficient power to supply the load and charge the battery and the battery (energy storage) system enters into the charging mode.

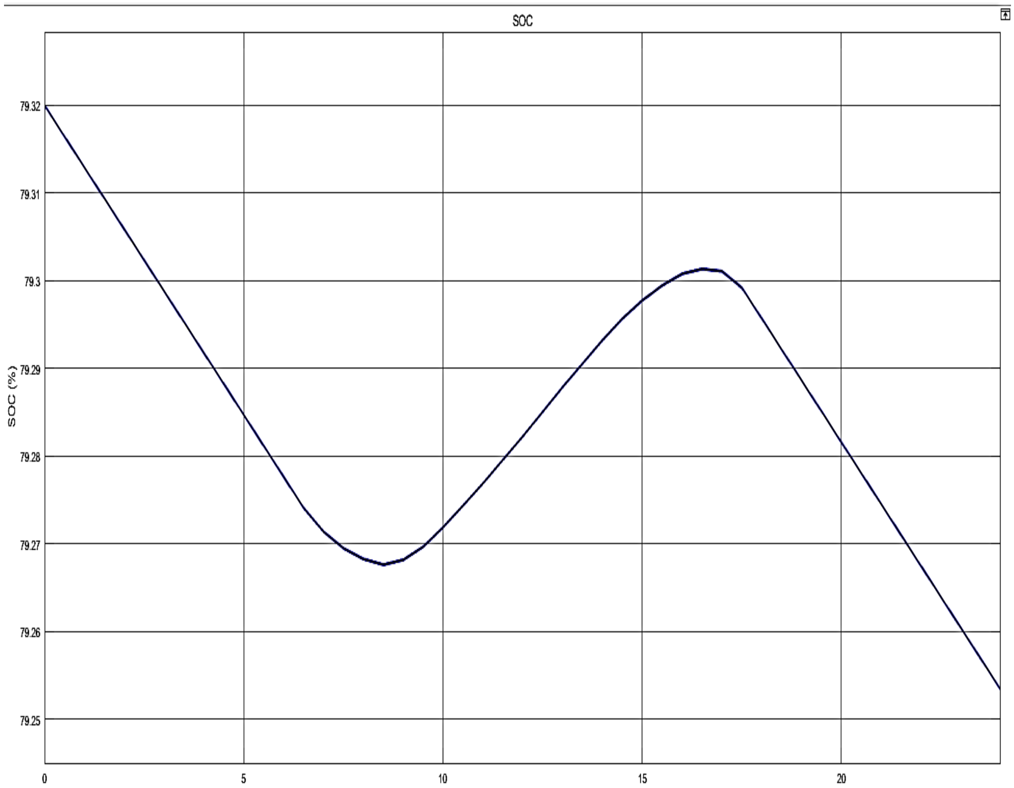

Figure 4. 18 Charging and discharging characteristics of the battery

Figure 4.19 below shows the voltage, current and power output of the buck convertor for 120V system appliance. It seen that regardless of the solar irradiation and load variation, the buck convertor produces constant voltage of magnitude of 120V DC throughout the day and voltage spikes with small magnitude observed at 06:00, 07:00, 13:00, 18:00 and 19:00. A large voltage spike also observed at 09:00 and 11:00. This voltage spikes caused due to sudden increasing and decreasing of the load. Between 06:00 and 07:00, between 11:00 and 13:00 and between 18:00 and 19:00, the load current reaches 10A. While during peak hours when large power consuming devices connected to the system, 26A observed between 09:00 and 11:00. Peak power output (3072W) recorded between 09:00 and 11:00.

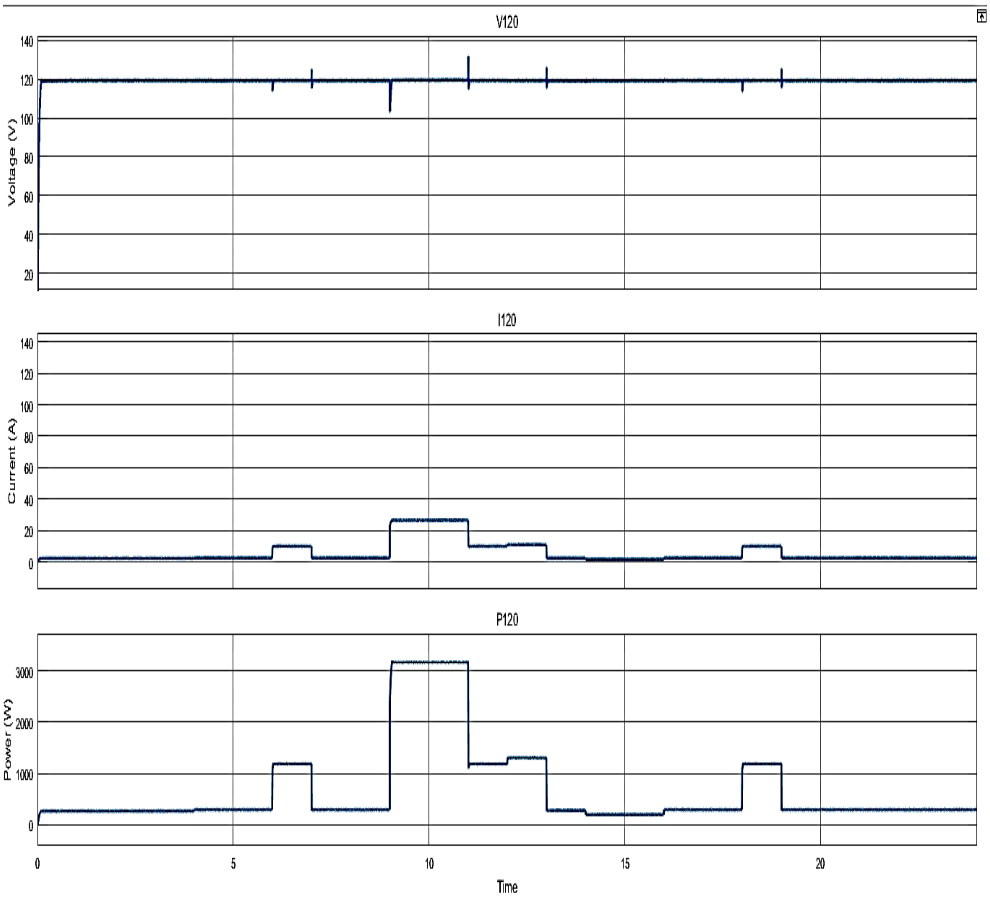

Figure 4. 19 The voltage, current and power output for 120V system appliance

Figure 4.20 below shows the voltage, current and power output of the buck convertor for 24V system appliance. It seen that regardless of the solar irradiation and load variation, the buck convertor produces constant voltage of magnitude of 24V DC throughout the day and voltage spikes with small magnitude happened at 05:00, 07:00, 11:00, 14:00, 19:00 and 20:00. A large voltage spike also observed at 18:00 and 22:00. Between 05:00 and 06:00, load current reaches 2A. Between 06:00 and 07:00, load current reaches 1.5A, and between 11:00 and 14:00 load current reaches 2.5A, between 18:00 and 19:00 load current reaches 4A, between 20:00 and 22:00 load current reaches 5A and while during peak hours when large power consuming devices are connected to the system between 19:00 and 20:00 the load current reaches 6.7A. Peak power output (160W) verified between 19:00 and 20:00.

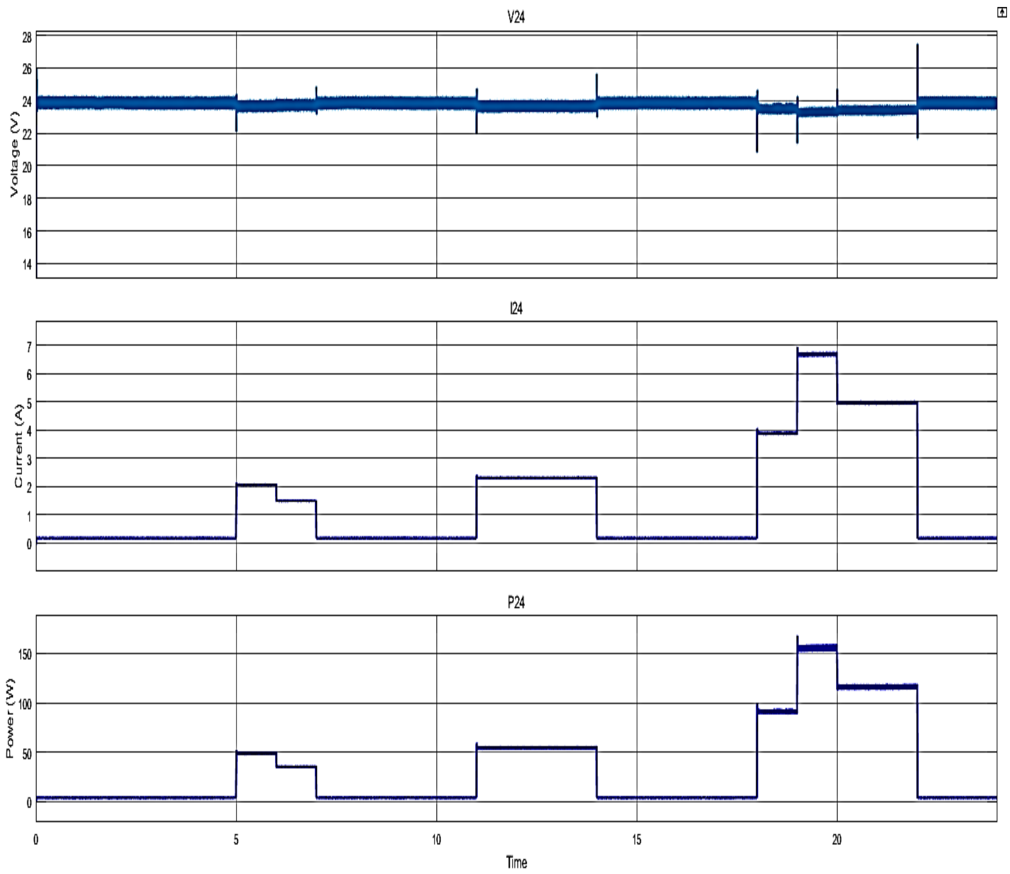

Figure 4. 20 The voltage, current and power output for 24V system appliance

Figure 4.21 below shows the voltage, current and power output of the buck convertor for 19.5V system appliance. It seen that regardless of the solar irradiation and load variations, the buck convertor produce constant voltage of magnitude of 19.5V DC throughout the day and voltage spikes with small magnitude happened at 13:00 and 20:00. A large voltage spike also observed at 12:00, 15:00, 19:00 and 21:00. Between 12:00 and 13:00, 19:00 and 20:00 load current reaches 13A, between 13:00 and 15:00 load current reaches 9A, and while during peak hours when large power consuming devices are connected to the system between 20:00 and 21:00 the load current reaches 19A. Peak power output (360W) verified between 19:00 and 20:00.

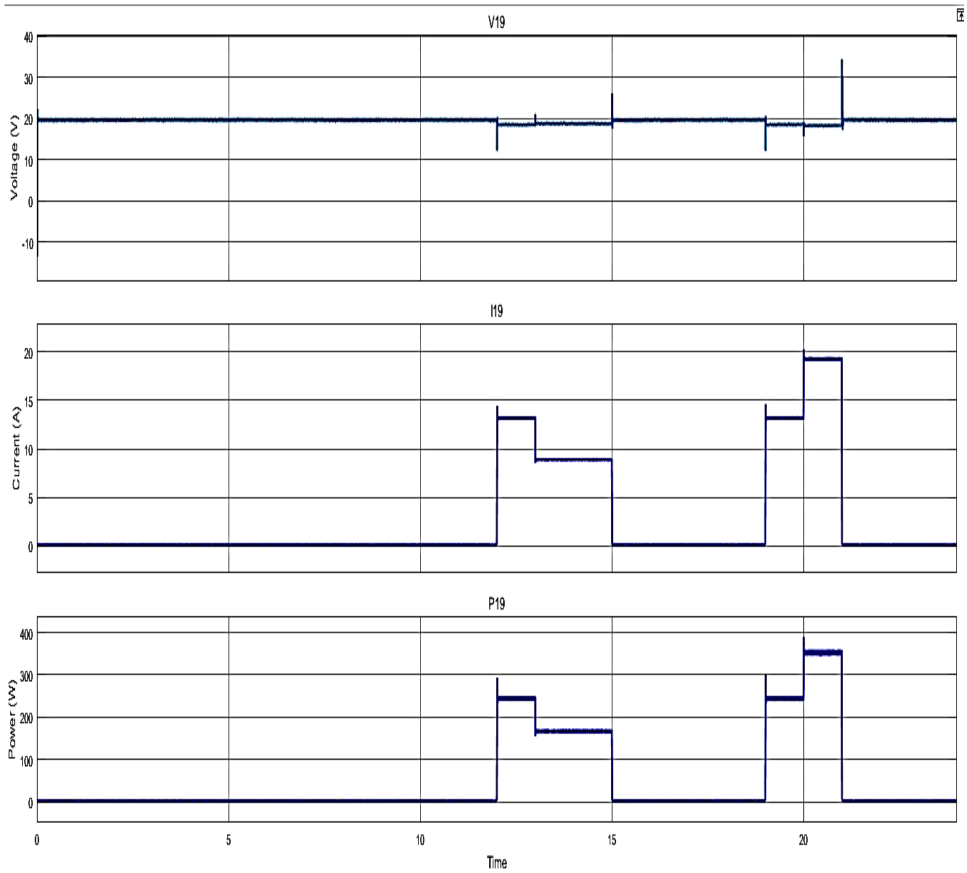

Figure 4. 21 The voltage, current and power output for 19.5V system appliance

The following Figure 4.22 shows the voltage, current and power output of the buck convertor for 5V system appliance. It seen that regardless of the solar irradiation and load variations, the buck convertor produce constant voltage of magnitude of 5V DC throughout the day and voltage spikes with small magnitude happened at 12:00, 13:00, 15:00, 18:00 and 19:00. A large voltage spike also observed at 20:00. Between 12:00 and 13:00, 18:00 and 19:00 load current reaches 3A, between 13:00 and 15:00 load current reaches 2A, and while during peak hours when large power consuming devices are connected to the system between 19:00 and 20:00 the load current reaches 5A. Peak power output (25W) verified between 19:00 and 20:00.

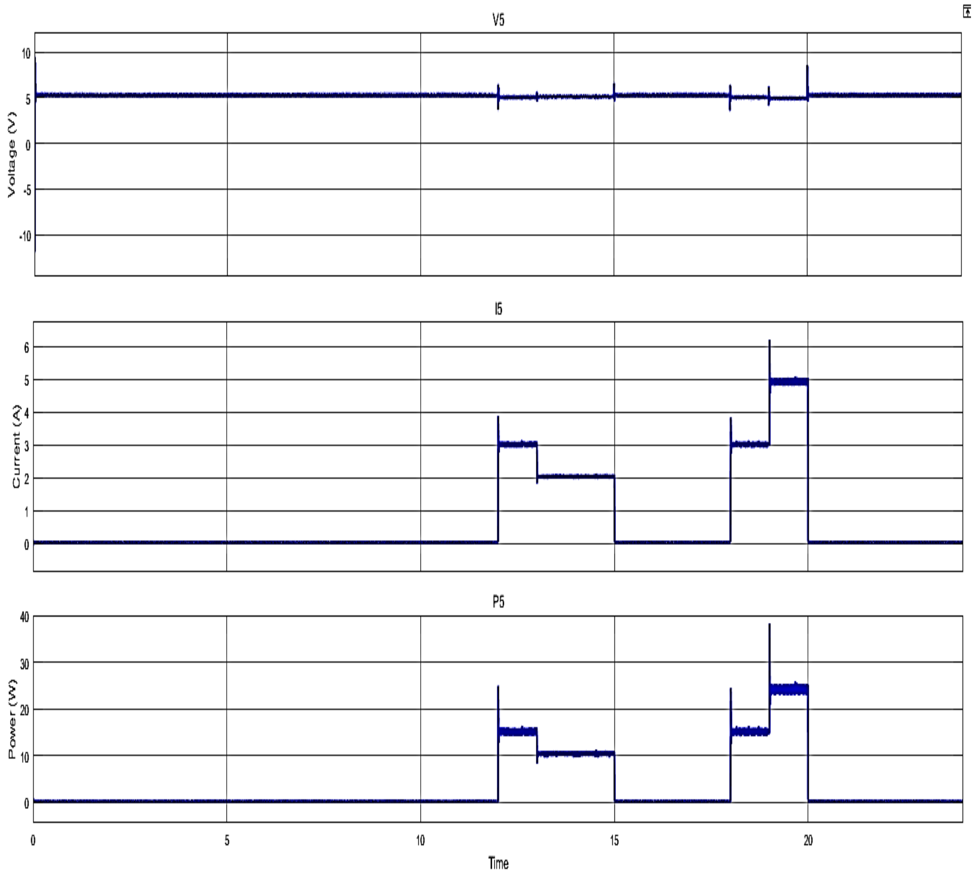

Figure 4. 22 The voltage, current and power output for 5V system appliance

CHAPTER 5

CONCLUSION, RECOMMENDATION AND FUTURE WORK

5.1 Conclusion

The research focused on the study, design and modeling of PV-powered DC-home with optimized storage appliance for rural electrification for Tullu Gudo Island. The energy resource, power requirement, solar irradiation and related data for this particular area obtained from National Aeronautics and Space Administration (NASA). The complete system modeled in MATLAB/Simulink software. The MPPT controller is used to generate maximum power point from PV source and bidirectional converter used to control the voltage level and the power flow between energy storage (battery) and DC-bus. The system voltages of 5V, 19.5V, 24V and 120V designed for meeting the DC load demand. The distribution network layout modeled for one (1) sampled DC homes. The design of these control voltage level were implemented by using MATLAB/Simulink.

The design of the buck converter was done by considering the equivalent circuit and its transfer functions in order to determine PID controller parameters (K_p, K_i, and K_d) values. There are no standard optimal days of autonomy for dc distribution system for residential applications. From the results obtained from HOMER simulation, two autonomy days are the optimal days for the battery (energy storage system) for rural electrification (Tullu Gudo Island) because the net present cost of the system is minimum ($46,290), the unit energy cost is ($0.689/kWh), and the size of battery (i.e. the coverage area) is reduced.

Currently, in Ethiopia, the existing electric power generation, transmission, and distribution costs are, on average, about $0.09 per kilowatt-hour (kWh), while the current tariff for electricity lies between $0.04 and $0.06 per kWh. However, this can be an acceptable alternative for people who have no access to electricity. Finally, the simulation result of PV powered DC-home system for different operating voltage system is verified.

Overall, the designed PV-powered DC home system has shown good results. This is due to the energy storage improvement by using solar insulation, hence reducing the total cost and cost of energy. Moreover, the optimized system was able to meet the modelled appliances consumption in the sample home. This has been clearly demonstrated by the results from HOMER and MATLAB/Simulink.

5.2 Recommendation

Especially for communities living far in areas where grid extension is not appropriate, the standalone DC micro grid project is very interesting to supply electricity to rural areas in all aspects like, power quality, reliability, sustainability and environmental protections. So Ethiopian government should create awareness by funding power system components that used for PV system installation and giving support to the people who want to use the technology, the goal of electrifying all areas of the country with distributed DC system achieved. The government can greatly reduce the deforestation rate renewable forms of standalone DC micro-grid energy will replace the currently used liquid fuel, gas, biomass or animal waste of forests in the country. Additionally, by implementing the proposed solution at large scale, the standalone DC micro grid distribution system can be integrated to the national gird and improve the reliability and power quality problem of the country.

5.3 Future Work

Based on the results obtained, future works may focus on developing the method to design hybrid BESS with ultra-capacitor energy storage systems to reduce the capacity requirements of BESS and extend the battery's lifetime. An ultra-capacitor can combined with BESS due to its high-power density and fast response. This hybrid battery and ultra-capacitor system is potentially a hopeful solution for both residential/commercial PV systems and utility-scale PV plant applications. The relationship between the cost of an ultra-capacitor and the advantages of ultra-capacitor to the battery storage system should investigate.

This research thesis was funded by Adama Science and Technology University under the grant number of ASTU/SM-R/069/19, Adama, Ethiopia.

References

[1] M. C. Kocer, C. C .Gezer, D. Gunes, M. A. Cinar, Bora Alboyak, and Ahmet Omen, " Assessment of Battery Storage Technologies for a Turkish Power Network," 2019.

[2] Opiyo, N.N., "a different storage focused pv based minigrid architectures for rural developing communities," *sustainable energy grids network,* vol. v, no. 9, pp. 75-99, 2018.

[3] D. Suchitra*, R. Jagatheesan, R. Santhana Venkatesam and V. Subramaniyan , "Comparative Study of Storage Devices for Stand-alone Hybrid Energy Systems," *Indian Journal of Science and Technology,* p. 45, 2016.

[4] M. Osama abed el-Raouf, Mohamed I. Mosaad, Mahmoud A. Al-Ahmar and Fahmy M El Bendary, "Tecno-Economic Analysis of Hybrid Renewable Energy Power Network for New Community in Egypt, Case Study New El-Farafra Oasis," *International Journal of Engineering Research and Advanced Technology (IJERAT),* vol. IV, no. 5, pp. 2454-6135, 2018.

[5] Raymoud H.Byrne, Tu A.Nguyen, David A.Copp, Babu R. Chalamala, and Imre Gyuk, "Energy Management and Optimization Methods for Grid Energy Storage Sytems," *IEEE,* p. 2741578, 2017.

[6] "https://www.scienceabc.com/innovation/ac-vs-dc-alternating-current-or-direct-current-which-is-better.html," [Online].

[7] "https://www.allaboutcircuits.com/textbook/alternating-current/chpt-3/more-on-the-skin-effect/," [Online].

[8] Diriba Kajela and Mukhdeep Singh Manshahia , "Optimization of Renewable Energy Systems," *IJSRST,* vol. 3, no. 8, pp. 2395-6011, 2017.

[9] Wenlong Jing*, Chean Hung Lai, S. H. Wallace Wong, M. L. Dennis Wong, "Battery - Super-capacitor Hybrid Energy Storage System in Standalone DC Microgrids," *IET Renewable Power Generation,* vol. 4, no. 11, 2016.

[10] R. K. Chauhan, B. S. Rajpurohit, R. E. Hebner, S. N. Singh, and F. M. Gonzalez-Longatt , "Voltage Standardization of DC Distribution System for Residential Buildings," *Clean Energy Technology,* vol. 4, no. 3, 2016.

[11] Bindu U. Kansara & B.R. Parekh, "Penetration of Renewable Energy Resources Based Dispatch Strategies for Isolated Hybrid Systems," *A. D. Patel Institute of Technology, BVM Engineering College, New Vidyanagar, Gujarat, India International Journal of Electrical and Electronics Engineering Research (IJEEER) ISSN 2250-155X* , vol. 3, no. 2, pp. 121-130, Jun 2013.

[12] S. T. Bahta, "Design and Analyzing of an Off-Grid Hybrid Renewable Energy System to Supply Electricity for Rural Areas," *Master of Science Thesis,* 2013.

[13] "en.wikipidia.org," Wikipedia, 26 February 2020. [Online]. Available: https://en.wikipedia.org/wiki/Growth_of_photovoltaics," [Online].

[14] Sharma, S., Jain, K.K. and Sharma, A., "Solar Cells: In Research and Applications A Review," *Materials Science and Applications,* vol. 6, pp. 1145-1155, 2015.

[15] Subodh Paudel, J.N. Shrestha, Fernando J. Neto, Jorge A.F. Ferreira, Muna Adhikari , "Optimization of Hybrid PV/Wind Power System for Remote Telecom Station," *IEEE International Conference on Power and Energy Systems (ICPS),* December 2011.

[16] Musta Cagatay Kocer, Ceyhun Cengiz, Mehmet Gezer, Doruk Gunes, Mehmet Aytac Cinar, Bora Alboyaci and Ahmet Onen, " Assessment of Battery Storage Technologies for a Turkish Power Network," *MDPI,* vol. 11, no. 3669, 2019.

[17] "eere/solar/articles," solar photovoltaic system design basics, 20 August 2013. [Online]. Available: https://www.energy.gov. [Accessed 8 March 2020].

[18] P. K. Pathak and A. R. Gupta, , "Battery Energy Storage System," *4th International Conference on Compututional Intelligence & Communication Technology (CICT) Ghaziabad,* pp. 1-9, 2018.

[19] "https://batteryuniversity.com/index.php/learn/article/secondary_batteries," secondary_batteries, 20 03 2020. [Online]. Available: http://www.batteryuniversity.com.

[20] Andreas Nyman and Henrik Ekstrom, "Modeling of the Lithium-ion Battery," January,2012.

[21] M. Khalid, "A Review on the Selected Applications of Battery-Supercapacitor Hybrid Energy Storage Systems for Microgrids," *Energies,* vol. 12, no. 4559, 2019.

[22] UmaShankar Patel, Ms. Dhaneshwari Sahu, Deepkiran Tirkey, "Maximum Power Point Tracking Using & Observe Algorithm and Compare With another Algorithm," *International Journal of Digital Application & Contemporary research,* vol. 2, no. 2, 2013.

[23] G. W. M. Sung Sae Lee, "“High-Efficiency Boost Half-Bridge Converter With Fast Boost Current Transferring ZVS Operation”," *IEEE Transactions on Power Electronics,* vol. 23, no. 4, pp. 1822-1829, 2008.

[24] J. E. Chaidez, "DC House Modeling and System Design," California Polytechnic State University , 2011.

[25] A. Getachew, "Study on Low Voltage Direct Current Distribution System Supplied by Solar Energy Master thesis," 2018.

[26] B. J. Williamson, " "project Edison: Smart DC,"," *ISGT Europe,* pp. pp. 1-10,, December 2011.

[27] B. G. F. Sandeep Anand, " Optimal voltage level for DC microgrids,," *in IECON 2010 - 36th Annual Conference on IEEE Industrial Electronics Society, U.S.A,* 2010.

[28] J.Pellis., "The DC low-voltage house. Graduation project," *Eindhoven University of Technology,* 1997.

[29] T. Bocklish, "Hybrid energy storage systems for renewable energy applications 9th International Energy Storage Conference," *IRES,* vol. 73 , pp. 103-111, 2015.

[30] D Ravi Prasad, Dr B.Rajesh Kamath, K.R Jagadisha, S.K Girish, "Smart DC Micro-grid for Effective Utilization," *International Journal of Scientific & Engineering Research,* vol. 3, no. 12, pp. 1-5, 2012.

[31] N.R. Rahmanov, N.M.Tabatabaei, K. Dursun,O.Z. Kerimov, "COMBINED AC-DC MICROGRIDS," *IJTPE,* vol. 4 , no. 12, pp. 158-161, 2012.

[32] Yongli Zhu, Chengxi Liu, Kai Sun, Di Shi and Zhiwei Wang, "Optimization of Battery Energy Storage to Improve Power System Oscillation Damping," *IEEE,* 2018.

[33] Kim, S. K., J. H. Jeon, C. H. Cho, and E. S. Kim, "Modeling and simulation of a grid-connected PV generation system for electromagnetic transient analysis," *in Solar Energy*, vol. 83, pp. 664-678, 2009.

[34] H. L. Tsai, "Insolation-oriented model of photovoltaic module using Matlab/Simulink," *in Solar Energy*, vol. 84, pp. 1318-1326, 2010.

[35] Femia, N., G. Petrone, G. Spagnuolo and M. Vitelli , "Optimizing sampling rate of P&OMPPT technique," *in Proceedings of the IEEE 35 Annual Power Electronics Specialists conference*, 2004.

[36] Tariq, A., and M. S. J. Asghar, "Development of microcontroller-based maximum power point tracker for a photovoltaic panel," *in Proceedings of the IEEE Power India Conference*, 2006.

[37] Sofla, M. A., and Lingfeng Wang, "Control of DC-DC bidirectional converters for interfacing batteries in microgrids," *in Power Systems Conference and Exposition (PSCE)*, 2011.

[38] Ramprabhakar, J., and K. Ragavan, "Dual bi-directional converter control for wind-solar-hydro system in grid connected and islanded operation," *in Power Electronics, Drives and Energy Systems (PEDES), IEEE International Conference*, 2012.

[39] W. Leslau, "Ziway Ethiopia Documents: Grammar and Dictionary," Wiesbaden, Otto Harrassowitz, p.xv. ISBN 3447041625, 1996.

[40] "/maps/ethiopia/(et01)/_tulloguddo/," 12 February 2020. [Online]. Available: http://www.getamap.net.

[41] A. Al-Akori, "PV Systems for Rural Health Facilities in Developing Areas," Report on International Energy Agency Photovoltaic Power Systems Programme (IEA-PVPS) T9-15, November 2014.

[42] G. L. (IED), "Rural Electrification with PV Hybrid Systems Overview and Recommendations for Further Deployment," International Energy Agency (IEA), July 2013.

[43] Ravi Prakash1, Sandeep Singh , "Designing and Modelling of Solar Photovoltaic Cell and Array," *IOSR Journal of Electrical and Electronics Engineering (IOSR-JEEE)*, vol. 11, no. 2, pp. 32-40, Appril 2016.

[44] M. Report, "Modeling and Control of dc/dc Boost Converter in FC systems," Professor Stefanopoulou, Wei Xi.

[45] Alivarani Mohapatra1, Byamakesh Nayak2, Chidurala Saiprakash3, " Adaptive Perturb & Observe MPPT for PV System with Experimental Validation," February 2019.

[46] Shafinaz A. Lopa, S. Hossain, M. K. Hasan, and T. K. Chakraborty , "Design and Simulation of DC - DC Converters," *International Research Journal of Engineering and Technology (IRJET)*, vol. 03, no. 01, pp. 2395 - 0072, Jan-2016.

[47] J. Ejury, "Buck Converter Design," Infineon Technologies North America (ITNA), Durham, January 2013.

[48] D. W. Hart, Power electronics, Book.

[49] R. S. Burns, Advanced Control Engineering, 2001.

[50] Low Wen Yao, Aziz, J. A., Pui Yee Kong, N. R. N. Idris, " Modeling of Lithium-Ion Battery Using MATLAB/Simulink," in *Low Wen Yao*, Skudai, Johor, Malaysia, 09 February 2014 IEEE.

[51] "articles/electronic_components/battery-technology," li-ion-lithium-ion-advantages-disadvantages., [Online]. Available: https://www.electronics-notes.com.

[52] Emma Raszmann, Kyri Baker, Ying Shi and Dane Christensen, " Modeling Stationary Lithium-Ion Batteries for Optimization and Predictive Control," *IEEE Power and Energy Conference Champaign*, February 23-24, 2017.

[53] R.A. Dougal, S. Liu, R.E. White, , "“Power and Life Extension of Battery Ultra-capacitor Hybrids”," *IEEE Transactions on Component and Packaging Technologies*, vol. 25, no. 1, p. 120-131, 2002.

[54] M. Rivera, "Small Wind / Photovoltaic Hybrid Renewable Energy System Optimization," *MSc Thesis, University of Puerto Rico., Puerto Rico*, 2008.

[55] Deepak Ravi, Bandi Mallikarjuna Reddy, Shimi S.L., Paulson Samuel, "Bidirectional dc to dc converters: An Overview of Various Topologies, Switching Schemes and Control Techniques," *International Journal of Engineering and Technology*, vol. 7, no. 4.5, pp. 360-365, 2018.

[56] M.-C. T. C.-H. H. Y.-G. L. Kuei-Hsiang Chao, "Design and Implementation of a Bidirectional DC-DC Converter for Stand-alone Photovoltaic Systems," *International Journal of Computer, Consumer and Control (IJ3C),* vol. 2, no. 3, 2013.

[57] Kou-Bin Liu, Chen-Yao Liu and Yi-Hua Liu, " Analysis and controller design of a universal bidirectional dc-dc converter," *energies,* 2016.

[58] L. H. L. N. S. D. I. Yen Yee Chia, " A load predictive energy management system for supercapacitor-battery hybrid energy storage system in solar application using the Support Vector Machine," *Journal Applied Energy,,* no. 137, pp. 588-602, 2015.

[59] Kiflom Gebrehiwot, Md. Alam Hossain Mondal, Claudia Ringler and Abiti Getaneh Gebremeskel , "Optimization and cost-benefit assessment of hybrid power systems for off-grid rural electrification in Ethiopia," *Energy,* no. 177, pp. 234-246, 2019.

[60] J. M. Eyer, J. J. Iannucci, and G. P. Corey, Energy Storage Benefits and Market Analysis Handbook A Study for the DOE Energy Storage Systems Program, Sandia: Sandia National Labratories, 2004.

[61] P. Susan Schoenung, " A Study for the DOE Energy Storage Systems Program," *Energy Storage Systems Cost Update,* 2011.

[62] I.˙. G.¨. a. N. Onat, " Cost Calculation Algorithm for Photovoltaic Systems, Marmara University, Turkey".

[63] M. K. M. S. K. K. Ajoya Kumar Pradhan, " Techno-Economic Evaluation of Stand-alone Hybrid Renewable Energy System for Remote Village Using HOMER-Pro Software," *International Journal of Applied Power Engineering (IJAPE),* vol. 6, no. 2, pp. 74-89, August 2017.

Appendices

Appendix A

Daily Load generator

```
function y = fcn(u)

%#codegen

if((u>=0)&&(u<=1))

    y=83;

elseif((u>=1)&&(u<=2))

    y=83;

elseif((u>=2)&&(u<=3))

       y=83;

elseif((u>=3)&&(u<=4))

        y=83;

elseif((u>=4)&&(u<=5))

        y=72;

elseif((u>=5)&&(u<=6))

        y=122;

elseif((u>=6)&&(u<=7))

        y=1108;

elseif((u>=7)&&(u<=8))

          y=72;

 elseif((u>=8)&&(u<=9))

          y=72;

 elseif((u>=9)&&(u<=10))

          y=3072;

 elseif((u>=10)&&(u<=11))
```

```
         y=3072;
 elseif((u>=11)&&(u<=12))
         y=1128;
 elseif((u>=12)&&(u<=13))
         y=1554;
 elseif((u>=13)&&(u<=14))
         y=324;
 elseif((u>=14)&&(u<=15))
         y=332;
 elseif((u>=15)&&(u<=16))
         y=142;
elseif((u>=16)&&(u<=17))
         y=72;
elseif((u>=17)&&(u<=18))
         y=72;
elseif((u>=18)&&(u<=19))
         y=1167;
elseif((u>=19)&&(u<=20))
         y=522;
elseif((u>=20)&&(u<=21))
y=669;
elseif((u>=21)&&(u<=22))
y=194;
elseif((u>=22)&&(u<=23))
y=72;
elseif((u>=23)&&(u<=24))
y=72;
```

```
else
    y=0;
end
```

Resistive Load model

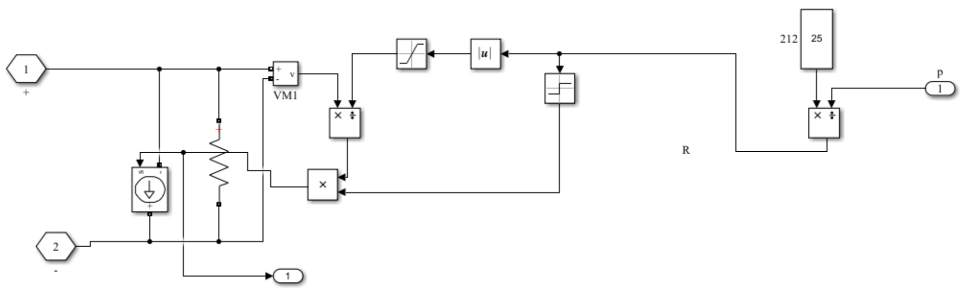

Appendix B

Converter with controller and specification

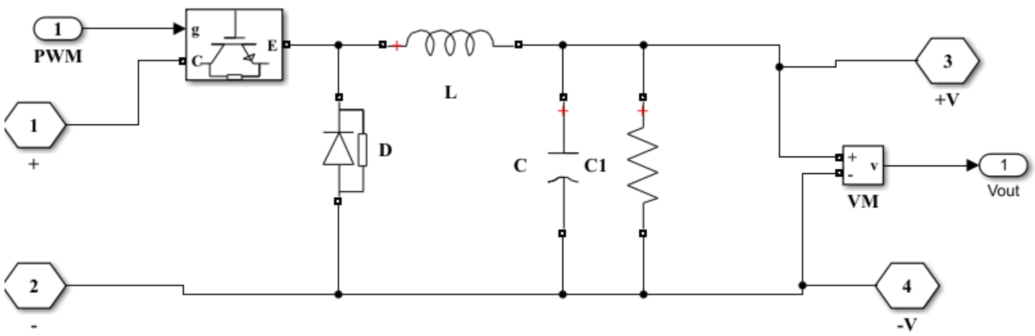

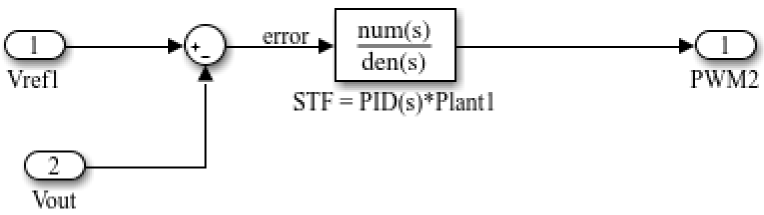

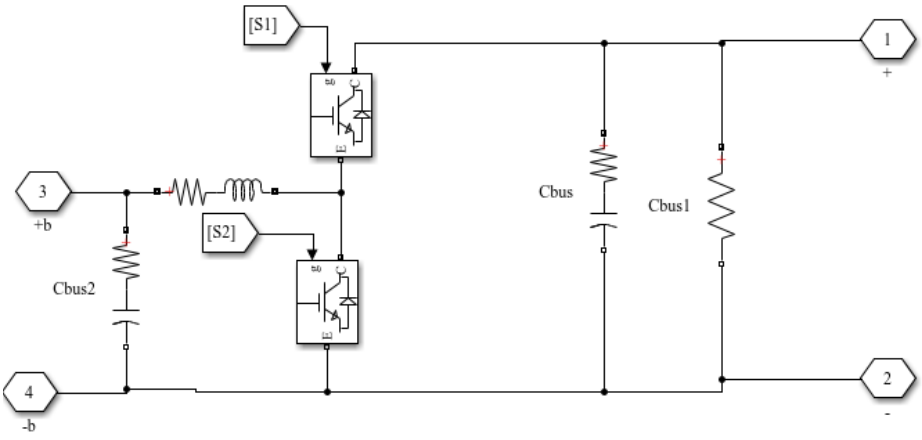

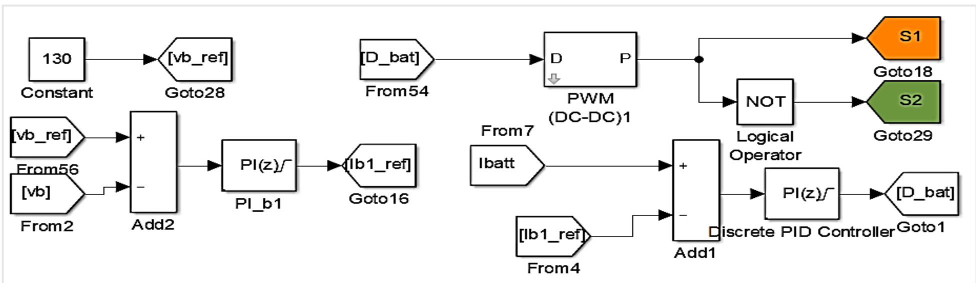

Brand	Eyonder
Product Name	DC power supply 72v
Model	EYD-DTD72S2430
Input rated voltage	72VDC
Input voltage range	40V~90VDC
Conversion Efficiency	96%
Output voltage	24VDC
Output current	30Amps
Output rated power	720Watts
Output peak power	125%
Voltage regulation	< 1%
Load regulation	< 2%
Ripple (full load test)	< 50mV
No-load current	< 20mA
Working Temperature	-40°c ~ +80°c
Waterproof rating	IP 68
Protections	Over-load, Over-current, Over-temperature, Short-circuit, Over-voltage
Machine size	160*113*35MM

N. Weight	1.5KG
Cooling way	Free air convection
Certifications	CE, RoHS
Others	White box packing

Plant response for buck converter

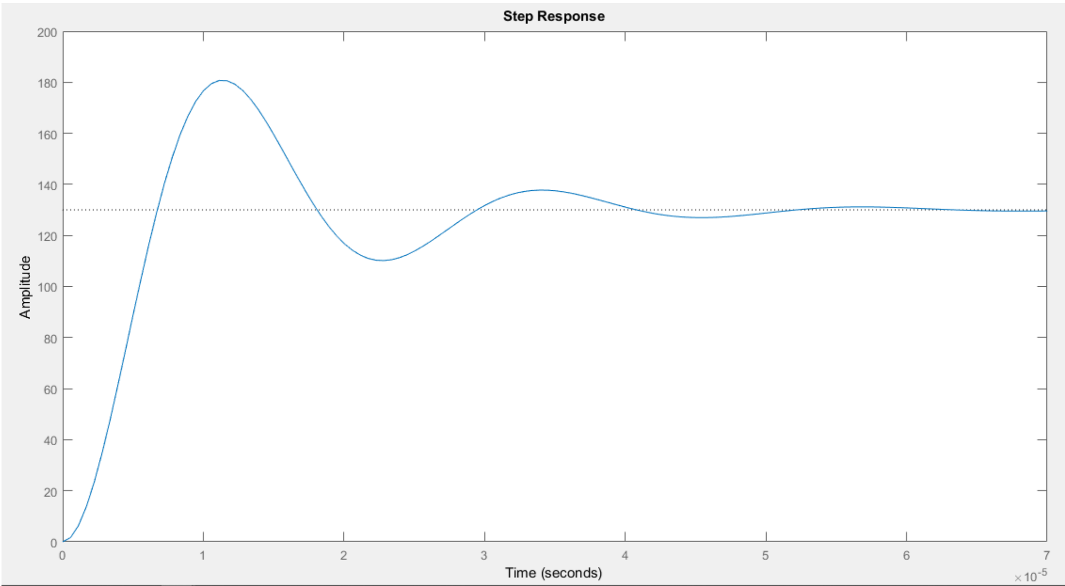

The overall response for PWM

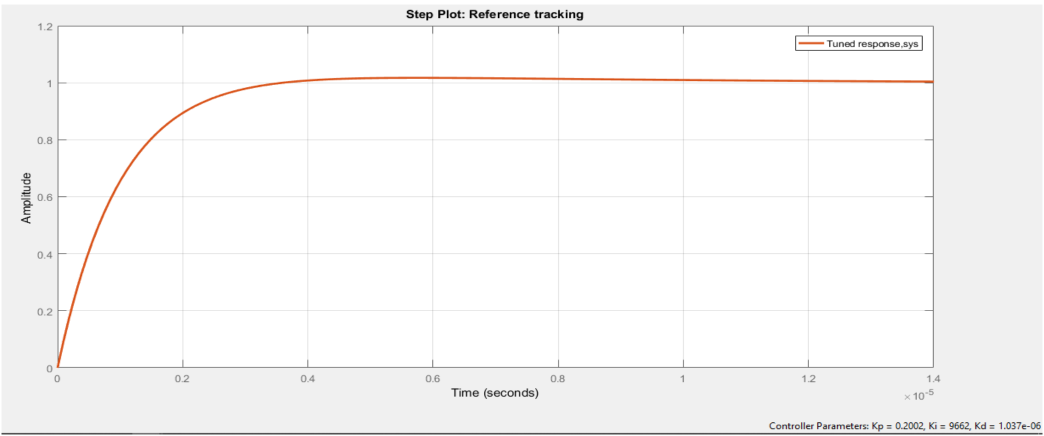

Appendix C

MPPT Controller

```
function Duty = MPPT_Control( V, I, deltaD_in)

Duty_init = 0.133;
Duty_min = 0;
Duty_max = 0.8;

persistent Vold Pold Duty_old;
if isempty (Vold)
   Vold=0;
   Pold=0;
   Duty_old=Duty_init;
end
P = V*I;
dV = V - Vold;
dP = P - Pold;
deltaD = deltaD_in;
if dP ~= 0
   if dP < 0
      if dV < 0
         Duty = Duty_old - deltaD;
      else
         Duty = Duty_old + deltaD;
      end
   else
      if dV < 0
         Duty = Duty_old + deltaD;
      else
         Duty = Duty_old - deltaD;
      end
   end
else
   Duty = Duty_old;
end
if Duty >= Duty_max || Duty<= Duty_min
   Duty=Duty_old;
end
Duty_old=Duty;
Vold=V;
Pold=P;

return
```

Outback Power FLEXmax FM80 MPPT Solar Charge Controller (FM80-150VDC)

Rating:

100% of100

1 Review Add Your Review

View Product Documents

$458.33

Maximum output of 80Amps DC Advanced MPPT charging algorithm 12, 24, 36, 48, and 60 Volt DC Battery Banks Built-in 80-character LCD display

Skip to the end of the image's gallery

Skip to the beginning of the image's gallery

Specifications:

- Nominal battery voltages: 12, 24, 36, 48, 60 Volts DC
- Maximum output current: 80 Amps DC at 104°F (40°C)
- Maximum PV array power: 12VDC systems: 1000 Watts; 24VDC systems: 2000 Watts; 48VDC systems: 4000 Watts
- Absolute maximum PV open circuit voltage: 150VDC, 145VDC start-up
- Maximum Efficiency: 98.44%
- Charging regulation stages: bulk, absorption, float, silent, & equalization
- Programmable voltage regulation and equalization set-points
- Standby power consumption: typically, < 1 Watt

- Built-in programmable auxiliary control output at 12VDC and 0.2ADC
- Data logging stores the last 128 days of data: amp-hours, watt-hours, time in float, peak watts, amps, and solar array voltage, max. battery voltage, min. battery voltage and absorb time, accumulated amp-hours, and kWh of production
- Active cooling and intelligent thermal management cooling (built-in fan)
- Designed for indoor installation
- Dimensions: 16.25"H x 5.75"W x 4.5"D
- Weight: 12.2 lb.
- 5-year warranty

Appendix D

Customers who viewed Rockville RWK0CU 0 AWG Gauge 100% Copper Complete Amp Installation Wire Kit… also viewed

20 Foot 1/0 Gauge Amp Kit Featuring 20% Oversized Cables - Complete 12V Audio Amplifier Installation & Wiring Kit 1 used and new from $84.99.

NVX True Spec 1/0 Gauge 100% Copper Single Amp Wiring Kit with 12 Gauge Speaker Wire [XAPK0] 3 used and new from $119.99.

KnuKonceptz Bassik 0 Gauge Complete Amplifier Installation Amp Wiring Kit with RCA

2 used and new from $31.99

Buy used:

$84.67

Rockville RWK41 4 Gauge Complete Car Amp Wiring Installation Wire Kit w/RCA's

Description:

The Rockville RWK41 4 AWG (American Wire Gauge) amp kit has the following differences over other amp kits on the market at this price point.

Features**:**

- 1 – 17’ High Grade Twisted Pair of 100% Copper RCA Cable
- 17’ – 4 Gauge Translucent Blue Superflex Power Cables
- 17’ – 18 Gauge Blue Remote Cable
- 17’ – 16 Gauge Clear Speaker Wire
- 3’ – 4 Gauge Clear Superflex Ground Wire
- Gold Plated AGU Heat Resistant Fuse Holder
- 60 Amp AGU Gold Plated Fuse
- 7’ Split Tube Loom
- Accessories Included: Wire Ties, Ring Terminals, Butt Connectors, Spades, and Grommets

2.0 out of 5 stars Fuse holder is garbage. Fire waiting to happen

Reviewed in the United States on January 1, 2020

Style: OFC Size: 0 Gauge Verified Purchase

True 0-gauge OFC however, there are things that can cause this install to be a fire hazard. I ended up purchasing a new fuse holder, which set me back another $40 on top of this kit.

Appendix E

48v 56v 60v 65v 70v 72v 80v 90v 96v 100v 110v 115v step down converter 120 to 12v 20a 240w buck isolated dc-to-dc power supply

US $48.75

- China
- Color: 20A
- 20A
- Input Voltage: 120V (48-120VDC)
- 120V(48-120VDC)
- Output Voltage: 12VDC
- 12VDC

Brand	Eyonder
Product Name	converter 120 to 12v
Model	EYD-DTD120S1220
Input rated voltage	120VDC
Input voltage range	48~120VDC
Conversion Efficiency	96%
Output voltage	12VDC
Output current	20Amps
Output rated power	240Watts
Output peak power	125%
Voltage regulation	< 1%
Load regulation	< 2%
Ripple (full load test)	< 50mV
No-load current	< 20mA
Working Temperature	-40°c ~ +80°c
Waterproof rating	IP 55

Protections	Over-load, Over-current, Over-temperature, Short-circuit, Over-voltage
Machine size	120*130*66MM
N. Weight	1.15KG
Cooling way	Free air convection
Certifications	CE, RoHS
Others	White box packing

High power step down buck input 40v~90v 46v 48v 50v 60v 70v 80v dc to dc power supply 72v to 24v 30a 720w boost converter

2 orders

US $68.75

China

Color: 30A

- 30A
- Input Voltage: 72V (40-90VDC)
- 72V(40-90VDC)
- Output Voltage: 24VDC
- 24VDC

Appendix F

Kyocera KC200GT (solar) and LiFePo4 (Li-ion) specification

12V 200Ah LiFeP04 Deep Cycle 2000 Times Solar Battery Rechargeable Outdoor Long Life Factory Price

Purchase Qty. / Reference FOB Price	
50-199 Pieces	US $179
200-499 Pieces	US $171.5
500+ Pieces	US $162.5

Standard capacity	200Ah
Rated voltage	12.8V
Maximum input current	40A
Maximum output current	80A
Charging voltage	14.4V~14.6V
Cut-off	2.5V single cell
Self-Discharge(25 degree)	<3%/month
Depth of discharge	Up to 95%
Cycle life	Discharge cycle 2000<1C/ Discharge cycle 4000<0.4C
Charge method(CC/CV)	Operation: -20~70° Degree/ Recommendation: 10~45° Degree
Warranty	5 Years

Specifications

Electrical Performance under Standard Test Conditions (*STC)

Maximum Power (Pmax)	200W (+10%/−5%)
Maximum Power Voltage (Vmpp)	26.3V
Maximum Power Current (Impp)	7.61A
Open Circuit Voltage (Voc)	32.9V
Short Circuit Current (Isc)	8.21A
Max System Voltage	600V
Temperature Coefficient of Voc	-1.23×10^{-1} V/℃
Temperature Coefficient of Isc	3.18×10^{-3} A/℃

*STC : Irradiance 1000W/m², AM1.5 spectrum, module temperture 25℃

Electrical Performance at 800W/m², NOCT, AM1.5

Maximum Power (Pmax)	142W
Maximum Power Voltage (Vmpp)	23.2V
Maximum Power Current (Impp)	6.13A
Open Circuit Voltage (Voc)	29.9V
Short Circuit Current (Isc)	6.62A

Cells

Number per Module	54

Module Characteristics

Length × Width × Depth	1425mm(56.2in)×990mm(39.0in)×36mm(1.4in)
Weight	18.5kg(40.7lbs.)
Cable	(+)720mm(28.3in),(-)1800mm(70.9in)

Junction Box Characteristics

Length × Width × Depth	113.6mm(4.5in)×76mm(3.0in)×9mm(0.4in)
IP Code	IP65

Reduction of Efficiency under Low Irradiance

Reduction	7.8%

Reduction of efficiency from an irrandiance of 1000W/m² to 200W/m² (module temperature 25℃)

Appendix G

DC Appliances

DC washing machine

Capacity (kg)	3kg	Tub Dimension (mm)	¢ 300x308
Spin Speed (rpm)	About 1000	Max water level (L)	26L
Input power (W)	180W	Gross/net weight(kg)	20/18
Net Dimensions (mm)	410x420x740	Voltage	12V
Packing Dimensions (mm)	470x465x800	Loading quantity(20/40/40'HQ)	180/375/457

Stand Solar BLDC Fan

Product Price: Rs 2,000 / Piece(s) Get Best Price

Specification:

- Body Type: Plastic
- Fan Size: 16 Inches
- Operating Voltage: 12 Volts DC
- Operating Volt Range: 10 to 15 V

- Power Consumption: 24 Watts
- Warranty: 1 Year

DC Refrigerator

Capacity	198L 12v 24v DC Refrigerator
Product Size(mm	500(L)x550(W)x1580(H)mm
Power Source	12v/24v DC Electricity and solar
Material	Coated material
Certification	CE,RoHS,GS,SAA
Place of Origin	China
Power	72W
Voltage	DC12v/24v,AC110v-240v, solar power
Brand Name	BEIER 12V UPRIGHT Bottom Freezer refrigerator
Model Number	BCD198 12V 24V DC Upright Refrigerator

Water purifier

Rs 12,000/Piece Get Latest Price

Purification Type	RO, UV, UF
Capacity	10-15 L
Inlet Water Pressure/Temp (Min)	0.3 kg / cm2 or 4.3psi / 10C
Inlet Water Pressure/Temp (Max)	3 kg / cm2 or 42.7psi / 35C

Booster Pump Voltage (Volt)	24 V DC
UV Lamp Wattage(Watt)	11 Watt

Coffee maker

Product Dimensions	9 x 5.14 x 7.07 inches
Item Weight	2.5 pounds
Manufacturer	BRENTWOOD
ASIN	B01CGC9AXC
Item model number	TS-213W
Customer Reviews	4.3 out of 5 stars
Best Sellers Rank	#138,607 in Home & Kitchen
Is Discontinued By Manufacturer	No
Fabric Type	Steel
Is Assembly Required?	No
Number of Pieces	1
Batteries Required	No
Included Components	Unit
Import Designation	Made in the USA or Imported